

CONVOLUTIONS THROUGH THE LENS OF TENSOR NETWORKS

Felix Dangel*

Vector Institute

661 University Ave., Toronto, Canada

ABSTRACT

Despite their simple intuition, convolutions are more tedious to analyze than dense layers, which complicates the generalization of theoretical and algorithmic ideas. We provide a new perspective onto convolutions through tensor networks (TNs) which allow reasoning about the underlying tensor multiplications by drawing diagrams, and manipulating them to perform function transformations, sub-tensor access, and fusion. We demonstrate this expressive power by deriving the diagrams of various autodiff operations and popular approximations of second-order information with full hyper-parameter support, batching, channel groups, and generalization to arbitrary convolution dimensions. Further, we provide convolution-specific transformations based on the connectivity pattern which allow to re-wire and simplify diagrams before evaluation. Finally, we probe computational performance, relying on established machinery for efficient TN contraction. Our TN implementation speeds up a recently-proposed KFAC variant up to 4.5 x and enables new hardware-efficient tensor dropout for approximate backpropagation.

1 INTRODUCTION

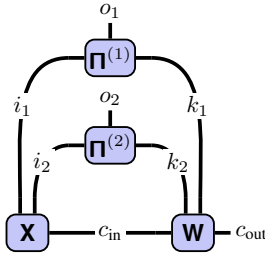
Convolutional neural networks (CNNs) [38] mark a milestone in the development of deep learning architectures. Despite the success of transformers [68], CNNs continue to be widely used and show competitive performance when incorporating architecture modernizations [41; 40] and attention [30; 70; 11; 39]. While the intuition behind convolution is simple to understand with graphical illustrations such as in Dumoulin & Visin [20], convolutions are more challenging to analyze than fully-connected layers in multi-layer perceptrons (MLPs). One reason is that the operation is hard to express in matrix expressions and—even when switching to index notation—compact expressions that are convenient to work with only exist for special hyper-parameter choices [e.g. 26; 2]. The many hyper-parameters of convolution and additional features like channel groups [35] introduce additional complexity. And related objects like (higher-order) derivatives and related routines for autodiff inherit this complexity. We observe a delay of analytical and algorithmic developments between CNNs and MLPs, e.g.

| | for MLPs | for CNNs |
|---|------------------|------------------|
| Approximate Hessian diagonal | 1989 | 2023 |
| Kronecker-factored curvature (KFAC, KFRA, KFLR) | 2015, 2017, 2017 | 2016, 2020, 2020 |
| Kronecker-factored quasi-Newton methods (KBFGS) | 2021 | 2022 |
| Neural tangent kernel (NTK) | 2018 | 2019 |
| Hessian rank | 2021 | 2023 |

Here, we seek to reduce this complexity gap by providing a new perspective onto convolutions through tensor networks (TN) [e.g. 52; 5; 8]. TNs express tensor multiplications as diagrams (Figure 1). Those simplify reading off structure like factorization, and can seamlessly be (i) manipulated to take derivatives or add batching, (ii) fused with other diagrams, and (iii) sliced to extract sub-tensors.

TNs are not only convenient for analytic investigations. The quantum computing/simulation communities [e.g. 63; 24; 72; 12] have developed established techniques to efficiently evaluate TNs. Those are accessible through a simple interface (`einsum`) and automate many optimizations like finding a high-quality contraction order or distributing computations. Our contributions are the following:

*fdangel@vectorinstitute.ai



$$= \text{Y} \text{ where } Y_{c_{\text{out}}, o_1, o_2} = \sum_{i_1, i_2, c_{\text{in}}, k_1, k_2} X_{c_{\text{in}}, i_1, i_2} \Pi_{i_1, o_1, k_1}^{(1)} \Pi_{i_2, o_2, k_2}^{(2)} W_{c_{\text{out}}, c_{\text{in}}, k_1, k_2}$$

Figure 1: TN representation of a 2d convolution with input \mathbf{X} and kernel \mathbf{W} (notation introduced in §2.3). The connectivity pattern along each dimension is made explicit via a tensor Π . Evaluating the indicated tensor multiplications (closed connections mean summation) yields the convolution’s result \mathbf{Y} .

- We use the TN format of convolution from Hayashi et al. [27] to derive diagrams for various autodiff routines and structural approximations of second-order information with support for all hyper-parameters, batching, channel groups, and arbitrary dimensions (Table 1).
- We present transformations based on structure in the connectivity pattern of real-world convolutions to re-wire TNs, enabling symbolic simplification before evaluation.
- We analyze the performance of a TN implementation, demonstrating speed-ups up to 4.5x for a recent KFAC variant, and use its flexibility to impose hardware-efficient dropout that reduces cost of randomized backpropagation via approximate TN contraction.

2 PRELIMINARIES

We briefly review 2d convolution (§2.1), provide a mathematical description of tensor multiplication (§2.2), introduce the graphical TN notation, and apply it to convolution (§2.3). We use bold lower-case (\mathbf{a}), upper-case (\mathbf{A}), and upper-case sans-serif (\mathbf{A}) symbols for vectors, matrices, and tensors. Entries follow the same convention but use regular font weight and $[\cdot]$ denotes slicing ($[\mathbf{A}]_{i,j} = A_{i,j}$). Parenthesized indices mean reshapes, e.g. $[\mathbf{a}]_{(i,j)} = [\mathbf{A}]_{i,j}$ where \mathbf{a} is the flattened matrix \mathbf{A} [57].

2.1 CONVOLUTION

2d convolutions process channels of two-dimensional signals $\mathbf{X} \in \mathbb{R}^{C_{\text{in}} \times I_1 \times I_2}$ with C_{in} channels of spatial dimensions¹ I_1, I_2 by sliding a collection of C_{out} filter banks, arranged in a kernel $\mathbf{W} \in \mathbb{R}^{C_{\text{out}} \times C_{\text{in}} \times K_1 \times K_2}$ with kernel size K_1, K_2 , over the input. The sliding operation depends on various hyperparameters (padding, stride, dilation, see [20]). At each step, the filters are contracted with the overlapping area, yielding the channel values of a pixel in the output $\mathbf{Y} \in \mathbb{R}^{C_{\text{out}} \times O_1 \times O_2}$ with spatial output dimensions O_1, O_2 . Optionally, a bias from $\mathbf{b} \in \mathbb{R}^{C_{\text{out}}}$ is added to each output channel.

One way to implement convolution is via matrix multiplication [9], similar to fully-connected layers. First, one extracts the overlapping patches from the input for each output, then flattens and column-stacks them into a matrix $[\mathbf{X}] \in \mathbb{R}^{C_{\text{in}} K_1 K_2 \times O_1 O_2}$, called the *unfolded input* (this operation is also called `im2col`). Multiplying a matrix view $\mathbf{W} \in \mathbb{R}^{C_{\text{out}} \times C_{\text{in}} K_1 K_2}$ of the kernel onto the unfolded input then yields a matrix view \mathbf{Y} of \mathbf{Y} (the vector of ones, $\mathbf{1}_{O_1 O_2}$, copies the bias for each channel),

$$\mathbf{Y} = \mathbf{W}[\mathbf{X}] + \mathbf{b} \mathbf{1}_{O_1 O_2}^T \in \mathbb{R}^{C_{\text{out}} \times O_1 O_2}. \quad (1)$$

An even closer perspective to fully-connected layers is to consider convolution as affine transformation of the flattened input $\mathbf{x} \in \mathbb{R}^{C_{\text{in}} I_1 I_2}$ into a vector view \mathbf{y} of \mathbf{Y} using a structured matrix $\mathbf{A}(\mathbf{W}) \in \mathbb{R}^{C_{\text{out}} O_1 O_2 \times C_{\text{in}} I_1 I_2}$ whose elements are contained in the kernel,

$$\mathbf{y} = \mathbf{A}(\mathbf{W})\mathbf{x} + \mathbf{b} \otimes \mathbf{1}_{O_1 O_2} \in \mathbb{R}^{C_{\text{out}} O_1 O_2}. \quad (2)$$

This dual perspective of unfolding the kernel instead of \mathbf{X} is uncommon in implementations, but used in theoretical works [e.g. 62] and highlights the similarity between convolutions and dense layers.

2.2 TENSOR MULTIPLICATION

Tensor multiplication unifies inner, element-wise (Hadamard), and outer (Kronecker) multiplication and relies on the input-output index relation to infer the multiplication type. We start with the binary case, then generalize to more inputs: Consider $\mathbf{A}, \mathbf{B}, \mathbf{C}$ whose index names are described by the index

¹We prefer I_1, I_2 over the more common choice H, W to simplify generalization to higher dimensions.

tuples S_1, S_2, S_3 where $S_3 \subseteq (S_1 \cup S_2)$ (converting tuples to sets if needed). Any multiplication of \mathbf{A} and \mathbf{B} can be described by the tensor multiplication operator $*_{(S_1, S_2, S_3)}$ with

$$\mathbf{C} = *_{(S_1, S_2, S_3)}(\mathbf{A}, \mathbf{B}) \Leftrightarrow [\mathbf{C}]_{S_3} = \sum_{(S_1 \cup S_2) \setminus S_3} [\mathbf{A}]_{S_1} [\mathbf{B}]_{S_2}, \quad (3)$$

summing over indices that are not present in the output. For example, for two matrices \mathbf{A}, \mathbf{B} , their product is $\mathbf{AB} = *_{((i,j), (j,k), (i,k))}(\mathbf{A}, \mathbf{B})$, their Hadamard product $\mathbf{A} \odot \mathbf{B} = *_{((i,j), (i,j), (i,j))}(\mathbf{A}, \mathbf{B})$, and their Kronecker product $\mathbf{A} \otimes \mathbf{B} = *_{((i,j), (k,l), ((i,k), (j,l)))}(\mathbf{A}, \mathbf{B})$. Libraries support this functionality via `einsum`, which takes a string encoding of S_1, S_2, S_3 , followed by \mathbf{A}, \mathbf{B} . It also accepts longer sequences $\mathbf{A}_1, \dots, \mathbf{A}_N$ with index tuples S_1, S_2, \dots, S_N and output index tuple S_{N+1} ,

$$\mathbf{A}_{N+1} = *_{(S_1, \dots, S_N, S_{N+1})}(\mathbf{A}_1, \dots, \mathbf{A}_N) \Leftrightarrow [\mathbf{A}_{N+1}]_{S_{N+1}} = \sum_{(\cup_{n=1}^N S_n) \setminus S_{N+1}} \left(\prod_{n=1}^N [\mathbf{A}_n]_{S_n} \right). \quad (4)$$

Binary and N -ary tensor multiplication are commutative: Simultaneously permuting operands and their index tuples does not change the result, $*_{(S_1, S_2, S_3)}(\mathbf{A}, \mathbf{B}) = *_{(S_2, S_1, S_3)}(\mathbf{B}, \mathbf{A})$ and $*_{(\dots, S_i, \dots, S_j, \dots)}(\dots, \mathbf{A}_i, \dots, \mathbf{A}_j, \dots) = *_{(\dots, S_j, \dots, S_i, \dots)}(\dots, \mathbf{A}_j, \dots, \mathbf{A}_i, \dots)$. They are also associative, i.e. we can multiply operands in any order. However, the notation becomes involved as it requires additional set arithmetic to detect when an index can be summed (see §F.1 for an example).

2.3 TENSOR NETWORKS & CONVOLUTION

A simpler way to understand tensor multiplications is via diagrams developed by e.g. Penrose [52]. Rank- K tensors are represented by nodes with K legs labelled by the index's name². For instance, \boxed{a}^{-i} denotes a vector \mathbf{a} , ${}^{i-}\boxed{B}^{-j}$ a matrix \mathbf{B} , and ${}^{i-}\boxed{C}^{-j-k}$ a rank-3 tensor \mathbf{C} . The 2d Kronecker delta $[\delta]_{i,j} = \delta_{i,j}$ is simply a line, ${}^{j-}\boxed{\delta}^{-i} = {}^{j-}\boxed{I}^{-i} = j \text{---} i$. Multiplications are indicated by connections between legs. For inner multiplication, we join the legs of the involved indices, e.g. the matrix multiplication diagram is ${}^{i-}\boxed{AB}^{-k} = {}^{i-}\boxed{A}^{-j} \text{---} {}^{j-}\boxed{B}^{-k}$. Element-wise multiplication is similar, but with a leg sticking out. For example, the Hadamard and Kronecker product diagrams are

$${}^{i-}\boxed{A \odot B}^{-j} = i \text{---} \left[\begin{array}{c} \boxed{A} \\ \boxed{B} \end{array} \right]^{-j}, \quad (i, k) \text{---} \boxed{A \otimes B} \text{---} (j, l) = (i, k) \left\langle \begin{array}{c} \boxed{A} \\ \boxed{B} \end{array} \right\rangle (j, l). \quad (5)$$

Note that the outer tensor product yields a rank-4 tensor which needs to be reshaped (indicated by black triangles³) to obtain a matrix. This syntax allows for extracting and embedding tensors along diagonals—e.g. taking a matrix diagonal, $\text{diag}(\mathbf{A})^{-i} = \boxed{A}^{-i}$, or forming a diagonal matrix, ${}^{i-}\text{diag}(\mathbf{a})^{-i} = {}^{i-}\boxed{a}^{-i}$ —and generalizes to larger diagonal blocks (§B). In the following, we stick to the simplest case to avoid the more advanced syntax. However, it shows the expressive power of TNs and is required to support common features of convolutions like channel groups.

Application to Convolution: We define a binary tensor $\mathbf{P} \in \{0, 1\}^{I_1 \times O_1 \times K_1 \times I_2 \times O_2 \times K_2}$ which represents the connectivity pattern between input, output, and kernel. $P_{i_1, o_1, k_1, i_2, o_2, k_2}$ is 1 if input locations (i_1, i_2) overlap with kernel positions (k_1, k_2) when computing output locations (o_1, o_2) and 0 otherwise. The spatial couplings are independent along each dimension, hence \mathbf{P} decomposes into $P_{i_1, o_1, k_1, i_2, o_2, k_2} = \prod_{i_1, o_1, k_1}^{(1)} \prod_{i_2, o_2, k_2}^{(2)}$ where the index pattern tensor $\prod^{(j)} \in \{0, 1\}^{I_j \times O_j \times K_j}$ encodes the connectivity along dimension j . With that, one obtains

$$Y_{\text{out}, o_1, o_2} = b_{\text{out}} + \sum_{c_{\text{in}}=1}^{C_{\text{in}}} \sum_{i_1=1}^{I_1} \sum_{i_2=1}^{I_2} \sum_{k_1=1}^{K_1} \sum_{k_2=1}^{K_2} X_{c_{\text{in}}, i_1, i_2} \prod_{i_1, o_1, k_1}^{(1)} \prod_{i_2, o_2, k_2}^{(2)} W_{\text{out}, c_{\text{in}}, k_1, k_2},$$

which translates into the TN diagram shown in Figure 1 if neglecting the bias.

3 TENSOR NETWORKS FOR CONVOLUTION OPERATIONS

We now demonstrate the elegance of TNs for computing derivatives (§3.1), autodiff operations (§3.2), and second-order information in the form of sub-tensors (§3.3) or structural approximations (§3.4) by graphical manipulation. For simplicity, we exclude batching (more generally, `vmap`-ing like in

²We use identical shapes for all tensors. Leg orientation does not assign properties like co-/contra-variance.

³Reshape can be seen as tensor multiplication with a one-hot tensor, but we decided to use a separate symbol to emphasize that it merely serves for re-interpreting the tensor and does not cause computations.

Table 1: Contraction expressions of operations related to 2d convolution. They include batching and channel groups, which are standard features in implementations. We describe each operation by an tuple of input tensors and a contraction string that uses the `einops` library’s syntax [57] which can express index (un-)grouping. Some quantities are only correct up to a scalar factor which is suppressed for brevity. See §B for visualizations and Table B2 for more operations.

| Operation | Operands | Contraction string (<code>einops</code> [57] convention) |
|--|--|--|
| Convolution (no bias) [27] | $\mathbf{X}, \Pi^{(1)}, \Pi^{(2)}, \mathbf{W}$ | "n (g c.in) i1 i2, i1 o1 k1, i2 o2 k2, (g c.out) c.in k1 k2 -> n (g c.out) o1 o2" |
| Unfolded input (<code>im2col</code>) | $\mathbf{X}, \Pi^{(1)}, \Pi^{(2)}$ | "n c.in i1 i2, i1 o1 k1, i2 o2 k2 -> n (c.in k1 k2) (o1 o2)" |
| Unfolded kernel (Toeplitz) | $\Pi^{(1)}, \Pi^{(2)}, \mathbf{W}$ | "i1 o1 k1, i2 o2 k2, c.out c.in k1 k2 -> (c.out o1 o2) (c.in i1 i2)" |
| Weight VJP | $\mathbf{X}, \Pi^{(1)}, \Pi^{(2)}, \mathbf{V}^{(Y)}$ | "n (g c.in) i1 i2, i1 o1 k1, i2 o2 k2, n (g c.out) o1 o2 -> (g c.out) c.in k1 k2" |
| Input VJP (transpose conv.) | $\mathbf{W}, \Pi^{(1)}, \Pi^{(2)}, \mathbf{V}^{(Y)}$ | "(g c.out) c.in k1 k2, i1 o1 k1, i2 o2 k2, n (g c.out) o1 o2 -> n (g c.in) i1 i2" |
| KFC/KFAC-expand [26; 22] | $\mathbf{X}, \Pi^{(1)}, \Pi^{(2)}, \mathbf{X}, \Pi^{(1)}, \Pi^{(2)}$ | "n (g c.in) i1 i2, i1 o1 k1, i2 o2 k2, n (g c.in) i1 i2, i1 o1 k1, i2 o2 k2 -> g (c.in k1 k2) (c.in k1 k2)" |
| KFAC-reduce [22] | $\mathbf{X}, \Pi^{(1)}, \Pi^{(2)}, \mathbf{X}, \Pi^{(1)}, \Pi^{(2)}$ | "n (g c.in) i1 i2, i1 o1 k1, i2 o2 k2, n (g c.in) i1 i2, i1 o1 k1, i2 o2 k2 -> g (c.k1 k2) (c.k1 k2)" |
| GGN Gram/NTK [17; 50; 48] | $\mathbf{X}, \Pi^{(1)}, \Pi^{(2)}, \mathbf{S}^{(Y)}, \mathbf{X}, \Pi^{(1)}, \Pi^{(2)}, \mathbf{S}^{(Y)}$ | "n (g c.in) i1 i2, i1 o1 k1, i2 o2 k2, c n (g c.out) o1 o2, n (g c.in) i1 i2, i1 o1 k1, i2 o2 k2, c n (g c.out) o1 o2 -> (c n) (c n)" |
| GGN/Cov.diagonal [16; 50] | $\mathbf{X}, \Pi^{(1)}, \Pi^{(2)}, \mathbf{S}^{(Y)}, \mathbf{X}, \Pi^{(1)}, \Pi^{(2)}, \mathbf{S}^{(Y)}$ | "n (g c.in) i1 i2, i1 o1 k1, i2 o2 k2, c n (g c.out) o1 o2, n (g c.in) i1 i2, i1 o1 k1, i2 o2 k2, c n (g c.out) o1 o2 -> c.out c.in k1 k2" |

JAX [7]) and channel groups. These can be achieved by adding a leg for the batch dimension and by un-grouping channels (see §B). Table 1 summarizes our derivations (with batching and groups).

As a warm-up, we identify the unfolded input and kernel from the matrix-multiplication view from Equations (1) and (2). They follow by contracting the index patterns with either the input or kernel,

$$\begin{aligned} \llbracket \mathbf{X} \rrbracket_{(c_{in}, k_1, k_2), (o_1, o_2)} &= \sum_{i_1=1}^{I_1} \sum_{i_2=1}^{I_2} \mathbf{X}_{c_{in}, i_1, i_2} \Pi_{i_1, o_1, k_1}^{(1)} \Pi_{i_2, o_2, k_2}^{(2)}, \\ \llbracket \mathbf{A}(\mathbf{W}) \rrbracket_{(c_{out}, o_1, o_2), (c_{in}, i_1, i_2)} &= \sum_{k_1=1}^{K_1} \sum_{k_2=1}^{K_2} \Pi_{i_1, o_1, k_1}^{(1)} \Pi_{i_2, o_2, k_2}^{(2)} \mathbf{W}_{c_{out}, c_{in}, k_1, k_2}, \end{aligned}$$

or, in diagram notation,

$$\llbracket \mathbf{X} \rrbracket_{(c_{in}, k_1, k_2), (o_1, o_2)} \quad \text{and} \quad \llbracket \mathbf{A}(\mathbf{W}) \rrbracket_{(c_{out}, o_1, o_2), (c_{in}, i_1, i_2)} \quad (6)$$

3.1 TENSOR NETWORK DIFFERENTIATION

Derivatives play a crucial role in theoretical and practical ML. First, we show that differentiating a TN diagram amounts to a simple graphical manipulation. Then, we derive the Jacobians of convolution. Consider an arbitrary TN represented by the tensor multiplication from Equation (4). The Jacobian tensor $[\mathbf{J}_{\mathbf{A}_j} \mathbf{A}_{N+1}]_{S_{N+1}, S'_j} = \partial[\mathbf{A}_{N+1}]_{S_{N+1}} / \partial[\mathbf{A}_j]_{S'_j}$ w.r.t. an input \mathbf{A}_j collects all partial derivatives and is addressed through indices $S_{n+1} \times S'_j$ with S'_j an independent copy of S_j . Assume that \mathbf{A}_j only enters once in the tensor multiplication. Then, taking the derivative of Equation (4) w.r.t. $[\mathbf{A}_j]_{S'_j}$ simply replaces the tensor by a Kronecker delta δ_{S_j, S'_j} ,

$$\frac{\partial[\mathbf{A}_{N+1}]_{S_{N+1}}}{\partial[\mathbf{A}_j]_{S'_j}} = \sum_{(U_{n=1}^N S_n) \setminus S_{n+1}} [\mathbf{A}_1]_{S_1} \cdots [\mathbf{A}_{j-1}]_{S_{j-1}} \left(\prod_{i \in S_j} \delta_{i, i'} \right) [\mathbf{A}_{j+1}]_{S_{j+1}} \cdots [\mathbf{A}_N]_{S_N}. \quad (7)$$

If an index $i \in S_j$ is summed, $i \notin S_{n+1}$, we can sum the Kronecker delta $\delta_{i, i'}$, effectively replacing all occurrences of i by i' . If instead i is part of the output index, $i \in S_{n+1}$, the Kronecker delta remains part of the Jacobian and imposes structure. Figures 2a and 2b illustrate this process in diagrams for differentiating a convolution w.r.t. its kernel. Equation (7) amounts to cutting out the argument of differentiation and assigning new indices to the resulting open legs (Figure 2a). Then, we can simplify the new legs connected to other tensors (Figure 2b). For the weight Jacobian $\mathbf{J}_{\mathbf{W}} \mathbf{Y}$, this introduces structure: If we re-interpret the two disjoint diagrams in Figure 2b as matrices, compare with the Kronecker diagram from Equation (5) and use Equation (6), we find $\llbracket \mathbf{X}^T \rrbracket \otimes \mathbf{I}_{C_{out}}$ for the Jacobian’s matrix view [e.g. 15]. Figure 2c shows the TN of the input Jacobian $\mathbf{J}_{\mathbf{X}} \mathbf{Y}$, which is given by a tensor view of the unfolded kernel, consistent with the matrix-vector perspective of Equation (2).

Differentiating a TN representation is more convenient than using matrix calculus [43] as it amounts to a simple graphical manipulation and does not rely on a flattening convention and therefore preserves

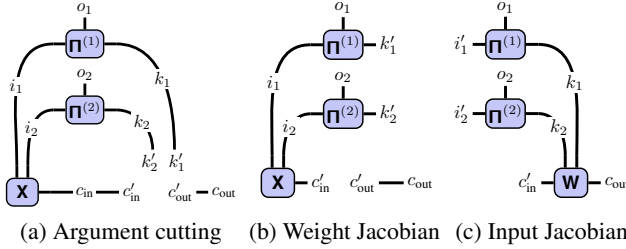


Figure 2: TN differentiation as graphical manipulation. (a) Differentiating a 2d convolution w.r.t. \mathbf{W} requires cutting it out of the diagram, introducing indices for open legs. (b) Weight Jacobian after simplifying the new legs connected to other tensors. (c) Same procedure applied to the Jacobian w.r.t. \mathbf{X} .

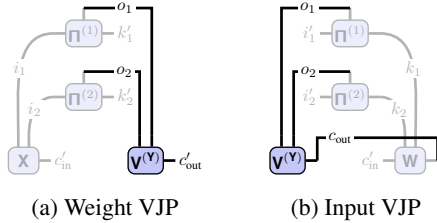


Figure 3: TNs of 2d convolution VJPs for backpropagation. Jacobians from Figure 2 are shaded, only their contraction with the vector $\mathbf{V}(\mathbf{Y})$ is highlighted. (a) VJP for the weight and (b) input Jacobian (transpose convolution). JVPs are similar, but contract vectors $\mathbf{V}(\mathbf{X}) \in \mathbb{R}^{C_{in} \times I_1 \times I_2}$, $\mathbf{V}(\mathbf{W}) \in \mathbb{R}^{C_{out} \times C_{in} \times K_1 \times K_2}$ with the input and kernel indices of $\mathbf{J}_X \mathbf{Y}$, $\mathbf{J}_W \mathbf{Y}$.

the full index structure. The resulting TN can still be translated back to matrix language, if desired. It also simplifies the computation of higher-order derivatives (e.g. $\partial^2 \mathbf{Y} / \partial \mathbf{W} \partial \mathbf{X}$), since differentiation yields another TN and can thus be repeated. If a tensor occurs more than once in a TN, the product rule applies and the derivative is a sum of TNs with one occurrence removed.

3.2 AUTOMATIC DIFFERENTIATION & CONNECTIONS TO TRANSPOSE CONVOLUTION

Although Jacobians can sometimes be useful, crucial routines for integration with autodiff are vector-Jacobian and Jacobian-vector products (VJPs, JVPs). Both are simple to realize with TNs due to access to full Jacobians. VJPs are used in backpropagation to pull back a tensor $\mathbf{V}(\mathbf{Y}) \in \mathbb{R}^{C_{out} \times O_1 \times O_2}$ from the output space. The VJP results are $\mathbf{V}(\mathbf{X}) \in \mathbb{R}^{C_{in} \times I_1 \times I_2}$ and $\mathbf{V}(\mathbf{W}) \in \mathbb{R}^{C_{out} \times C_{in} \times K_1 \times K_2}$ are

$$\mathbf{V}_{c'_{in}, i'_1, i'_2}(\mathbf{X}) = \sum_{c_{out}, o_1, o_2} \mathbf{V}_{c_{out}, o_1, o_2}(\mathbf{Y}) \frac{\partial Y_{c_{out}, o_1, o_2}}{\partial X_{c'_{in}, i'_1, i'_2}}, \quad \mathbf{V}_{c'_{out}, c'_{in}, k'_1, k'_2}(\mathbf{W}) = \sum_{c_{out}, o_1, o_2} \mathbf{V}_{c_{out}, o_1, o_2}(\mathbf{Y}) \frac{\partial Y_{c_{out}, o_1, o_2}}{\partial W_{c'_{out}, c'_{in}, k'_1, k'_2}}.$$

Both are simply new TNs constructed from contracting the vector with the respective Jacobian, see Figure 3 (VJPs are analogous). Note that the input VJP is often used as a definition for transpose convolution [20]. In the matrix-multiplication perspective (Equation (2)), this operation is defined relative to a convolution with kernel \mathbf{W} by multiplication with $\mathbf{A}(\mathbf{W})^\top$, i.e. using the same connectivity pattern but mapping from the convolution’s output space to its input space. The TN diagram makes this sharing explicit as the same Π ’s are used, and provides a clean definition of transpose convolution.⁴

3.3 EXACT SECOND-ORDER INFORMATION

Last, we look at second-order information of a loss. Its computation can be phrased as backpropagation with a final extraction step [18] which contains less standard operations like Jacobian-matrix products (JMPs) and sub-tensor extraction. TNs can express this extraction step in a single diagram.

Consider a datum (\mathbf{x}, \mathbf{t}) and its loss $\ell(\mathbf{w}) = \ell(\mathbf{f}, \mathbf{t})$ where $\mathbf{f} := f_{\mathbf{w}}(\mathbf{x}) \in \mathbb{R}^C$ is the prediction of a CNN with a convolution with flattened kernel \mathbf{w} and flattened output \mathbf{y} (derivations carry over to a batch loss). The kernel’s generalized Gauss-Newton (GGN) matrix [60] $\mathbf{G}(\mathbf{w}) = (\mathbf{J}_{\mathbf{w}} \mathbf{f})^\top \nabla_{\mathbf{f}}^2 \ell(\mathbf{J}_{\mathbf{w}} \mathbf{f}) \in \mathbb{R}^{C_{out} \times C_{in} \times K_1 \times K_2 \times C_{out} \times C_{in} \times K_1 \times K_2}$ is a positive semi-definite Hessian proxy preferred by many applications [e.g. 19; 44] and coincides with the Fisher information matrix for many common losses [45]. It is the self-outer product of a backpropagated symmetric factorization $\mathbf{S}(\mathbf{y}) = (\mathbf{J}_{\mathbf{y}} \mathbf{f})^\top \mathbf{S}(\mathbf{f}) \in \mathbb{R}^{C_{out} \times O_1 \times O_2 \times C}$ of the loss Hessian, $\nabla_{\mathbf{f}}^2 \ell(\mathbf{f}, \mathbf{y}) = \mathbf{S}(\mathbf{f})(\mathbf{S}(\mathbf{f}))^\top$. During backpropagation, the convolution extracts information about $\mathbf{G}(\mathbf{w}) = (\mathbf{J}_{\mathbf{w}} \mathbf{y})^\top \mathbf{S}(\mathbf{y})(\mathbf{S}(\mathbf{y}))^\top \mathbf{J}_{\mathbf{w}} \mathbf{y}$.

In TN notation, this is easy to express without flattening: We simply compose two VJP diagrams from Figure 3a with an extra leg (MJP) and add the outer-product contraction to obtain the tensor version $\mathbf{G}(\mathbf{W}) \in \mathbb{R}^{C_{out} \times C_{in} \times K_1 \times K_2 \times C_{out} \times C_{in} \times K_1 \times K_2}$ of $\mathbf{G}(\mathbf{w})$ (Figure 4a). The GGN is often further

⁴In standalone implementations of transpose convolution, one must supply an additional parameter to unambiguously reconstruct the convolution’s input dimension (see §C for how to compute Π in this case).

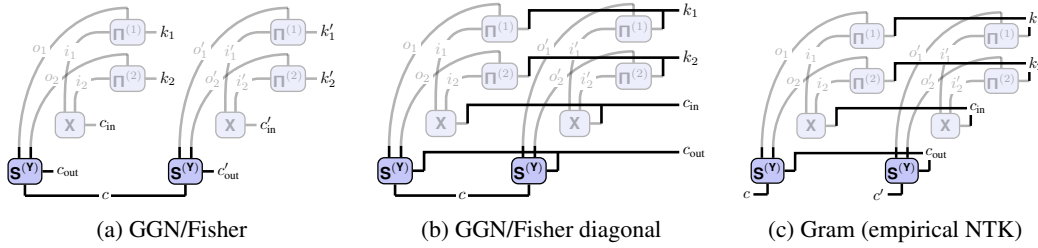


Figure 4: TN composition and sub-tensor extraction for second-order information. Weight MJPs from Figure 3a are shaded. (a) exact and (b) diagonal of the kernel’s GGN (the same applies to structurally similar matrices like the gradient covariance [34]). (c) TN of the GGN Gram matrix.

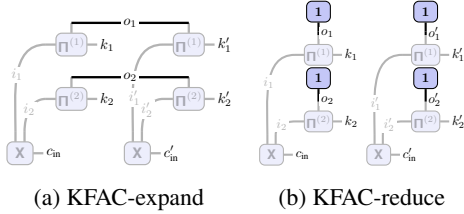


Figure 5: TNs of input-based Kronecker factors for block-diagonal Fisher/GGN approximations. The unfolded input is shaded, only additional contractions are highlighted. (a) Ω (KFC/KFAC-expand) from Grosse & Martens [26] and (b) $\hat{\Omega}$ (KFAC-reduce) from Eschenhagen [22] (in practice, the vectors of ones that effectively sum out an index are not physically required).

approximated by sub-tensors as it is too large. These slicing operations are also easy to integrate into the diagrams, e.g. to extract diagonal elements (Figure 4b [16; 50]), or mini-block diagonals (Figure B10 [15; 3]). This also removes redundant computations compared to computing, then slicing, the matrix. The same ideas apply to the GGN Gram matrix $(S^{(w)})^\top S^{(w)} \in \mathbb{R}^{C \times C}$ (Figure 4c). It contains the GGN spectrum [17] and is related to the empirical NTK for square loss [48].

3.4 KRONECKER-FACTORED APPROXIMATE CURVATURE (KFAC)

Sub-tensors of second-order information yield low-memory, easy-to-invert curvature proxies. Other works have developed structural GGN/Fisher approximations based on Kronecker factorization [46; 26; 22; 47] for architectures including CNNs. Their computation involves the unfolded input and libraries that provide access to them [16; 50] rely on `im2col`. We briefly present their TNs which can avoid building up $[\mathbf{X}]$ and thus reduce memory and run time (§5.1).

KFC (KFAC-expand): Grosse & Martens [26] introduce a Kronecker approximation for the kernel’s GGN, $G(w) \approx \Omega \otimes \Gamma$ where $\Gamma \in \mathbb{R}^{C_{\text{out}} \times C_{\text{out}}}$ and the input-based factor is $\Omega = [\mathbf{X}]^\top [\mathbf{X}] \in \mathbb{R}^{C_{\text{in}} K_1 K_2 \times C_{\text{in}} K_1 K_2}$ (Figure 5a), the unfolded input’s self-inner product (averaged over a batch).

KFAC-reduce: Eschenhagen [22] generalized KFAC to graph neural networks and transformers based on the concept of weight sharing, also present in convolutions. They identify two approximations—KFAC-expand and KFAC-reduce—the former of which corresponds to KFC [26]. The latter shows similar performance in downstream tasks, but is cheaper to compute. It relies on the column-averaged unfolded input, i.e. the average over all patches sharing the same weights. KFAC-reduce approximates $G(w) \approx \hat{\Omega} \otimes \hat{\Gamma}$ with $\hat{\Gamma} \in \mathbb{R}^{C_{\text{out}} \times C_{\text{out}}}$ and $\hat{\Omega} = 1/(O_1 O_2)^2 (\mathbf{1}_{O_1 O_2}^\top [\mathbf{X}])^\top \mathbf{1}_{O_1 O_2}^\top [\mathbf{X}] \in \mathbb{R}^{C_{\text{in}} K_1 K_2 \times C_{\text{in}} K_1 K_2}$ (Figure 5b; averaged over a batch).

4 TENSOR NETWORK TRANSFORMATIONS & IMPLEMENTATION ASPECTS

Many convolutions in real-world CNNs use highly structured connectivity patterns. This enables diagram simplifications of the TNs presented in §3, which we describe here (§4.1). We also briefly mention implementation aspects for efficient TN contraction (§4.2).

4.1 CONVOLUTION INDEX PATTERN STRUCTURE

The index pattern Π encodes the connectivity of a convolution and depends on its hyperparameters. Along one dimension, $\Pi = \Pi(I, K, S, P, D)$ with input size I , kernel size K , stride S , padding

P , and dilation D . We provide pseudo-code for computing Π in §C which is easy to implement efficiently with standard functions from any numerical library (Algorithm C1). Since Π is binary and has size linear in I, O, K , it is cheap to pre-compute and cache. In 1-based index notation, it is the logical expression expressed by the Kronecker delta

$$[\Pi(I, K, S, P, D)]_{i,o,k} = \delta_{i,1+(k-1)D+(o-1)S-P}, \quad i=1,\dots,I, \quad o=1,\dots,O, \quad k=1,\dots,K \quad (8)$$

with spatial output size $O(I, K, S, P, D) = 1 + \lfloor (I+2P-(K+(K-1)(D-1)))/S \rfloor$. In the following, we will assume the absence of boundary pixels that don't overlap with the kernel, that is

$$I + 2P - (K + (K - 1)(D - 1)) \bmod S = 0, \quad (9)$$

where the floor operation in $O(I, K, S, P, D)$ is obsolete. This can always be assured by narrowing \mathbf{X} before a convolution. Based on our hyper-parameter analysis of real-world CNNs (§D), we identify:

Transformation 1 (Dense convolutions) Assume Equation (9). For $K = S$ with default padding and dilation ($P = 0, D = 1$), patches are adjacent non-overlapping tiles, accessible by un-grouping the input index i into a tuple index (\tilde{i}, \tilde{k}) of size $I/K \times K$:

$$[\Pi(I, K, K, 0, 1)]_{i,o,k} = [\Pi(I, K, K, 0, 1)]_{(\tilde{i}, \tilde{k}), o, k} = \delta_{\tilde{i}, o} \delta_{\tilde{k}, k}.$$

'Trivial' convolutions ($K = S = 1$) are a special case with identity pattern $[\Pi(I, 1, 1, 0, 1)]_{i,o,k} = \delta_{i,o}$.

Dense convolutions with $K = S = 1$ are very common⁵. DenseNets [32] rely on them, but they are also featured by MobileNets [29; 58] and ResNets [28]. InceptionV3 [66] has 2d 'mixed dense' convolutions that are 'trivial' along one spatial dimension.

Transformation 2 (Down-sampling convolutions) For $S > K$ with default padding and dilation ($P = 0, D = 1$), some elements do not overlap with the kernel. If the input dimension i is summed, all participating tensors can be pruned to remove the explicit zeros. Assume $I \bmod S = 0$. Then, pruning amounts to un-grouping i into (i', s) of size $I/S \times S$, narrowing s to K entries, and grouping back into an index \tilde{i} of size KI/S . After pruning, the index pattern represents a dense convolution with input size KI/S , kernel size K , and stride K . In a contraction with some tensor \mathbf{V} ,

$$\sum_{i=1}^I [\mathbf{V}]_{\dots, i, \dots} [\Pi(I, K, S > K, 0, 1)]_{i, o, k} = \sum_{\tilde{i}=1}^{KI/S} [\tilde{\mathbf{V}}]_{\dots, \tilde{i}, \dots} [\Pi(KI/S, K, K, 0, 1)]_{\tilde{i}, o, k}$$

with sub-tensor $[\tilde{\mathbf{V}}]_{\dots, \tilde{i}, \dots} = [[\mathbf{V}]_{\dots, (i', s), \dots}]_{\dots, (:, :K), \dots}$ where $:K$ means narrowing to K elements.

Transformation 2 converts down-sampling convolutions to dense convolutions, which can be further simplified with Transformation 1. We find down-sampling convolutions with $S = 2 > K = 1$ in ResNet18 [28], ResNext101 [69], and WideResNet101 [71]. Those convolutions discard 75% of their input! Knowledge that an operation only consumes a fraction of its input could be used to eliminate those 'dead' computations in preceding operations, reducing FLOPS and memory.

Transformation 3 (Kernel-output dimension swap) Assume Equation (9). Transposing kernel and output dimensions in an index pattern yields another index pattern with same input size, kernel size $O(I, K, S, P, D)$, and swapped stride and dilation:

$$[\Pi(I, K, S, P, D)]_{i, o, k} = [\Pi(I, O, D, P, S)]_{i, k, o}.$$

This transformation is easy to see from the symmetry of (k, D) and (o, S) in Equation (8) and $O(I, K, S, P, D)$. It converts index pattern contractions over output into kernel dimensions, like in convolutions. An example is the weight VJP from Figure 3a, which—after swapping kernel and output dimensions—resembles the TN for convolution from Figure 1 with kernel \mathbf{V} . Rochette et al. [56] use this to phrase the computation of per-example gradients as convolution.

§C.3 presents more properties of Π based on the sub-sampling interpretation of stride and dilation along the output and kernel dimensions. We also provide a transformation for swapping input and output dimensions, relating convolution and transpose convolution as described in [20].

⁵While we did not identify dense convolutions with $K = S > 2$, pooling layers often use non-overlapping patches. Average pooling can be seen as grouped convolution ($G = C_{in}$) with constant factorized kernel, and hence expressed as dense convolution. This view is interesting for convolutions that directly feed into average pooling layers, such as in `densenet201` as it allows to merge convolution and pooling into a single TN.

4.2 IMPLEMENTATION ASPECTS

Contraction order optimization: There exist various orders in which to carry out the summations in a TN and their performance can vary by orders of magnitude. One extreme approach is to carry out all summations via nested for-loops. This so-called Feynman path integral algorithm requires little memory, but many FLOPS since it does not re-cycle intermediate results. The other extreme is sequential pair-wise contraction. This builds up intermediate results and can greatly reduce FLOPS. The schedule is represented by a binary tree, but the underlying search is in general at least #P-hard [13]. Fortunately, there exist heuristics to find high-quality contraction trees for TNs with hundreds of tensors [31; 24; 12], implemented in packages like `opt_einsum` [63].

Index slicing & distributing computations: A common problem with high-quality schedules is that intermediates exceed memory. Dynamic slicing [31] (e.g. `cotengra` [24]) is a simple method to decompose a contraction until it becomes feasible by breaking it up into smaller identical sub-tasks whose aggregation adds a small overhead. This enables peak memory reduction and distribution.

Sparsity: Π is sparse as only a small fraction of the input overlaps with the kernel for each output element. For a convolution with stride $S < K$ and otherwise default parameters ($P = 0, D = 1$) that satisfies Equation (9), for fixed output and kernel indices k, o , there is exactly one non-zero entry in $[\Pi]_{:,o,k}$. Hence $\text{nnz}(\Pi) = OK$, which corresponds to a sparsity of $1/I$. Padding leads to more kernel elements that do not contribute to an output pixel, and therefore a sparser Π . For down-sampling and dense convolutions, we showed how Π 's algebraic structure allows to simplify the contraction. However, if that is not possible, Π contains explicit zeros that add unnecessary FLOPS. One—admittedly involved—way to circumvent this is to match the contraction sequences with TNs of operations with efficient implementations (like `im2col`, (transpose) convolution), using transformations such as Transformation 3 or introducing identity tensors to complete a template. This was done in [56; 14] to re-phrase computing per-sample gradients and `im2col` with convolutions.

Approximate contraction & structured dropout: TNs offer a principled approach for stochastic approximation via Monte-Carlo estimation to save memory and run time at the cost of accuracy. The basic idea is best explained on a matrix product $C := AB = \sum_{n=1}^N [A]_{:,n} [B]_{n,:}$ with $A \in \mathbb{R}^{I \times N}, B \in \mathbb{R}^{N \times O}$. To approximate the sum, we introduce a distribution over n 's range, then use column-row-sampling (CRS) [1] to form an unbiased Monte-Carlo approximation with sampled indices, which only requires the sub-matrices with active column-row pairs. Bernoulli-CRS samples without replacement by assigning a Bernoulli random variable $\text{Bernoulli}(\pi_n)$ with probability π_n for column-row pair n to be included in the contraction. The Bernoulli estimator is $\tilde{C} := \sum_{n=1}^N z_n/\pi_n [A]_{n,:} [B]_{n,:}$ with $z_n \sim \text{Bernoulli}(\pi_n)$. With a shared keep probability, $\pi_n := p$, this yields the unbiased estimator $C' = 1/p \sum_{n=1, \dots, N} A' B'$ where $A' = AK$ and $B' = KB$ with $K = \text{diag}(z_1, \dots, z_N)$ are the sub-matrices of A, B containing the active column-row pairs. CRS applies to a single contraction. For TNs with multiple sums, we can apply it individually. Also, we can impose a distribution over the result indices, which leads to computing a (scaled) sub-tensor.

5 EXPERIMENTS

5.1 RUN TIME EVALUATION

We implement the presented TNs in PyTorch [51], which amounts to generating contraction string and operands⁶. The simplifications from Transformations 1 and 2 are a post-processing step that modifies them. To find a contraction schedule, we use `opt_einsum` [63] with default settings. We extract the unique convolutions of 8 architectures for ImageNet and smaller data sets, then compare some operations from Table 1 with their standard implementation on an Nvidia Tesla T4 GPU (16 GB); see §E for all details. Due to space constraints, we highlight important insights here and provide references to the corresponding material in the appendix.

In general, the performance gap between specialized and TN implementation decreases the less common an operation is (Figure E14); from forward pass (inference & training), to VJPs (training),

⁶`einsum` does not yet support index un-grouping, so we must reshape manually before and after.

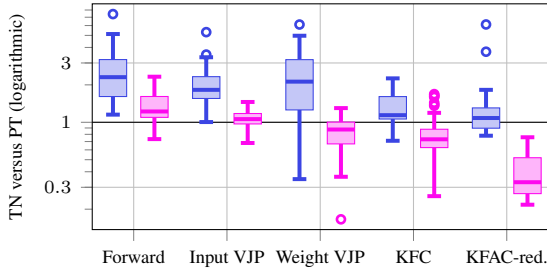


Figure 6: Ratio of TN versus standard implementation run times (without and with simplifications) on some of the derived operations for dense convolutions. Box plots contain data from dense convolutions of 8 CNNs. With simplifications, convolution and input VJP achieve median ratios slightly above 1, and the TN implementation is faster for weight VJP, KFC & KFAC-reduce.

to KFAC (training with a second-order method). This is intuitive as more frequently used routines have likely enjoyed more performance optimization efforts.

Impact of TN simplifications: While general convolutions remain unaffected (Figure E15d), mixed dense, dense, and down-sampling convolutions consistently enjoy significant run time improvements when applying the transformations of §4 (Figures E15a to E15c). As an example, we show the performance comparison for the dense convolutions in Figure 6: The performance ratio’s median between TN and highly specialized forward and input VJP is close to 1, which means both require almost the same time. In the median, the TN even outperforms PyTorch’s highly optimized weight VJP, also for down-sampling convolutions (Figure E18). For KFC, the median performance ratios are well below 1 for dense, mixed dense, and sub-sampling convolutions (Figure E19).

KFAC-reduce: For all convolution types, the TN implementation achieves its largest improvements for $\hat{\Omega}$ and consistently outperforms the PyTorch implementation in the median when simplifications are enabled (Figure E20). This stems from the explicit access to the connectivity pattern: The default implementation unfolds the input, takes the row-average, then forms the outer product. The TN does not need to build up $[\mathbf{X}]$ in memory and instead averages the index pattern tensors. This reduces peak memory and run time. We observe performance ratios of up to 0.22 x which corresponds to a speed-up of roughly 4.5 x (Table E8). This significantly reduces the cost of a second-order optimizer based on KFAC-reduce, for which computing (and inverting) the Kronecker factors adds most overhead⁷.

5.2 RANDOMIZED AUTODIFF VIA APPROXIMATE TENSOR CONTRACTION

CRS is an interesting alternative to gradient checkpointing [25] to lower memory consumption of backpropagation [49; 10; 1]. We focus on unbiased gradient approximations by applying the exact forward pass, and CRS when computing the weight VJP, which requires storing a sub-tensor of \mathbf{X} .

For convolutions, the approximations of existing work are somewhat limited. Adelman et al. [1] restrict to sampling \mathbf{X} along c_{in} , which eliminates the gradient of many filters as the index is part of the output. The randomized gradient would thus only train a sub-tensor of the kernel per step. Oktay et al. [49]; Chen et al. [10] apply unstructured dropout to \mathbf{X} , store it in sparse form, and restore the sparsified tensor during the backward pass. This reduces memory, but does not reduce computation.

The TN view is more flexible and can tackle spatial dimensions with CRS. This reduces memory to the same extent, but also run time due to fewer contractions. Importantly, it does not zero out the gradient signal for entire filters. In Figure 7 we compare the gradient approximation errors of channel and spatial sub-sampling. For the same memory reduction, spatial sub-sampling yields a smaller approximation error on both real and randomly generated data. E.g., instead of keeping 75 % of channels, we can achieve the same approximation quality using only 35 % of pixels.

6 RELATED WORK

Structured convolutions: We use the TN formulation of convolution from Hayashi et al. [27] whose focus lies on connecting factorizations of the kernel to existing structured convolutions (depth-wise separable [29; 58], factored [66], bottleneck [28], flattened/CP decomposed, low-rank

⁷Recently, [53] showed that using only the input-based factor (setting $\mathbf{\Gamma} \propto \mathbf{I}$) yields good performance for training deep neural networks. For such methods, computing (and inverting) $\mathbf{\Omega}$ represents the main bottleneck.

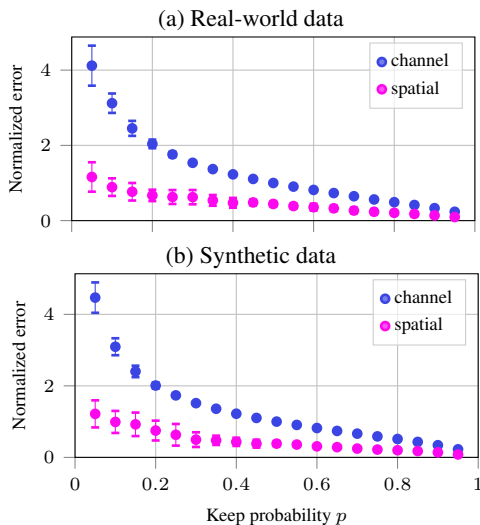


Figure 7: Sub-sampling spatial axes is more effective than sampling channels on both (a) real-world and (b) synthetic data. We take the untrained All-CNN-C [65; 59] for CIFAR-100 with cross-entropy loss, disable dropout, and modify the convolutions to use a fraction p of \mathbf{X} when computing the weight gradient via Bernoulli-CRS. For mini-batches of size 128, we compute the deterministic gradients for all kernels, then flatten and concatenate them into a vector \mathbf{g} ; likewise for its proxy $\hat{\mathbf{g}}$. CRS is described by $(p_{c_{in}}, p_{i_1}, p_{i_2})$, the keep rates along the channel and spatial dimensions. We compare **channel** and **spatial** sampling with same memory reduction, i.e. $(p, 1, 1)$ and $(1, \sqrt{p}, \sqrt{p})$. To measure approximation quality, we use the normalized residual norm $\|\mathbf{g} - \hat{\mathbf{g}}\|_2 / \|\mathbf{g}\|_2$ and report mean and standard deviation of 10 different model and batch initializations.

filter [64; 55; 67]) and explore new factorizations. Our work focuses on operations related to convolutions, diagram manipulations, the index pattern structure, and the performance/flexibility of TNs. Structured convolutions integrate seamlessly with our derivations by swapping the kernel with its factorized diagram.

Higher-order autodiff: ML frameworks prioritize differentiating scalar-valued objectives once. A recent line of works [36; 37; 42] developed a tensor calculus framework for computing (higher-order) derivatives of matrix/tensor-valued functions, along with compilation techniques based on linear algebra and common sub-expression elimination (CSE). By phrasing convolution as tensor multiplication, we allow it to be integrated into such frameworks and make it amenable to their optimizations. Our convolution-specific simplifications complement existing techniques.

7 CONCLUSION

We proposed using tensor networks (TNs), a diagrammatic representation of tensor multiplications, to simplify the analysis and provide white-box implementations of convolutions, as well as related routines for autodiff and approximation of second-order information. We illustrated their elegance and expressiveness to apply function transformations (differentiation, batching) and partial operand access (diagonal extraction) by simple graphical manipulations. Concretely, we derived the diagrams of the above operations, supporting all hyper-parameters of convolution, features like channel groups and batching, and generalization to arbitrary dimensions. TNs enable automated performance optimization via contraction tree search, symbolic simplification, and distribution through a single interface (`einsum`). We extended those techniques by convolution-specific simplifications based on structure in the connectivity pattern and demonstrated their effectiveness to speed-up computations.

We believe that TNs are a versatile tool to simplify the analysis of convolutions and open up new algorithmic possibilities due to their simplicity and flexibility, while offering abstractions for automated performance optimization. Our results motivate their application to efficient approximation of higher-order information (up to 4.5 x speedup on a recently proposed KFAC variant) and randomized autodiff with structured dropout to reduce cost. We look forward to exploring those, among others, in more detail in future work.

ACKNOWLEDGMENTS

The author would like to thank Luca Thiede for providing feedback to the manuscript.

REFERENCES

- [1] Menachem Adelman, Kfir Levy, Ido Hakimi, and Mark Silberstein. Faster neural network training with approximate tensor operations. In *Advances in Neural Information Processing Systems (NeurIPS)*, 2021.
- [2] Sanjeev Arora, Simon S Du, Wei Hu, Zhiyuan Li, Russ R Salakhutdinov, and Ruosong Wang. On exact computation with an infinitely wide neural net. *Advances in neural information processing systems (NeurIPS)*, 2019.
- [3] Achraf Bahamou, Donald Goldfarb, and Yi Ren. A mini-block fisher method for deep neural networks. In *International Conference on Artificial Intelligence and Statistics (AISTATS)*, 2023.
- [4] Suzanna Becker and Yann Lecun. Improving the convergence of back-propagation learning with second-order methods. 1989.
- [5] Jacob Biamonte and Ville Bergholm. Tensor networks in a nutshell, 2017.
- [6] Aleksandar Botev, Hippolyt Ritter, and David Barber. Practical Gauss-Newton optimisation for deep learning. In *International Conference on Machine Learning (ICML)*, 2017.
- [7] James Bradbury, Roy Frostig, Peter Hawkins, Matthew James Johnson, Chris Leary, Dougal Maclaurin, and Skye Wanderman-Milne. JAX: composable transformations of Python+NumPy programs, 2018.
- [8] Jacob C Bridgeman and Christopher T Chubb. Hand-waving and interpretive dance: an introductory course on tensor networks. *Journal of Physics A: Mathematical and theoretical*, 2017.
- [9] Kumar Chellapilla, Sidd Puri, and Patrice Simard. High performance convolutional neural networks for document processing. In *International Workshop on Frontiers in Handwriting Recognition*, 2006.
- [10] Joya Chen, Kai Xu, Yuhui Wang, Yifei Cheng, and Angela Yao. DropIT: Dropping intermediate tensors for memory-efficient DNN training. In *International Conference on Learning Representations (ICLR)*, 2023.
- [11] Yinpeng Chen, Xiyang Dai, Mengchen Liu, Dongdong Chen, Lu Yuan, and Zicheng Liu. Dynamic convolution: Attention over convolution kernels. In *IEEE/CVF conference on computer vision and pattern recognition (CVPR)*, 2020.
- [12] The cuQuantum development team. cuQuantum SDK: A high-performance library for accelerating quantum information science, 2023.
- [13] Carsten Damm, Markus Holzer, and Pierre McKenzie. The complexity of tensor calculus. *computational complexity*, 2002.
- [14] Felix Dangel. unfoldNd: (n=1,2,3)-dimensional unfold (im2col) and fold (col2im) in pytorch, 2021.
- [15] Felix Dangel, Stefan Harmeling, and Philipp Hennig. Modular block-diagonal curvature approximations for feedforward architectures. In *International Conference on Artificial Intelligence and Statistics (AISTATS)*, 2020.
- [16] Felix Dangel, Frederik Kunstner, and Philipp Hennig. BackPACK: Packing more into backprop. In *International Conference on Learning Representations (ICLR)*, 2020.
- [17] Felix Dangel, Lukas Tatzel, and Philipp Hennig. ViViT: Curvature access through the generalized gauss-newton’s low-rank structure. *Transactions on Machine Learning Research (TMLR)*, 2022.
- [18] Felix Julius Dangel. Backpropagation beyond the gradient. 2023.
- [19] Erik Daxberger, Agustinus Kristiadi, Alexander Immer, Runa Eschenhagen, Matthias Bauer, and Philipp Hennig. Laplace redux - effortless bayesian deep learning. In *Advances in Neural Information Processing Systems (NeurIPS)*, 2021.
- [20] Vincent Dumoulin and Francesco Visin. A guide to convolution arithmetic for deep learning. 2016.
- [21] Mohamed Elsayed and A. Rupam Mahmood. HesScale: Scalable computation of hessian diagonals. 2023.
- [22] Runa Eschenhagen. Kronecker-factored approximate curvature for linear weight-sharing layers. 2022.
- [23] Donald Goldfarb, Yi Ren, and Achraf Bahamou. Practical quasi-newton methods for training deep neural networks, 2021.
- [24] Johnnie Gray and Stefanos Kourtis. Hyper-optimized tensor network contraction. *Quantum*, 2021.

-
- [25] Andreas Griewank and Andrea Walther. *Evaluating derivatives: principles and techniques of algorithmic differentiation*. SIAM, 2008.
- [26] Roger Grosse and James Martens. A kronecker-factored approximate Fisher matrix for convolution layers. In *International Conference on Machine Learning (ICML)*, 2016.
- [27] Kohei Hayashi, Taiki Yamaguchi, Yohei Sugawara, and Shin-ichi Maeda. Exploring unexplored tensor network decompositions for convolutional neural networks. In *Advances in Neural Information Processing Systems (NeurIPS)*, 2019.
- [28] Kaiming He, Xiangyu Zhang, Shaoqing Ren, and Jian Sun. Deep residual learning for image recognition. In *IEEE conference on computer vision and pattern recognition (CVPR)*, 2016.
- [29] Andrew G Howard, Menglong Zhu, Bo Chen, Dmitry Kalenichenko, Weijun Wang, Tobias Weyand, Marco Andreetto, and Hartwig Adam. Mobilenets: Efficient convolutional neural networks for mobile vision applications. 2017.
- [30] Jie Hu, Li Shen, and Gang Sun. Squeeze-and-excitation networks. In *IEEE/CVF conference on computer vision and pattern recognition (CVPR)*, 2018.
- [31] Cupjin Huang, Fang Zhang, Michael Newman, Xiaotong Ni, Dawei Ding, Junjie Cai, Xun Gao, Tenghui Wang, Feng Wu, Gengyan Zhang, et al. Efficient parallelization of tensor network contraction for simulating quantum computation. *Nature Computational Science*, 2021.
- [32] Gao Huang, Zhuang Liu, Laurens Van Der Maaten, and Kilian Q Weinberger. Densely connected convolutional networks. In *IEEE conference on computer vision and pattern recognition (CVPR)*, 2017.
- [33] Arthur Jacot, Franck Gabriel, and Clément Hongler. Neural tangent kernel: Convergence and generalization in neural networks, 2020.
- [34] Stanislaw Jastrzebski, Maciej Szymczak, Stanislav Fort, Devansh Arpit, Jacek Tabor, Kyunghyun Cho*, and Krzysztof Geras*. The break-even point on optimization trajectories of deep neural networks. In *International Conference on Learning Representations (ICLR)*, 2020.
- [35] Alex Krizhevsky, Ilya Sutskever, and Geoffrey E. Hinton. Imagenet classification with deep convolutional neural networks. In *Advances in Neural Information Processing Systems (NeurIPS)*, 2012.
- [36] Sören Laue, Matthias Mitterreiter, and Joachim Giesen. Computing higher order derivatives of matrix and tensor expressions. *Advances in Neural Information Processing Systems (NeurIPS)*, 2018.
- [37] Sören Laue, Matthias Mitterreiter, and Joachim Giesen. A simple and efficient tensor calculus. In *AAAI Conference on Artificial Intelligence*, 2020.
- [38] Y. LeCun, B. Boser, J. S. Denker, D. Henderson, R. E. Howard, W. Hubbard, and L. D. Jackel. Backpropagation applied to handwritten zip code recognition. *Neural Computation*, 1989.
- [39] Chao Li, Aojun Zhou, and Anbang Yao. Omni-dimensional dynamic convolution. In *International Conference on Learning Representations (ICLR)*, 2022.
- [40] Shiwei Liu, Tianlong Chen, Xiaohan Chen, Xuxi Chen, Qiao Xiao, Boqian Wu, Tommi Kärkkäinen, Mykola Pechenizkiy, Decebal Constantin Mocanu, and Zhangyang Wang. More convnets in the 2020s: Scaling up kernels beyond 51x51 using sparsity. In *International Conference on Learning Representations (ICLR)*, 2023.
- [41] Zhuang Liu, Hanzi Mao, Chao-Yuan Wu, Christoph Feichtenhofer, Trevor Darrell, and Saining Xie. A convnet for the 2020s. *IEEE/CVF Conference on Computer Vision and Pattern Recognition (CVPR)*, 2022.
- [42] Linjian Ma, Jiayu Ye, and Edgar Solomonik. Autohoot: Automatic high-order optimization for tensors. In *International Conference on Parallel Architectures and Compilation Techniques (PACT)*, 2020.
- [43] J. R. Magnus and H. Neudecker. *Matrix Differential Calculus with Applications in Statistics and Econometrics*. Probabilistics and Statistics. 1999.
- [44] James Martens. Deep learning via Hessian-free optimization. In *International Conference on Machine Learning (ICML)*, 2010.
- [45] James Martens. New insights and perspectives on the natural gradient method, 2020.
- [46] James Martens and Roger Grosse. Optimizing neural networks with Kronecker-factored approximate curvature. In *International Conference on Machine Learning (ICML)*, 2015.

-
- [47] James Martens, Jimmy Ba, and Matt Johnson. Kronecker-factored curvature approximations for recurrent neural networks. In *International Conference on Learning Representations (ICLR)*, 2018.
- [48] Roman Novak, Jascha Sohl-Dickstein, and Samuel S. Schoenholz. Fast finite width neural tangent kernel. In *International Conference on Machine Learning (ICML)*, 2022.
- [49] Deniz Oktay, Nick McGreivy, Joshua Aduol, Alex Beatson, and Ryan P Adams. Randomized automatic differentiation. In *International Conference on Learning Representations (ICLR)*, 2021.
- [50] Kazuki Osawa, Satoki Ishikawa, Rio Yokota, Shigang Li, and Torsten Hoefer. Asdl: A unified interface for gradient preconditioning in pytorch, 2023.
- [51] Adam Paszke, Sam Gross, Francisco Massa, Adam Lerer, James Bradbury, Gregory Chanan, Trevor Killeen, Zeming Lin, Natalia Gimelshein, Luca Antiga, Alban Desmaison, Andreas Kopf, Edward Yang, Zachary DeVito, Martin Raison, Alykhan Tejani, Sasank Chilamkurthy, Benoit Steiner, Lu Fang, Junjie Bai, and Soumith Chintala. PyTorch: An imperative style, high-performance deep learning library. In *Advances in Neural Information Processing Systems (NeurIPS)*. 2019.
- [52] Roger Penrose. Applications of negative dimensional tensors. *Combinatorial Mathematics and its Applications*, 1971.
- [53] Felix Petersen, Tobias Sutter, Christian Borgelt, Dongsung Huh, Hilde Kuehne, Yuekai Sun, and Oliver Deussen. ISAAC newton: Input-based approximate curvature for newton’s method. In *International Conference on Learning Representations (ICLR)*, 2023.
- [54] Yi Ren, Achraf Bahamou, and Donald Goldfarb. Kronecker-factored quasi-newton methods for deep learning, 2022.
- [55] Roberto Rigamonti, Amos Sironi, Vincent Lepetit, and Pascal Fua. Learning separable filters. In *IEEE Conference on Computer Vision and Pattern Recognition (CVPR)*, 2013.
- [56] Gaspar Rochette, Andre Manoel, and Eric W. Tramel. Efficient per-example gradient computations in convolutional neural networks, 2019.
- [57] Alex Rogozhnikov. Einops: Clear and reliable tensor manipulations with einstein-like notation. In *International Conference on Learning Representations (ICLR)*, 2022.
- [58] Mark Sandler, Andrew Howard, Menglong Zhu, Andrey Zhmoginov, and Liang-Chieh Chen. Mobilenetv2: Inverted residuals and linear bottlenecks. In *IEEE conference on computer vision and pattern recognition (CVPR)*, 2018.
- [59] Frank Schneider, Lukas Balles, and Philipp Hennig. DeepOBS: A deep learning optimizer benchmark suite. In *International Conference on Learning Representations (ICLR)*, 2019.
- [60] Nicol N Schraudolph. Fast curvature matrix-vector products for second-order gradient descent. *Neural computation*, 2002.
- [61] Sidak Pal Singh, Gregor Bachmann, and Thomas Hofmann. Analytic insights into structure and rank of neural network hessian maps. *Advances in Neural Information Processing Systems (NeurIPS)*, 2021.
- [62] Sidak Pal Singh, Thomas Hofmann, and Bernhard Schölkopf. The hessian perspective into the nature of convolutional neural networks. 2023.
- [63] Daniel G. A. Smith and Johnnie Gray. opt_einsum - A python package for optimizing contraction order for einsum-like expressions. *Journal of Open Source Software (JOSS)*, 2018.
- [64] Steven W. Smith. The scientist and engineer’s guide to digital signal processing. 1997.
- [65] Jost Tobias Springenberg, Alexey Dosovitskiy, Thomas Brox, and Martin Riedmiller. Striving for simplicity: The all convolutional net, 2015.
- [66] Christian Szegedy, Vincent Vanhoucke, Sergey Ioffe, Jon Shlens, and Zbigniew Wojna. Rethinking the inception architecture for computer vision. In *IEEE conference on computer vision and pattern recognition (CVPR)*, 2016.
- [67] Cheng Tai, Tong Xiao, Yi Zhang, Xiaogang Wang, et al. Convolutional neural networks with low-rank regularization. 2015.

-
- [68] Ashish Vaswani, Noam Shazeer, Niki Parmar, Jakob Uszkoreit, Llion Jones, Aidan N Gomez, Łukasz Kaiser, and Illia Polosukhin. Attention is all you need. In *Advances in Neural Information Processing Systems (NeurIPS)*, 2017.
- [69] Saining Xie, Ross Girshick, Piotr Dollár, Zhuowen Tu, and Kaiming He. Aggregated residual transformations for deep neural networks. In *IEEE conference on computer vision and pattern recognition (CVPR)*, 2017.
- [70] Brandon Yang, Gabriel Bender, Quoc V Le, and Jiquan Ngiam. Condconv: Conditionally parameterized convolutions for efficient inference. *Advances in Neural Information Processing Systems (NeurIPS)*, 2019.
- [71] Sergey Zagoruyko and Nikos Komodakis. Wide residual networks. 2016.
- [72] Fang Zhang. A parallel tensor network contraction algorithm and its applications in quantum computation. 2020.

CONVOLUTIONS THROUGH THE LENS OF TENSOR NETWORKS (SUPPLEMENTARY MATERIAL)

In this supplementary material we provide additional details of the main text. Overview:

| | | |
|----------|---|-----------|
| A | Limitations | 16 |
| B | Visual Tour of Tensor Network Operations for Convolutions | 16 |
| B.1 | Convolution & First-order Derivatives | 16 |
| B.2 | Exact Second-order Information | 16 |
| B.3 | Kronecker-factored Approximate Curvature (KFAC) | 19 |
| B.4 | Further Operations & Extensive Overview | 19 |
| C | Implementation Details | 23 |
| C.1 | Index Pattern Tensor Computation for Convolutions | 23 |
| C.2 | Index Pattern Tensor for Standalone Transpose Convolution | 23 |
| C.3 | Additional Index Pattern Properties | 23 |
| D | Convolution Layer Hyper-parameter Analysis | 24 |
| E | Performance Evaluation Details (GPU) | 27 |
| E.1 | Protocol & Overview | 27 |
| E.2 | Forward Pass | 29 |
| E.3 | Input VJP | 32 |
| E.4 | Weight VJP | 35 |
| E.5 | KFC Factor (KFAC-expand) | 38 |
| E.6 | KFAC-reduce Factor | 41 |
| F | Miscellaneous | 44 |
| F.1 | Example: Associativity of Tensor Multiplication | 44 |

A LIMITATIONS

Here we comment on limitations on our approach.

No common sub-expression elimination (CSE): Our implementation relies on `opt_einsum` which focuses on contraction order optimization. This optimization is efficient when all operands are different. However, with multiple occurrences of operands, computing shared sub-expressions might be an advantageous optimization approach which `opt_einsum` does not account for. The second-order quantity TNs from §3.3 and 3.4 contain such sub-expressions, for instance $[\mathbf{X}]$ and $\mathbf{1}_{O_1 O_2}^\top [\mathbf{X}]$ in KFAC-expand and KFAC-reduce, and $\mathbf{S}^{(W)}$ in the GGN quantities from Figure 4. The efficiency of CSE depends on how costly the shared tensor is to compute. For instance, computing $\mathbf{S}^{(W)}$ is expensive and therefore CSE is the more suitable optimization technique. For the input-based Kronecker factors which require the unfolded input, either contraction path optimization or CSE might be better. This is because the optimal contraction order may not correspond to 2x input unfolding and exhibit more parallelism which may lead to faster run times on a GPU. It would be interesting to integrate CSE into the contraction path optimization and develop a heuristic to choose a contraction path, for instance based on a weighted sum of FLOPs and memory.

No index slicing: We mention index slicing as a technique to reduce peak memory of, and distribute, TN contractions. However, our implementation does not use index slicing, although there are packages like `cotengra` [24] with an interface similar to `opt_einsum`. We did not experiment with index slicing as our benchmark uses a single GPU and did not encounter out-of-memory errors. Still, we mention this technique, as, in combination with CSE, it could automatically reduce peak memory of the GGN quantities from Figure 4 which suffer from high memory requirements.

B VISUAL TOUR OF TENSOR NETWORK OPERATIONS FOR CONVOLUTIONS

Here, we extend the presented operations with a batch axis and allow for grouped convolutions.

B.1 CONVOLUTION & FIRST-ORDER DERIVATIVES

Adding a batch dimension (vmap-ing): Adding a batch axis to all presented operations is trivial. We only need to add an additional leg to the batched tensors, and connect these legs via element-wise or inner multiplication, depending on whether the result tensor is batched or not.

Grouped convolutions: Grouped convolutions were originally proposed by Krizhevsky et al. [35] and allow for parallelizing, distributing, and reducing the parameters of the convolution operation. They split C_{in} input channels into G groups of size $\tilde{C}_{\text{in}} := C_{\text{in}}/G$, then perform independent convolutions per group, each producing $\tilde{C}_{\text{out}} := C_{\text{out}}/G$ output channels which are concatenated in the output. Each group uses a kernel \mathbf{W}_g of size $\tilde{C}_{\text{out}} \times \tilde{C}_{\text{in}} \times K_1 \times K_2$. These kernels are stacked into a single tensor $\mathbf{W} \in \mathbb{R}^{C_{\text{out}}, \tilde{C}_{\text{in}}, K_1, K_2}$ such that $[\mathbf{W}]_{(g, :, :, :)} = \mathbf{W}_g$. To support groups, we thus decompose the channel indices into $c_{\text{in}} := (\tilde{c}_{\text{in}}, g)$ and $c_{\text{out}} := (\tilde{c}_{\text{out}}, g)$. For the forward pass this yields the grouped convolution (without bias)

$$Y_{(g, \tilde{c}_{\text{out}}), o_1, o_2} = \sum_{i_1, i_2, \tilde{c}_{\text{in}}, k_1, k_2} X_{(g, \tilde{c}_{\text{in}}), i_1, i_2} \Pi_{i_1, o_1, k_1}^{(1)} \Pi_{i_2, o_2, k_2}^{(2)} W_{(g, \tilde{c}_{\text{out}}), c_{\text{in}}, k_1, k_2}. \quad (\text{B10})$$

Figure B8a shows the batched version of Equation (B10) as TN. Applying the differentiation rule from §3 leads to the Jacobians and VJPs shown in the remaining panels of Figure B8.

B.2 EXACT SECOND-ORDER INFORMATION

In Figure B11 we show the TNs for the GGN diagonal and the GGN Gram matrix (empirical NTK matrix) from Figure 4 extended by channel groups and a batch axis.

Diagonal block extraction: Combined with index un-grouping, diagonal extraction generalizes to larger blocks: Let $\mathbf{A} \in \mathbb{R}^{KI \times KJ}$ be a matrix of K horizontally and vertically concatenated blocks

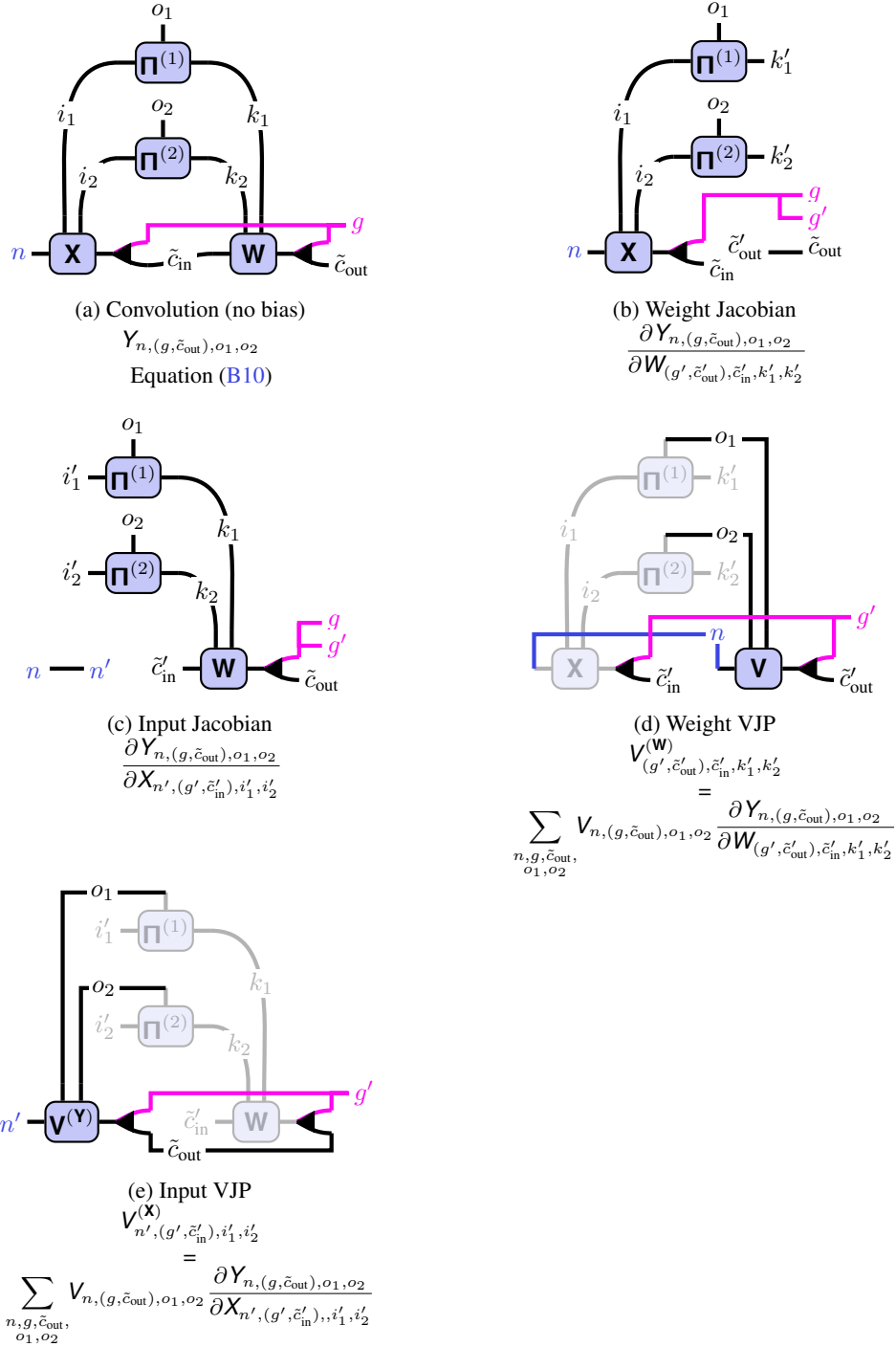
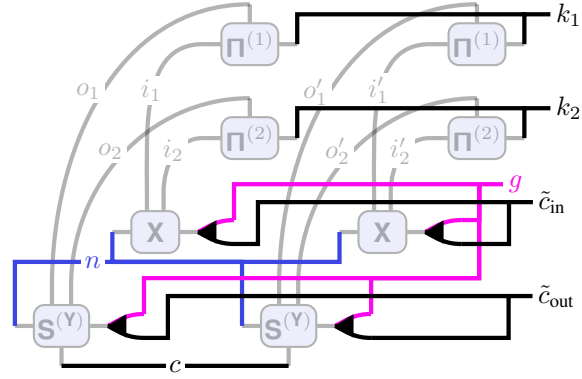


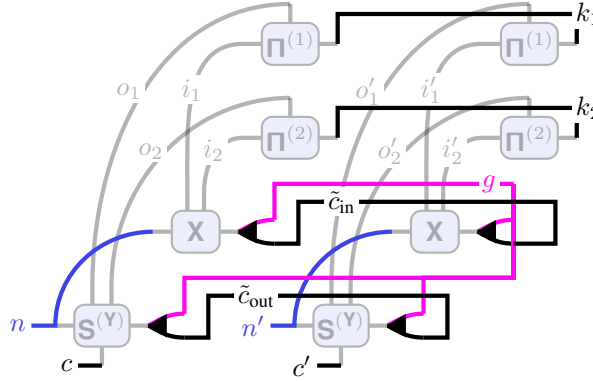
Figure B8: TNs of the (a) forward pass, (b, c) Jacobians, and (d, e) VJPs with **batch axis** and **channel groups**. They generalize Figures 1 to 3 from the main text. For the VJPs, the Jacobians are shaded.

$\mathbf{A}^{(k_1,k_2)} \in \mathbb{R}^{I \times J}$, $k_i = 1 \dots, K$. We can extract the diagonal blocks by restoring the sub-structure, then taking the diagonal along the K -dimensional index,

$$k_l^j = \left\{ \mathbf{A}^{(k,k)} \right\} - j = \begin{matrix} & & k & & \\ & & \swarrow & & \searrow \\ & & (k,i) & \mathbf{A} & (k,j) \\ & & \swarrow & & \searrow \\ & & i & & j \end{matrix}$$



(a) GGN diagonal



(b) GGN Gram matrix (empirical NTK)

Figure B9: TNs of (a) the GGN diagonal and (b) the GGN Gram matrix with **batching** and **channel groups**. They extend Figures 4b and 4c from the main text.

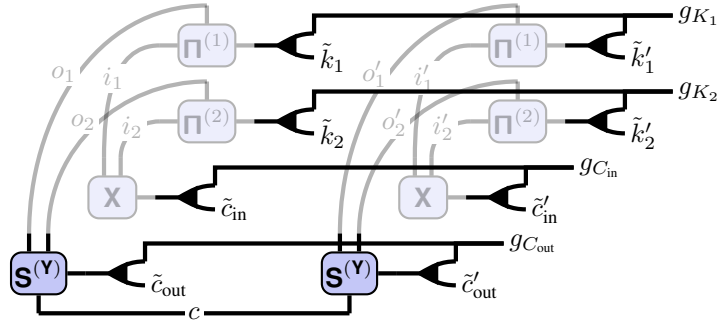


Figure B10: TN of a GGN mini-block diagonal without batching and channel groups.

We can apply this procedure to the GGN from Figure 4a. Assume we want to divide the output channel, input channel, and spatial dimensions into $G_{C_{out}}, G_{C_{in}}, G_{K_1}, G_{K_2}$ groups. A group will thus be indexed with a tuple $(g_{C_{out}}, g_{C_{in}}, g_{K_1}, g_{K_2})$ and the corresponding GGN block will be of dimension $C_{out}/G_{C_{out}} \times C_{in}/G_{C_{in}} \times K_1/G_{K_1} \times K_2/G_{K_2} \times C_{out}/G_{C_{out}} \times C_{in}/G_{C_{in}} \times K_1/G_{K_1} \times K_2/G_{K_2}$ and correspond to the GGN for $[\mathbf{W}]_{(g_{C_{out}}, :), (g_{C_{in}}, :), (g_{K_1}, :), (g_{K_2}, :)}$. This process of un-grouping the output dimensions, then taking the diagonal along the group indices, is illustrated in Figure B10. Note that if we choose $G_{C_{out}} = C_{out}, G_{C_{in}} = C_{in}, G_{K_1} = K_1, G_{K_2} = K_2$, each block will be a single number and hence we recover the GGN diagonal from Figure 4b. If instead we $G_{C_{out}} = G_{C_{in}} G_{K_1} G_{K_2} = 1$, we obtain the full GGN from Figure 4a. The outlined schemes allows to extract mini-blocks of arbitrary size along the diagonal (subject to the total dimension).

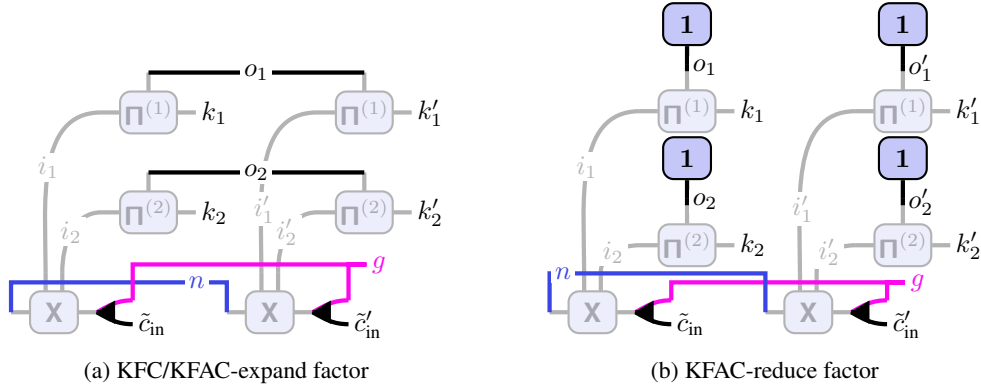


Figure B11: TN diagrams of input-based factors in Kronecker approximations of the GGN for convolutions with **batching** and **channel groups**. They extend Figure 5 from the main text.

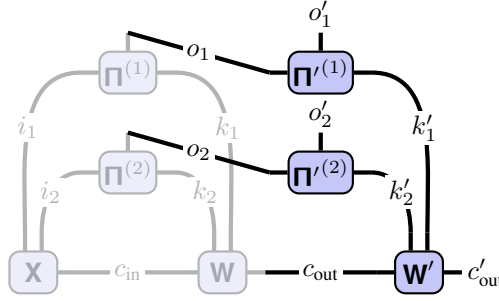


Figure B12: TN of two consecutive convolutions without groups and without batch axis.

B.3 KRONECKER-FACTORED APPROXIMATE CURVATURE (KFAC)

We were unable to find a definition of KFAC for grouped convolutions. Hence, we derive it here and present the TN diagrams. We use the perspective that grouped convolutions are independent convolutions over channel groups which are then concatenated. For each of those convolutions, we can then apply established the KFAC approximation for convolutions without groups. For a group g we have the kernel $\mathbf{W}_g = [\mathbf{W}]_{(g,:),:,,:}$ and the unfolded input of its associated input channels, $[\mathbf{X}_g] = [\mathbf{X}]_{(g,:),:,,:} = [[\mathbf{X}]_{(g,:),:,,:}]$ (or $[\mathbf{X}_{n,g}] = [\mathbf{X}_n]_{(g,:),:,,:} = [[\mathbf{X}_n]_{(g,:),:,,:}]$ in the batched setting).

KFC/KFAC-expand grouped convolutions: Applying the regular KFC approximation to the kernel of group g , this yields the Fisher approximation $\Omega_g \otimes \Gamma_g$ with $\Gamma_g \in \mathbb{R}^{\tilde{C}_{\text{out}} \times \tilde{C}_{\text{out}}}$ and $\Omega_g = 1/N \sum_{n=1}^N [\mathbf{X}_{n,g}]^\top [\mathbf{X}_{n,g}] \in \mathbb{R}^{\tilde{C}_{\text{in}} K_1 K_2 \times \tilde{C}_{\text{in}} K_1 K_2}$ where $\mathbf{X}_{n,g}$ is the input tensor for sample n and group g (remember the index structure $\mathbf{X}_{n,(g,\tilde{c}_{\text{in}}),i_1,i_2}$). Figure B11a shows the diagram for $\{N \Omega_g\}_{g=1}^G$.

KFAC-reduce for grouped convolutions: Proceeding in the same way, but using the unfolded input averaged over output locations, we obtain the Fisher approximation $\hat{\Omega}_g \otimes \hat{\Gamma}_g$ with $\hat{\Gamma}_g \in \mathbb{R}^{\tilde{C}_{\text{out}} \times \tilde{C}_{\text{out}}}$ and $\hat{\Omega}_g = 1/N (O_1 O_2)^2 \sum_{n=1}^N (\mathbf{1}_{O_1 O_2}^\top [\mathbf{X}_{n,g}])^\top \mathbf{1}_{O_1 O_2}^\top [\mathbf{X}_{n,g}] \in \mathbb{R}^{\tilde{C}_{\text{in}} K_1 K_2 \times \tilde{C}_{\text{in}} K_1 K_2}$ for the kernel of group g . Figure B11b shows the diagram for $\{N (O_1 O_2)^2 \hat{\Omega}_g\}_{g=1}^G$.

B.4 FURTHER OPERATIONS & EXTENSIVE OVERVIEW

Consecutive convolutions: We can chain two, or more, convolutions into a single TN diagram (Figure B12) to obtain a deep linear CNN [62] similar to deep linear networks which are popular for analytical studies.

Convolution weight/input JVPs: In the main text, we derived the Jacobians of convolution (§3.1) which can be used to derive the JVPs. A JVP propagates perturbations $\mathbf{V}^{(\mathbf{W})} \in \mathbb{R}^{C_{\text{out}} \times C_{\text{in}} \times K_1 \times K_2}$ and $\mathbf{V}^{(\mathbf{X})} \in \mathbb{R}^{C_{\text{in}} \times I_1 \times I_2}$ in the input space to perturbations in the output space by contracting the perturbation with the Jacobian. See Table B2 for the general einsum expressions.

Batched convolution weight VJP: To obtain per-sample gradients, the weight VJP must be carried out without summing over the batch axis which amounts to keeping the batch index in the output index tuple.

VJPs and JVPs of im2col: With the TN differentiation technique described in §3.1 we can compute the Jacobian of the unfolding operation, then contract it with perturbations $V^{(\mathbf{X})} \in \mathbb{R}^{C_{\text{in}} \times K_1 \times K_2}$ in input space to obtain the JVP, or with perturbations $V^{(\mathbb{I}\mathbf{X})} \in \mathbb{R}^{O_1 O_2 \times C_{\text{in}} K_1 K_2}$ to obtain the VJP.

Approximate Hessian diagonals (HesScale/BL89): Becker & Lecun [4]; Elsayed & Mahmood [21] proposed approximate procedures for the Hessian diagonal which cost roughly a gradient. They can be understood as modifications of the Hessian backpropagation equations from Dangel et al. [15].

Consider a layer with input \mathbf{x} , output \mathbf{y} , and weights \mathbf{w} inside a sequential feedforward neural network (for a convolutional layer, these correspond to the flattened input, output, and kernel). To compute per-layer Hessians of a loss ℓ , each layer backpropagates its incoming Hessian $\nabla_{\mathbf{y}}^2 \ell$ according to [15]

$$\begin{aligned}\nabla_{\mathbf{x}}^2 \ell &= (\mathbf{J}_{\mathbf{x}\mathbf{y}})^\top \nabla_{\mathbf{y}}^2 \ell(\mathbf{J}_{\mathbf{x}\mathbf{y}}) + \sum_i \frac{\partial \ell}{\partial y_i} \nabla_{\mathbf{x}}^2 y_i, \\ \nabla_{\mathbf{w}}^2 \ell &= (\mathbf{J}_{\mathbf{w}\mathbf{y}})^\top \nabla_{\mathbf{y}}^2 \ell(\mathbf{J}_{\mathbf{w}\mathbf{y}}) + \sum_i \frac{\partial \ell}{\partial y_i} \nabla_{\mathbf{w}}^2 y_i.\end{aligned}\tag{B11}$$

The scheme of [4; 21] imposes diagonal structure on the backpropagated quantity. A layer receives a backpropagated diagonal $\mathbf{d}^{(\mathbf{y})}$ such that $\text{diag}(\mathbf{d}^{(\mathbf{y})}) \approx \nabla_{\mathbf{y}}^2 \ell$, and backpropagates it according to Equation (B11), but with a post-processing step to obtain a diagonal backpropagated quantity,

$$\begin{aligned}\mathbf{d}^{(\mathbf{x})} &= \text{diag} \left((\mathbf{J}_{\mathbf{x}\mathbf{y}})^\top \text{diag}(\mathbf{d}^{(\mathbf{y})}) (\mathbf{J}_{\mathbf{x}\mathbf{y}}) \right) + \text{diag} \left(\sum_i \frac{\partial \ell}{\partial y_i} \nabla_{\mathbf{x}}^2 y_i \right), \\ \mathbf{d}^{(\mathbf{w})} &= \text{diag} \left((\mathbf{J}_{\mathbf{w}\mathbf{y}})^\top \text{diag}(\mathbf{d}^{(\mathbf{y})}) (\mathbf{J}_{\mathbf{w}\mathbf{y}}) \right) + \text{diag} \left(\sum_i \frac{\partial \ell}{\partial y_i} \nabla_{\mathbf{w}}^2 y_i \right),\end{aligned}\tag{B12}$$

where $\text{diag}(\mathbf{d}^{(\mathbf{x})}) \approx \nabla_{\mathbf{x}}^2 \ell$ and $\text{diag}(\mathbf{d}^{(\mathbf{w})}) \approx \nabla_{\mathbf{w}}^2 \ell$ is an approximation to the Hessian diagonal.

For convolutional layers, which are linear in the input and weight, the second summands are zero due to $\nabla_{\mathbf{x}}^2 y_i = \mathbf{0} = \nabla_{\mathbf{w}}^2 y_i$. The first terms of Equation (B12) require (i) embedding a diagonal vector into a matrix, (ii) applying MJPs and JMPs, and (iii) extracting the result’s diagonal. Those can be expressed as a single TN. We show the diagrams in Figure B13, using tensors rather than their flattened versions, that is $(\mathbf{x}, \mathbf{y}, \mathbf{w}, \mathbf{d}^{(\mathbf{x})}, \mathbf{d}^{(\mathbf{y})}, \mathbf{d}^{(\mathbf{w})}) \rightarrow (\mathbf{X}, \mathbf{Y}, \mathbf{W}, \mathbf{D}^{(\mathbf{X})}, \mathbf{D}^{(\mathbf{Y})}, \mathbf{D}^{(\mathbf{W})})$.

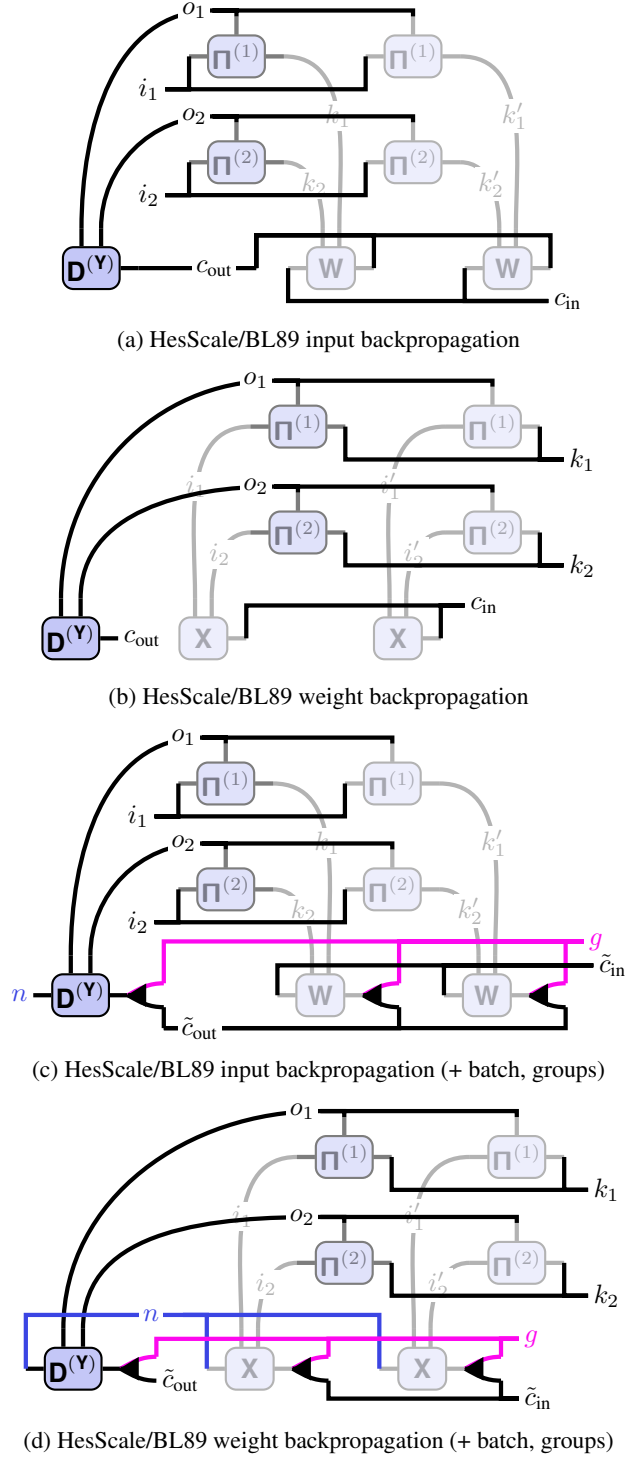


Figure B13: TN diagrams for HesScale/BL89 [4; 21] backpropagations through convolutional layers to approximate the Hessian diagonals $\mathbf{D}^{(X)}$, $\mathbf{D}^{(W)}$. JMPs and MJPs are shaded. (a, b) show the simple versions without batching and without channel groups. (c, d) include **batching** and **channel groups**.

Table B2: Extensive list of convolution and related operations (extension from Table 1 in the main text). All operations consider two spatial dimensions and support batching and channel groups. Generalization to other dimensions follow by introducing more spatial indices i_3, o_3, \dots and kernel indices k_3, \dots .

| Operation | Operands | Contraction string (einops [57] convention) |
|--|--|--|
| Convolution (no bias) [27] | $\mathbf{X}, \Pi^{(1)}, \Pi^{(2)}, \mathbf{W}$ | "n (g c.in) i1 i2, i1 o1 k1, i2 o2 k2, (g c.out) c.in k1 k2 -> n (g c.out) o1 o2" |
| Unfolded input (im2col) | $\mathbf{X}, \Pi^{(1)}, \Pi^{(2)}$ | "n c.in i1 i2, i1 o1 k1, i2 o2 k2 -> n (c.in k1 k2) (o1 o2)" |
| Unfolded kernel (Toeplitz) | $\Pi^{(1)}, \Pi^{(2)}, \mathbf{W}$ | "i1 o1 k1, i2 o2 k2, c.out c.in k1 k2 -> (c.out o1 o2) (c.in i1 i2)" |
| Convolution weight VJP | $\mathbf{X}, \Pi^{(1)}, \Pi^{(2)}, \mathbf{V}^{(Y)}$ | "n (g c.in) i1 i2, i1 o1 k1, i2 o2 k2, n (g c.out) o1 o2 -> c.out c.in k1 k2" |
| Convolution input VJP (transpose convolution) | $\mathbf{W}, \Pi^{(1)}, \Pi^{(2)}, \mathbf{V}^{(Y)}$ | "(g c.out) c.in k1 k2, i1 o1 k1, i2 o2 k2, n (g c.out) o1 o2 -> n (g c.in) i1 i2" |
| Convolution weight VJP (per-sample/batched) [56] | $\mathbf{X}, \Pi^{(1)}, \Pi^{(2)}, \mathbf{V}^{(Y)}$ | "n (g c.in) i1 i2, i1 o1 k1, i2 o2 k2, n (g c.out) o1 o2 -> n (g c.out) c.in k1 k2" |
| Convolution weight JVP | $\mathbf{X}, \Pi^{(1)}, \Pi^{(2)}, \mathbf{V}^{(W)}$ | "n (g c.in) i1 i2, i1 o1 k1, i2 o2 k2, (g c.out) c.in k1 k2 -> n (g c.out) o1 o2" |
| Convolution input JVP | $\mathbf{W}, \Pi^{(1)}, \Pi^{(2)}, \mathbf{V}^{(X)}$ | "(g c.out) c.in i1 i2, i1 o1 k1, i2 o2 k2, n (g c.in) i1 i2 -> n (g c.out) o1 o2" |
| im2col VJP | $\Pi^{(1)}, \Pi^{(2)}, \mathbf{V}^{(X)}$ | "i1 o1 k1, i2 o2 k2, n (c.in k1 k2) (o1 o2) -> n c.in i1 i2" |
| im2col JVP | $\Pi^{(1)}, \Pi^{(2)}, \mathbf{V}^{(X)}$ | "i1 o1 k1, i2 o2 k2, n c.in i1 i2 -> n (c.in k1 k2) (o1 o2)" |
| KFC/KFAC-expand [26; 22] | $\mathbf{X}, \Pi^{(1)}, \Pi^{(2)}, \mathbf{X}, \Pi^{(1)}, \Pi^{(2)}$ | "n (g c.in) i1 i2, i1 o1 k1, i2 o2 k2, n (g c.in) i1. i2., i1. o1 k1., i2. o2 k2. -> g (c.in k1 k2) (c.in k1. k2.)" |
| KFAC-reduce [22] | $\mathbf{X}, \Pi^{(1)}, \Pi^{(2)}, \mathbf{X}, \Pi^{(1)}, \Pi^{(2)}$ | "n (g c.in) i1 i2, i1 o1 k1, i2 o2 k2, n (g c.in) i1. i2., i1. o1 k1., i2. o2 k2. -> g (c k1 k2) (c. k1. k2.)" |
| GGN Gram/empirical NTK matrix [17; 50; 48] | $\mathbf{X}, \Pi^{(1)}, \Pi^{(2)}, \mathbf{S}^{(Y)}, \mathbf{X}, \Pi^{(1)}, \Pi^{(2)}, \mathbf{S}^{(Y)}$ | "n (g c.in) i1 i2, i1 o1 k1, i2 o2 k2, c n (g c.out) o1 o2, n. (g c.in) i1. i2., i1. o1 k1., i2. o2 k2., c n. (g c.out) o1. o2. -> (c n) (c. n.)" |
| GGN/Fisher diagonal [16; 50] | $\mathbf{X}, \Pi^{(1)}, \Pi^{(2)}, \mathbf{S}^{(Y)}, \mathbf{X}, \Pi^{(1)}, \Pi^{(2)}, \mathbf{S}^{(Y)}$ | "n (g c.in) i1 i2, i1 o1 k1, i2 o2 k2, c n (g c.out) o1 o2, n (g c.in) i1. i2., i1. o1 k1., i2. o2 k2., c n (g c.out) o1. o2. -> (g c.out) c.in k1 k2" |
| GGN/Fisher diagonal (per-sample/batched) | $\mathbf{X}, \Pi^{(1)}, \Pi^{(2)}, \mathbf{S}^{(Y)}, \mathbf{X}, \Pi^{(1)}, \Pi^{(2)}, \mathbf{S}^{(Y)}$ | "n (g c.in) i1 i2, i1 o1 k1, i2 o2 k2, c n (g c.out) o1 o2, n (g c.in) i1. i2., i1. o1 k1., i2. o2 k2., c n (g c.out) o1. o2. -> n (g c.out) c.in k1 k2" |
| Approximate weight Hessian diagonal [4; 21] | $\mathbf{X}, \Pi^{(1)}, \Pi^{(2)}, \mathbf{D}^{(Y)}, \mathbf{X}, \Pi^{(1)}, \Pi^{(2)}$ | "n (g c.in) i1 i2, i1 o1 k1, i2 o2 k2, n (g c.out) o1 o2, n (g c.in) i1. i2., i1. o1 k1., i2. o2 k2 -> (g c.out) c.in k1 k2" |
| Approximate input Hessian diagonal [4; 21] | $\mathbf{W}, \Pi^{(1)}, \Pi^{(2)}, \mathbf{D}^{(Y)}, \mathbf{W}, \Pi^{(1)}, \Pi^{(2)}$ | "(g c.out) c.in k1 k2, i1 o1 k1, i2 o2 k2, n (g c.out) o1 o2, (g c.out) c.in k1. k2., i1 o1 k1., i2 o2 k2. -> n (g c.in) i1 i2" |
| Approximate weight Hessian diagonal (per-sample/batched) | $\mathbf{X}, \Pi^{(1)}, \Pi^{(2)}, \mathbf{D}^{(Y)}, \mathbf{X}, \Pi^{(1)}, \Pi^{(2)}$ | "n (g c.in) i1 i2, i1 o1 k1, i2 o2 k2, n (g c.out) o1 o2, n (g c.in) i1. i2., i1. o1 k1., i2. o2 k2 -> n (g c.out) c.in k1 k2" |

C IMPLEMENTATION DETAILS

Here we present details on the index pattern computation, and additional transformations.

C.1 INDEX PATTERN TENSOR COMPUTATION FOR CONVOLUTIONS

Algorithm C1 lists pseudo-code for the index pattern computation from the convolution hyper-parameters K, S, P, D , and the spatial input dimension I , that is $\mathbf{\Pi}(I, K, S, P, D)$. *Unlike in the main text, we use 0-based indexing which is more common in numerical libraries.* For self-consistency, we re-state the relation of the hyper-parameters to output dimension from [20, Relationship 15],

$$O(I, K, S, P, D) = 1 + \left\lfloor \frac{I + 2P - K - (K - 1)(D - 1)}{S} \right\rfloor. \quad (\text{C13})$$

Algorithm C1 Computing the convolution index pattern tensor $\mathbf{\Pi}$ for a spatial dimension.

Require: Input size $I \in \mathbb{N}^+$, kernel size $K \in \mathbb{N}^+$, stride $S \in \mathbb{N}^+$, padding $P \in \mathbb{N}_0^+$, dilation $D \in \mathbb{N}^+$

```

 $O \leftarrow 1 + \left\lfloor \frac{I + 2P - K - (K - 1)(D - 1)}{S} \right\rfloor$   $\triangleright$  Compute output dimension [20, Relationship 15]
 $\mathbf{\Pi} \leftarrow \mathbf{0}_{I \times O \times K}$   $\triangleright$  Initialize index pattern tensor
for  $o = 0, \dots, O - 1, k = 0, \dots, K - 1$  do  $\triangleright$  Use 0-based indexing!
   $i \leftarrow kD + oS - P$   $\triangleright$  Reconstruct contributing input element
  if  $0 \leq i \leq I - 1$  then  $\triangleright$  Check in bounds
     $\mathbf{\Pi}_{i, o, k} \leftarrow 1$ 
  end if
end for
return Index pattern tensor  $\mathbf{\Pi} \in \{0, 1\}^{I \times O \times K}$ 

```

C.2 INDEX PATTERN TENSOR FOR STANDALONE TRANSPOSE CONVOLUTION

Although a transpose convolution is defined w.r.t. a reference convolution with hyper-parameters K, S, P, D , most libraries offer standalone implementations of transpose convolution. We describe the transpose convolution by its associated convolution, that is as a mapping from $\mathbb{R}^{C_{\text{out}} \times O_1 \times O_2}$ (the convolution's output space) to $\mathbb{R}^{C_{\text{in}} \times I_1 \times I_2}$ (the convolution's input space). For convolution with $S > 1$, we cannot infer I from O, K, S, P, D , as multiple I s map to the same O if $(I + 2P - K - (K - 1)(D - 1)) \bmod S \neq 0$ (see the floor operation in Algorithm C1). We need to either supply I directly, or the remainder

$$A = I - S \left\lfloor \frac{I + 2P - K - (K - 1)(D - 1)}{S} \right\rfloor$$

(often called `output_padding`) to make I unambiguous. Then, we compute

$$I = (O - 1)S - 2P + D(K - 1) + A + 1. \quad (\text{C14})$$

to get $I(O, A)$ and call Algorithm C1 to obtain $\mathbf{\Pi}(I(O, A), K, S, P, D)$.

C.3 ADDITIONAL INDEX PATTERN PROPERTIES

For completeness, we state additional index pattern tensor properties here (using 1-based indexing):

Transformation C4 (Sub-sampling interpretation of stride) *Strided convolutions ($S > 1$) sub-sample non-strided convolutions along the output dimension, ignoring all but every S th output [20]. In other words, $[\mathbf{\Pi}(I, K, S, P, D)]_{i, o, k} = [\mathbf{\Pi}(I, K, 1, P, D)]_{i, 1 + S(o-1), k}$ or, in tensor notation $([\cdot]::S$ denotes slicing with steps of S),*

$$\mathbf{\Pi}(I, K, S, P, D) = [\mathbf{\Pi}(I, K, 1, P, D)]_{::S, :, \cdot}$$

Transformation C5 (Sub-sampling interpretation of dilation) *Dilated convolutions ($D > 1$) with kernel size K sub-sample the kernel of a non-dilated convolution of kernel size $K + (D -$*

$1)(K - 1)$, ignoring all but every D th kernel element. In other words, $[\mathbf{\Pi}(I, K, S, P, D)]_{i,o,k} = [\mathbf{\Pi}(I, K + (K - 1)(D - 1), S, P, 1)]_{i,o,1+D(k-1)}$ or, in tensor notation,

$$\mathbf{\Pi}(I, K, S, P, D) = [\mathbf{\Pi}(I, K + (K - 1)(D - 1), S, P, 1)]_{:, :, : : D}.$$

Transformation C6 (Transpose convolution as convolution) Assume Equation (9). Consider a non-strided ($S = 1$), non-dilated ($D = 1$) convolution with index pattern $\mathbf{\Pi}(I, K, 1, P, 1)$ and output dimension $O(I, K, 1, P, 1)$. Transposing the spatial dimensions and flipping the kernel dimension yields another index pattern with modified padding $P' = K - P - 1$. In other words, for all $i = 1, \dots, I, k = 1, \dots, K, o = 1, \dots, O$

$$[\mathbf{\Pi}(I, K, 1, P, 1)]_{i,o,k} = [\mathbf{\Pi}(O, K, 1, P', 1)]_{o,i,K+1-k}.$$

D CONVOLUTION LAYER HYPER-PARAMETER ANALYSIS

Here we give an overview of and characterize convolutions in popular architectures (see Table D3). We include moderately deep CNNs on Fashion MNIST, CIFAR-10, and CIFAR-100 from the DeepOBS benchmark [59], and deep CNNs on ImageNet (AlexNet, ResNet18, InceptionV3, MobileNetV2, ResNext101). Regarding the hyper-parameters, we make the following observations:

- Many CNNs do not use a bias term. This is because the output of those layers feeds directly into a batch normalization layer, which is invariant under the addition of a bias term.
- All investigated convolutions use default dilation.
- Group convolutions are rarely used. MobileNetV2 (Table D3h) uses group convolutions that interpret each individual channel as a group. ResNext101 (Table D3f) uses group convolutions that interpret a collection of channels as a group.
- Many networks use dense convolutions, that is convolutions with unit kernel size ($K = 1$), unit stride ($S = 1$), and no padding ($P = 0$). These convolutions have a trivial index pattern and can therefore be simplified.
- InceptionV3 (Table D3g) uses two-dimensional convolutions with one trivial dimension ('mixed dense') with unit kernel size, unit stride, and no padding along one direction. For this spatial dimension, the index pattern can be simplified.
- ResNet18 (Table D3e) and ResNext101 (Table D3f) use convolutions with $S > K$ for down-sampling whose kernel only overlaps with a fraction of the input. The index pattern can be simplified.

Table D3: Hyper-parameters of convolutions in different CNNs. For convolutions with identical hyper-parameters, we only show one instance and its multiplicity.

(a) 3c3d, CIFAR-10 (3, 32, 32)

| Name (count) | Input shape | Output shape | Kernel | Stride | Padding | Dilation | Groups | Bias | Type |
|--------------|--------------|--------------|--------|--------|---------|----------|--------|------|---------|
| conv1.0 (1) | (3, 32, 32) | (64, 28, 28) | (5, 5) | (1, 1) | (0, 0) | (1, 1) | 1 | Yes | General |
| conv2.0 (1) | (64, 14, 14) | (96, 12, 12) | (3, 3) | (1, 1) | (0, 0) | (1, 1) | 1 | Yes | General |
| conv3.1 (1) | (96, 8, 8) | (128, 6, 6) | (3, 3) | (1, 1) | (0, 0) | (1, 1) | 1 | Yes | General |

(b) 2c2d, Fashion MNIST (1, 28, 28)

| Name (count) | Input shape | Output shape | Kernel | Stride | Padding | Dilation | Groups | Bias | Type |
|--------------|--------------|--------------|--------|--------|---------|----------|--------|------|---------|
| conv1.1 (1) | (1, 32, 32) | (32, 28, 28) | (5, 5) | (1, 1) | (0, 0) | (1, 1) | 1 | Yes | General |
| conv2.1 (1) | (32, 18, 18) | (64, 14, 14) | (5, 5) | (1, 1) | (0, 0) | (1, 1) | 1 | Yes | General |

(c) All-CNN-C, CIFAR-100 (3, 32, 32)

| Name (count) | Input shape | Output shape | Kernel | Stride | Padding | Dilation | Groups | Bias | Type |
|--------------|---------------|---------------|--------|--------|---------|----------|--------|------|---------|
| conv1.1 (1) | (3, 34, 34) | (96, 32, 32) | (3, 3) | (1, 1) | (0, 0) | (1, 1) | 1 | Yes | General |
| conv2.1 (1) | (96, 34, 34) | (96, 32, 32) | (3, 3) | (1, 1) | (0, 0) | (1, 1) | 1 | Yes | General |
| conv3.1 (1) | (96, 33, 33) | (96, 16, 16) | (3, 3) | (2, 2) | (0, 0) | (1, 1) | 1 | Yes | General |
| conv4.1 (1) | (96, 18, 18) | (192, 16, 16) | (3, 3) | (1, 1) | (0, 0) | (1, 1) | 1 | Yes | General |
| conv5.1 (1) | (192, 18, 18) | (192, 16, 16) | (3, 3) | (1, 1) | (0, 0) | (1, 1) | 1 | Yes | General |
| conv6.1 (1) | (192, 17, 17) | (192, 8, 8) | (3, 3) | (2, 2) | (0, 0) | (1, 1) | 1 | Yes | General |
| conv7.0 (1) | (192, 8, 8) | (192, 6, 6) | (3, 3) | (1, 1) | (0, 0) | (1, 1) | 1 | Yes | General |
| conv8.1 (1) | (192, 6, 6) | (192, 6, 6) | (1, 1) | (1, 1) | (0, 0) | (1, 1) | 1 | Yes | Dense |
| conv9.1 (1) | (192, 6, 6) | (100, 6, 6) | (1, 1) | (1, 1) | (0, 0) | (1, 1) | 1 | Yes | Dense |

(d) AlexNet, Imagenet (3, 256, 256)

| Name (count) | Input shape | Output shape | Kernel | Stride | Padding | Dilation | Groups | Bias | Type |
|-----------------|---------------|---------------|----------|--------|---------|----------|--------|------|---------|
| features.0 (1) | (3, 256, 256) | (64, 63, 63) | (11, 11) | (4, 4) | (2, 2) | (1, 1) | 1 | Yes | General |
| features.3 (1) | (64, 31, 31) | (192, 31, 31) | (5, 5) | (1, 1) | (2, 2) | (1, 1) | 1 | Yes | General |
| features.6 (1) | (192, 15, 15) | (384, 15, 15) | (3, 3) | (1, 1) | (1, 1) | (1, 1) | 1 | Yes | General |
| features.8 (1) | (384, 15, 15) | (256, 15, 15) | (3, 3) | (1, 1) | (1, 1) | (1, 1) | 1 | Yes | General |
| features.10 (1) | (256, 15, 15) | (256, 15, 15) | (3, 3) | (1, 1) | (1, 1) | (1, 1) | 1 | Yes | General |

(e) ResNet18, Imagenet (3, 256, 256)

| Name (count) | Input shape | Output shape | Kernel | Stride | Padding | Dilation | Groups | Bias | Type |
|---------------------------|---------------|----------------|--------|--------|---------|----------|--------|------|---------|
| conv1 (1) | (3, 256, 256) | (64, 128, 128) | (7, 7) | (2, 2) | (3, 3) | (1, 1) | 1 | No | General |
| layer1.0.conv1 (4) | (64, 64, 64) | (64, 64, 64) | (3, 3) | (1, 1) | (1, 1) | (1, 1) | 1 | No | General |
| layer2.0.conv1 (1) | (64, 64, 64) | (128, 32, 32) | (3, 3) | (2, 2) | (1, 1) | (1, 1) | 1 | No | General |
| layer2.0.conv2 (3) | (128, 32, 32) | (128, 32, 32) | (3, 3) | (1, 1) | (1, 1) | (1, 1) | 1 | No | General |
| layer2.0.downsample.0 (1) | (64, 64, 64) | (128, 32, 32) | (1, 1) | (2, 2) | (0, 0) | (1, 1) | 1 | No | Down |
| layer3.0.conv1 (1) | (128, 32, 32) | (256, 16, 16) | (3, 3) | (2, 2) | (1, 1) | (1, 1) | 1 | No | General |
| layer3.0.conv2 (3) | (256, 16, 16) | (256, 16, 16) | (3, 3) | (1, 1) | (1, 1) | (1, 1) | 1 | No | General |
| layer3.0.downsample.0 (1) | (128, 32, 32) | (256, 16, 16) | (1, 1) | (2, 2) | (0, 0) | (1, 1) | 1 | No | Down |
| layer4.0.conv1 (1) | (256, 16, 16) | (512, 8, 8) | (3, 3) | (2, 2) | (1, 1) | (1, 1) | 1 | No | General |
| layer4.0.conv2 (3) | (512, 8, 8) | (512, 8, 8) | (3, 3) | (1, 1) | (1, 1) | (1, 1) | 1 | No | General |
| layer4.0.downsample.0 (1) | (256, 16, 16) | (512, 8, 8) | (1, 1) | (2, 2) | (0, 0) | (1, 1) | 1 | No | Down |

(f) ResNext101_32x8d, ImageNet (3, 256, 256)

| Name (count) | Input shape | Output shape | Kernel | Stride | Padding | Dilation | Groups | Bias | Type |
|---------------------------|----------------|----------------|--------|--------|---------|----------|--------|------|---------|
| conv1 (1) | (3, 256, 256) | (64, 128, 128) | (7, 7) | (2, 2) | (3, 3) | (1, 1) | 1 | No | General |
| layer1.0.conv1 (2) | (64, 64, 64) | (256, 64, 64) | (1, 1) | (1, 1) | (0, 0) | (1, 1) | 1 | No | Dense |
| layer1.0.conv2 (3) | (256, 64, 64) | (256, 64, 64) | (3, 3) | (1, 1) | (1, 1) | (1, 1) | 32 | No | General |
| layer1.0.conv3 (5) | (256, 64, 64) | (256, 64, 64) | (1, 1) | (1, 1) | (0, 0) | (1, 1) | 1 | No | Dense |
| layer2.0.conv1 (1) | (256, 64, 64) | (512, 64, 64) | (1, 1) | (1, 1) | (0, 0) | (1, 1) | 1 | No | Dense |
| layer2.0.conv2 (1) | (512, 64, 64) | (512, 32, 32) | (3, 3) | (2, 2) | (1, 1) | (1, 1) | 32 | No | General |
| layer2.0.conv3 (7) | (512, 32, 32) | (512, 32, 32) | (1, 1) | (1, 1) | (0, 0) | (1, 1) | 1 | No | Dense |
| layer2.0.downsample.0 (1) | (256, 64, 64) | (512, 32, 32) | (1, 1) | (2, 2) | (0, 0) | (1, 1) | 1 | No | Down |
| layer2.1.conv2 (3) | (512, 32, 32) | (512, 32, 32) | (3, 3) | (1, 1) | (1, 1) | (1, 1) | 32 | No | General |
| layer3.0.conv1 (1) | (512, 32, 32) | (1024, 32, 32) | (1, 1) | (1, 1) | (0, 0) | (1, 1) | 1 | No | Dense |
| layer3.0.conv2 (1) | (1024, 32, 32) | (1024, 16, 16) | (3, 3) | (2, 2) | (1, 1) | (1, 1) | 32 | No | General |
| layer3.0.conv3 (45) | (1024, 16, 16) | (1024, 16, 16) | (1, 1) | (1, 1) | (0, 0) | (1, 1) | 1 | No | Dense |
| layer3.0.downsample.0 (1) | (512, 32, 32) | (1024, 16, 16) | (1, 1) | (2, 2) | (0, 0) | (1, 1) | 1 | No | Down |
| layer3.1.conv2 (22) | (1024, 16, 16) | (1024, 16, 16) | (3, 3) | (1, 1) | (1, 1) | (1, 1) | 32 | No | General |
| layer4.0.conv1 (1) | (1024, 16, 16) | (2048, 16, 16) | (1, 1) | (1, 1) | (0, 0) | (1, 1) | 1 | No | Dense |
| layer4.0.conv2 (1) | (2048, 16, 16) | (2048, 8, 8) | (3, 3) | (2, 2) | (1, 1) | (1, 1) | 32 | No | General |
| layer4.0.conv3 (5) | (2048, 8, 8) | (2048, 8, 8) | (1, 1) | (1, 1) | (0, 0) | (1, 1) | 1 | No | Dense |
| layer4.0.downsample.0 (1) | (1024, 16, 16) | (2048, 8, 8) | (1, 1) | (2, 2) | (0, 0) | (1, 1) | 1 | No | Down |
| layer4.1.conv2 (2) | (2048, 8, 8) | (2048, 8, 8) | (3, 3) | (1, 1) | (1, 1) | (1, 1) | 32 | No | General |

(g) InceptionV3, Imagenet (3, 299, 299)

| Name (count) | Input shape | Output shape | Kernel | Stride | Padding | Dilation | Groups | Bias | Type |
|----------------------------------|----------------|----------------|--------|--------|---------|----------|--------|------|-----------|
| Conv2d.1a_3x3.conv (1) | (3, 299, 299) | (32, 149, 149) | (3, 3) | (2, 2) | (0, 0) | (1, 1) | 1 | No | General |
| Conv2d.2a_3x3.conv (1) | (32, 149, 149) | (32, 147, 147) | (3, 3) | (1, 1) | (0, 0) | (1, 1) | 1 | No | General |
| Conv2d.2b_3x3.conv (1) | (32, 147, 147) | (64, 147, 147) | (3, 3) | (1, 1) | (1, 1) | (1, 1) | 1 | No | General |
| Conv2d.3b_1x1.conv (1) | (64, 73, 73) | (80, 73, 73) | (1, 1) | (1, 1) | (0, 0) | (1, 1) | 1 | No | Dense |
| Conv2d.4a_3x3.conv (1) | (80, 73, 73) | (192, 71, 71) | (3, 3) | (1, 1) | (0, 0) | (1, 1) | 1 | No | General |
| Mixed_5b.branch1x1.conv (2) | (192, 35, 35) | (64, 35, 35) | (1, 1) | (1, 1) | (0, 0) | (1, 1) | 1 | No | Dense |
| Mixed_5b.branch5x5_1.conv (1) | (192, 35, 35) | (48, 35, 35) | (1, 1) | (1, 1) | (0, 0) | (1, 1) | 1 | No | Dense |
| Mixed_5b.branch5x5_2.conv (3) | (48, 35, 35) | (64, 35, 35) | (5, 5) | (1, 1) | (2, 2) | (1, 1) | 1 | No | General |
| Mixed_5b.branch3x3dbl_2.conv (4) | (64, 35, 35) | (96, 35, 35) | (3, 3) | (1, 1) | (1, 1) | (1, 1) | 1 | No | General |
| Mixed_5b.branch3x3dbl_3.conv (3) | (96, 35, 35) | (96, 35, 35) | (3, 3) | (1, 1) | (1, 1) | (1, 1) | 1 | No | General |
| Mixed_5b.branch_pool.conv (1) | (192, 35, 35) | (32, 35, 35) | (1, 1) | (1, 1) | (0, 0) | (1, 1) | 1 | No | Dense |
| Mixed_5c.branch1x1.conv (3) | (256, 35, 35) | (64, 35, 35) | (1, 1) | (1, 1) | (0, 0) | (1, 1) | 1 | No | Dense |
| Mixed_5c.branch5x5_1.conv (1) | (256, 35, 35) | (48, 35, 35) | (1, 1) | (1, 1) | (0, 0) | (1, 1) | 1 | No | Dense |
| Mixed_5d.branch1x1.conv (4) | (288, 35, 35) | (64, 35, 35) | (1, 1) | (1, 1) | (0, 0) | (1, 1) | 1 | No | Dense |
| Mixed_5d.branch5x5_1.conv (1) | (288, 35, 35) | (48, 35, 35) | (1, 1) | (1, 1) | (0, 0) | (1, 1) | 1 | No | Dense |
| Mixed_6a.branch3x3.conv (1) | (288, 35, 35) | (384, 17, 17) | (3, 3) | (2, 2) | (0, 0) | (1, 1) | 1 | No | General |
| Mixed_6a.branch3x3dbl_3.conv (1) | (96, 35, 35) | (96, 17, 17) | (3, 3) | (2, 2) | (0, 0) | (1, 1) | 1 | No | General |
| Mixed_6b.branch1x1.conv (12) | (768, 17, 17) | (192, 17, 17) | (1, 1) | (1, 1) | (0, 0) | (1, 1) | 1 | No | Dense |
| Mixed_6b.branch7x7_1.conv (2) | (768, 17, 17) | (128, 17, 17) | (1, 1) | (1, 1) | (0, 0) | (1, 1) | 1 | No | Dense |
| Mixed_6b.branch7x7_2.conv (2) | (128, 17, 17) | (128, 17, 17) | (1, 7) | (1, 1) | (0, 3) | (1, 1) | 1 | No | Dense mix |
| Mixed_6b.branch7x7_3.conv (1) | (128, 17, 17) | (192, 17, 17) | (7, 1) | (1, 1) | (3, 0) | (1, 1) | 1 | No | Dense mix |
| Mixed_6b.branch7x7dbl_2.conv (2) | (128, 17, 17) | (128, 17, 17) | (7, 1) | (1, 1) | (3, 0) | (1, 1) | 1 | No | Dense mix |
| Mixed_6b.branch7x7dbl_5.conv (1) | (128, 17, 17) | (192, 17, 17) | (1, 7) | (1, 1) | (0, 3) | (1, 1) | 1 | No | Dense mix |
| Mixed_6c.branch7x7_1.conv (4) | (768, 17, 17) | (160, 17, 17) | (1, 1) | (1, 1) | (0, 0) | (1, 1) | 1 | No | Dense |
| Mixed_6c.branch7x7_2.conv (4) | (160, 17, 17) | (160, 17, 17) | (1, 7) | (1, 1) | (0, 3) | (1, 1) | 1 | No | Dense mix |
| Mixed_6c.branch7x7_3.conv (2) | (160, 17, 17) | (192, 17, 17) | (7, 1) | (1, 1) | (3, 0) | (1, 1) | 1 | No | Dense mix |
| Mixed_6c.branch7x7dbl_2.conv (4) | (160, 17, 17) | (160, 17, 17) | (7, 1) | (1, 1) | (3, 0) | (1, 1) | 1 | No | Dense mix |
| Mixed_6c.branch7x7dbl_5.conv (2) | (160, 17, 17) | (192, 17, 17) | (1, 7) | (1, 1) | (0, 3) | (1, 1) | 1 | No | Dense mix |
| Mixed_6e.branch7x7_2.conv (4) | (192, 17, 17) | (192, 17, 17) | (1, 7) | (1, 1) | (0, 3) | (1, 1) | 1 | No | Dense mix |
| Mixed_6e.branch7x7_3.conv (4) | (192, 17, 17) | (192, 17, 17) | (7, 1) | (1, 1) | (3, 0) | (1, 1) | 1 | No | Dense mix |
| AuxLogits.conv0.conv (1) | (768, 5, 5) | (128, 5, 5) | (1, 1) | (1, 1) | (0, 0) | (1, 1) | 1 | No | Dense |
| AuxLogits.conv1.conv (1) | (128, 5, 5) | (768, 1, 1) | (5, 5) | (1, 1) | (0, 0) | (1, 1) | 1 | No | General |
| Mixed_7a.branch3x3_2.conv (1) | (192, 17, 17) | (320, 8, 8) | (3, 3) | (2, 2) | (0, 0) | (1, 1) | 1 | No | General |
| Mixed_7a.branch7x7x3_4.conv (1) | (192, 17, 17) | (192, 8, 8) | (3, 3) | (2, 2) | (0, 0) | (1, 1) | 1 | No | General |
| Mixed_7b.branch1x1.conv (1) | (1280, 8, 8) | (320, 8, 8) | (1, 1) | (1, 1) | (0, 0) | (1, 1) | 1 | No | Dense |
| Mixed_7b.branch3x3_1.conv (1) | (1280, 8, 8) | (384, 8, 8) | (1, 1) | (1, 1) | (0, 0) | (1, 1) | 1 | No | Dense |
| Mixed_7b.branch3x3_2a.conv (4) | (384, 8, 8) | (384, 8, 8) | (1, 3) | (1, 1) | (0, 1) | (1, 1) | 1 | No | Dense mix |
| Mixed_7b.branch3x3_2b.conv (4) | (384, 8, 8) | (384, 8, 8) | (3, 1) | (1, 1) | (1, 0) | (1, 1) | 1 | No | Dense mix |
| Mixed_7b.branch3x3dbl_1.conv (1) | (1280, 8, 8) | (448, 8, 8) | (1, 1) | (1, 1) | (0, 0) | (1, 1) | 1 | No | Dense |
| Mixed_7b.branch3x3dbl_2.conv (2) | (448, 8, 8) | (384, 8, 8) | (3, 3) | (1, 1) | (1, 1) | (1, 1) | 1 | No | General |
| Mixed_7b.branch_pool.conv (1) | (1280, 8, 8) | (192, 8, 8) | (1, 1) | (1, 1) | (0, 0) | (1, 1) | 1 | No | Dense |
| Mixed_7c.branch1x1.conv (1) | (2048, 8, 8) | (320, 8, 8) | (1, 1) | (1, 1) | (0, 0) | (1, 1) | 1 | No | Dense |
| Mixed_7c.branch3x3_1.conv (1) | (2048, 8, 8) | (384, 8, 8) | (1, 1) | (1, 1) | (0, 0) | (1, 1) | 1 | No | Dense |
| Mixed_7c.branch3x3dbl_1.conv (1) | (2048, 8, 8) | (448, 8, 8) | (1, 1) | (1, 1) | (0, 0) | (1, 1) | 1 | No | Dense |
| Mixed_7c.branch_pool.conv (1) | (2048, 8, 8) | (192, 8, 8) | (1, 1) | (1, 1) | (0, 0) | (1, 1) | 1 | No | Dense |

(h) MobileNetV2, Imagenet (3, 256, 256)

| Name (count) | Input shape | Output shape | Kernel | Stride | Padding | Dilation | Groups | Bias | Type |
|--------------------------|----------------|----------------|--------|--------|---------|----------|--------|------|---------|
| features.0.0 (1) | (3, 256, 256) | (32, 128, 128) | (3, 3) | (2, 2) | (1, 1) | (1, 1) | 1 | No | General |
| features.1.conv.0.0 (1) | (32, 128, 128) | (32, 128, 128) | (3, 3) | (1, 1) | (1, 1) | (1, 1) | 32 | No | General |
| features.1.conv.1 (1) | (32, 128, 128) | (16, 128, 128) | (1, 1) | (1, 1) | (0, 0) | (1, 1) | 1 | No | Dense |
| features.2.conv.0.0 (1) | (16, 128, 128) | (96, 128, 128) | (1, 1) | (1, 1) | (0, 0) | (1, 1) | 1 | No | Dense |
| features.2.conv.1.0 (1) | (96, 128, 128) | (96, 64, 64) | (3, 3) | (2, 2) | (1, 1) | (1, 1) | 96 | No | General |
| features.2.conv.2 (1) | (96, 64, 64) | (24, 64, 64) | (1, 1) | (1, 1) | (0, 0) | (1, 1) | 1 | No | Dense |
| features.3.conv.0.0 (2) | (24, 64, 64) | (144, 64, 64) | (1, 1) | (1, 1) | (0, 0) | (1, 1) | 1 | No | Dense |
| features.3.conv.1.0 (1) | (144, 64, 64) | (144, 64, 64) | (3, 3) | (1, 1) | (1, 1) | (1, 1) | 144 | No | General |
| features.3.conv.2 (1) | (144, 64, 64) | (24, 64, 64) | (1, 1) | (1, 1) | (0, 0) | (1, 1) | 1 | No | Dense |
| features.4.conv.1.0 (1) | (144, 64, 64) | (144, 32, 32) | (3, 3) | (2, 2) | (1, 1) | (1, 1) | 144 | No | General |
| features.4.conv.2 (1) | (144, 32, 32) | (32, 32, 32) | (1, 1) | (1, 1) | (0, 0) | (1, 1) | 1 | No | Dense |
| features.5.conv.0.0 (3) | (32, 32, 32) | (192, 32, 32) | (1, 1) | (1, 1) | (0, 0) | (1, 1) | 1 | No | Dense |
| features.5.conv.1.0 (2) | (192, 32, 32) | (192, 32, 32) | (3, 3) | (1, 1) | (1, 1) | (1, 1) | 192 | No | General |
| features.5.conv.2 (2) | (192, 32, 32) | (32, 32, 32) | (1, 1) | (1, 1) | (0, 0) | (1, 1) | 1 | No | Dense |
| features.7.conv.1.0 (1) | (192, 32, 32) | (192, 16, 16) | (3, 3) | (2, 2) | (1, 1) | (1, 1) | 192 | No | General |
| features.7.conv.2 (1) | (192, 16, 16) | (64, 16, 16) | (1, 1) | (1, 1) | (0, 0) | (1, 1) | 1 | No | Dense |
| features.8.conv.0.0 (4) | (64, 16, 16) | (384, 16, 16) | (1, 1) | (1, 1) | (0, 0) | (1, 1) | 1 | No | Dense |
| features.8.conv.1.0 (4) | (384, 16, 16) | (384, 16, 16) | (3, 3) | (1, 1) | (1, 1) | (1, 1) | 384 | No | General |
| features.8.conv.2 (3) | (384, 16, 16) | (64, 16, 16) | (1, 1) | (1, 1) | (0, 0) | (1, 1) | 1 | No | Dense |
| features.11.conv.2 (1) | (384, 16, 16) | (96, 16, 16) | (1, 1) | (1, 1) | (0, 0) | (1, 1) | 1 | No | Dense |
| features.12.conv.0.0 (3) | (96, 16, 16) | (576, 16, 16) | (1, 1) | (1, 1) | (0, 0) | (1, 1) | 1 | No | Dense |
| features.12.conv.1.0 (2) | (576, 16, 16) | (576, 16, 16) | (3, 3) | (1, 1) | (1, 1) | (1, 1) | 576 | No | General |
| features.12.conv.2 (2) | (576, 16, 16) | (96, 16, 16) | (1, 1) | (1, 1) | (0, 0) | (1, 1) | 1 | No | Dense |
| features.14.conv.1.0 (1) | (576, 16, 16) | (576, 8, 8) | (3, 3) | (2, 2) | (1, 1) | (1, 1) | 576 | No | General |
| features.14.conv.2 (1) | (576, 8, 8) | (160, 8, 8) | (1, 1) | (1, 1) | (0, 0) | (1, 1) | 1 | No | Dense |
| features.15.conv.0.0 (3) | (160, 8, 8) | (960, 8, 8) | (1, 1) | (1, 1) | (0, 0) | (1, 1) | 1 | No | Dense |
| features.15.conv.1.0 (3) | (960, 8, 8) | (960, 8, 8) | (3, 3) | (1, 1) | (1, 1) | (1, 1) | 960 | No | General |
| features.15.conv.2 (2) | (960, 8, 8) | (160, 8, 8) | (1, 1) | (1, 1) | (0, 0) | (1, 1) | 1 | No | Dense |
| features.17.conv.2 (1) | (960, 8, 8) | (320, 8, 8) | (1, 1) | (1, 1) | (0, 0) | (1, 1) | 1 | No | Dense |
| features.18.0 (1) | (320, 8, 8) | (1280, 8, 8) | (1, 1) | (1, 1) | (0, 0) | (1, 1) | 1 | No | Dense |

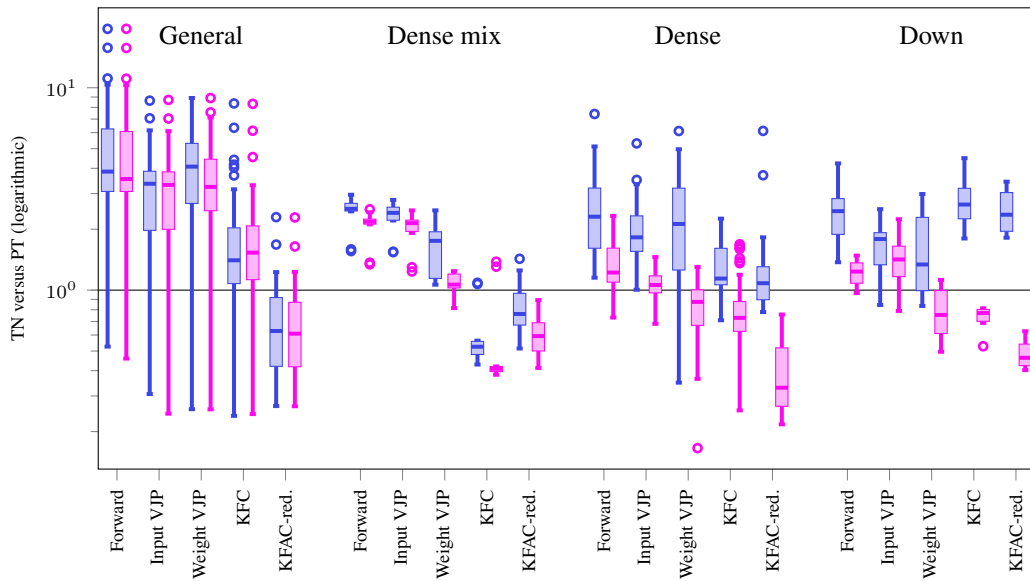


Figure E14: Benchmark overview. We measure the performance ratios of our TN implementation w.r.t. a base line in PyTorch (PT). Blue boxes show the performance ratios of TN versus PT, second-color boxes show the performance ratios of TN+opt versus PT.

E PERFORMANCE EVALUATION DETAILS (GPU)

Here we provide all details on the run time evaluation from the main text. We consider the convolutions from the CNNs from §D. Experiments were carried out on an Nvidia Tesla T4 (16 GB memory). We use a batch size of 32 for the ImageNet architectures, and 128 for the others.

E.1 PROTOCOL & OVERVIEW

We compare different implementations of the same operations in PyTorch. The base line (referred by ‘PT’) uses PyTorch’s built-in functionalities for convolutions and related operations, such as `torch.nn.functional.conv2d` (forward), `torch.nn.functional.unfold` (KFC, KFAC-reduce), and PyTorch’s built-in automatic differentiation `torch.autograd.grad` (VJPs).

Our TN implementation (referred by ‘TN’) sets up operands and the string-valued equation for each routine. Optionally, we can apply the simplifications from §4 as a post-processing step before contraction, which yields a modified equation and operand list (‘TN + opt’). Finally, we determine the contraction path using `opt_einsum.contract_path` and perform the contraction with its PyTorch back-end (`opt_einsum.contract`). We only measure the contraction time as in practical settings, the contraction path search would be executed once, then cached. We also exclude final operations to obtain the correct shape or scale (flattening, reshaping, scaling by constant) in all implementations (including the base line).

For each operation and each convolution layer, we perform 50 independent repetitions and report the minimum time in tables. To summarize those tables, we extract the performance ratios, that is the TN implementation’s run time divided by the base line’s. Ratios larger than 1 mean that the TN implementation is slower, ratios smaller than 1 indicate that it is faster than the base line. We collect those ratios for the different convolution types (general, mixed dense, dense, sub-sampling) and display them separately using box plots. Each operation has two boxes, corresponding to the un-simplified (TN), and the simplified (TN + opt) implementation. For the box plots, we use `matplotlib`’s default settings (a box extends from the first quartile to the third quartile of the data, with a line at the median; whiskers extend from the box by 1.5x the inter-quartile range; flier points are those past the end of the whiskers). Figure E14 summarizes the entire GPU benchmark. Figure E15 shows the same information with each convolution type as an individual plot.

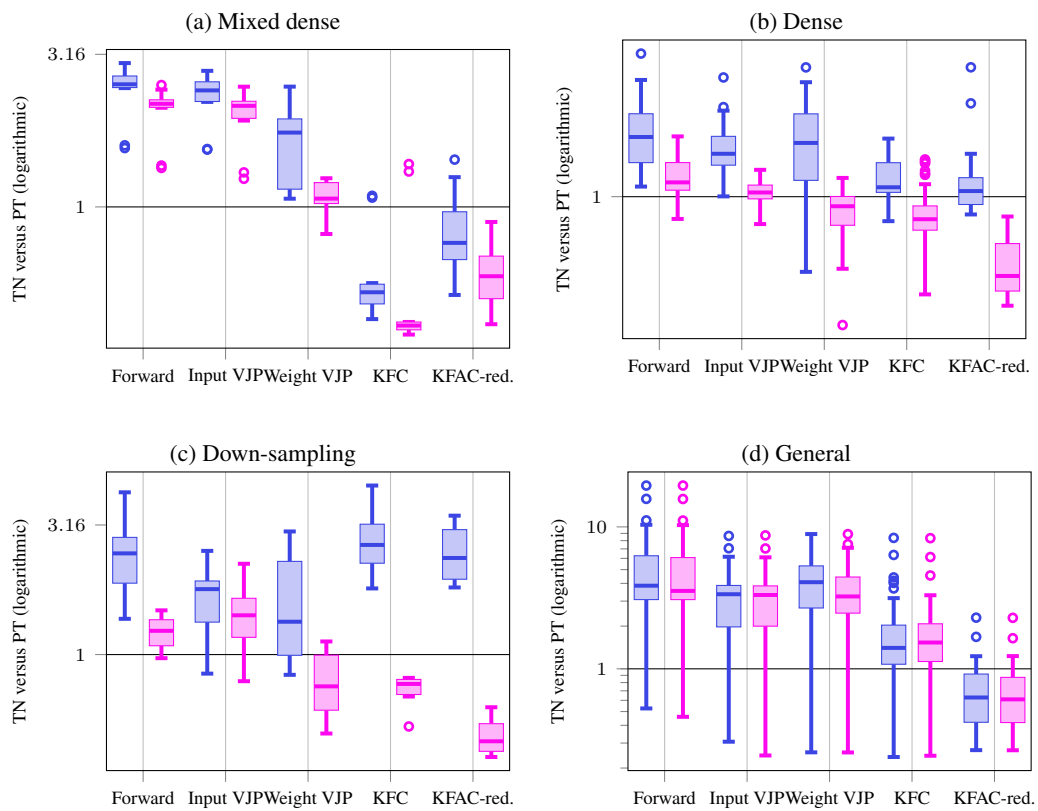


Figure E15: Impact of **TN simplifications** (non-simplified performance ratios shown in **blue**). TN simplifications improve performance on **(a)** mixed dense, **(b)** dense, and **(c)** down-sampling convolutions. **(d)** General convolutions are not affected by TN simplifications.

E.2 FORWARD PASS

We compare TN and TN+opt with PyTorch's `torch.nn.functional.conv2d`. Figure E16 visualizes the performance ratios for different convolution categories. Table E4 contains the detailed run times and performance factors.

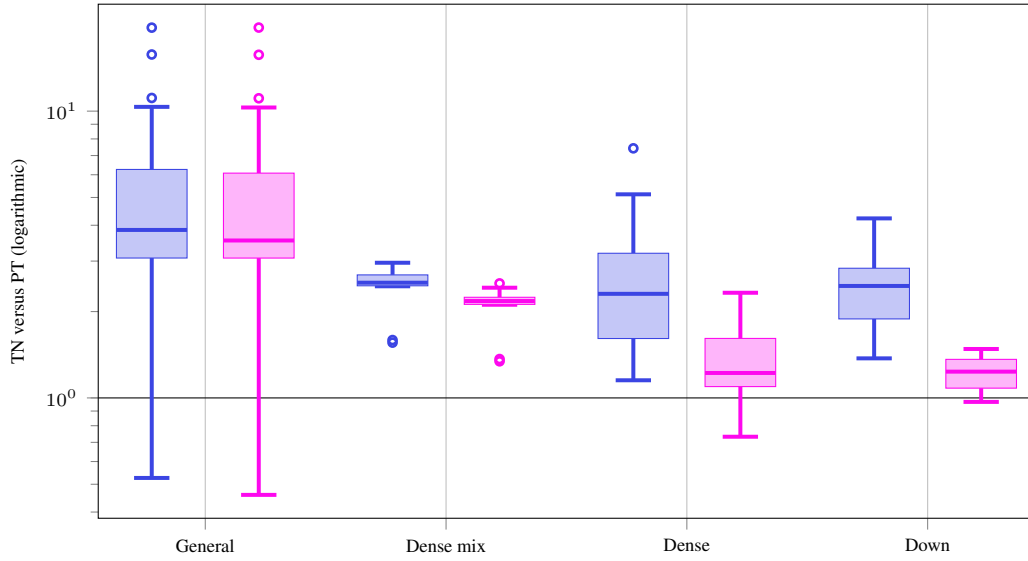


Figure E16: Forward pass performance ratios of TN versus PT and TN+opt versus PT for different convolution types on GPU.

Table E4: Forward pass performance comparison on GPU.

(a) 3c3d, CIFAR-10, input shape (128, 3, 32, 32)

| Name | TN [s] | PT [s] | Factor | TN + opt [s] | PT [s] | Factor | Type |
|---------|----------------------|----------------------|--------|----------------------|----------------------|--------|---------|
| conv1.0 | $1.26 \cdot 10^{-3}$ | $4.63 \cdot 10^{-4}$ | 2.73 x | $1.23 \cdot 10^{-3}$ | $4.64 \cdot 10^{-4}$ | 2.64 x | General |
| conv2.0 | $1.91 \cdot 10^{-3}$ | $4.52 \cdot 10^{-4}$ | 4.22 x | $1.79 \cdot 10^{-3}$ | $4.53 \cdot 10^{-4}$ | 3.95 x | General |
| conv3.1 | $1.21 \cdot 10^{-3}$ | $4.11 \cdot 10^{-4}$ | 2.94 x | $1.16 \cdot 10^{-3}$ | $4.10 \cdot 10^{-4}$ | 2.83 x | General |

(b) F-MNIST 2c2d, input shape (128, 1, 28, 28)

| Name | TN [s] | PT [s] | Factor | TN + opt [s] | PT [s] | Factor | Type |
|---------|----------------------|----------------------|--------|----------------------|----------------------|--------|---------|
| conv1.1 | $8.21 \cdot 10^{-4}$ | $2.25 \cdot 10^{-4}$ | 3.65 x | $7.67 \cdot 10^{-4}$ | $2.25 \cdot 10^{-4}$ | 3.41 x | General |
| conv2.1 | $3.56 \cdot 10^{-3}$ | $7.43 \cdot 10^{-4}$ | 4.79 x | $3.24 \cdot 10^{-3}$ | $7.83 \cdot 10^{-4}$ | 4.14 x | General |

(c) CIFAR-100 All-CNN-C, input shape (128, 3, 32, 32)

| Name | TN [s] | PT [s] | Factor | TN + opt [s] | PT [s] | Factor | Type |
|---------|----------------------|----------------------|--------|----------------------|----------------------|--------|---------|
| conv1.1 | $1.01 \cdot 10^{-3}$ | $4.20 \cdot 10^{-4}$ | 2.41 x | $9.45 \cdot 10^{-4}$ | $4.19 \cdot 10^{-4}$ | 2.25 x | General |
| conv2.1 | $1.94 \cdot 10^{-2}$ | $3.09 \cdot 10^{-3}$ | 6.26 x | $1.88 \cdot 10^{-2}$ | $3.10 \cdot 10^{-3}$ | 6.08 x | General |
| conv3.1 | $8.56 \cdot 10^{-3}$ | $2.86 \cdot 10^{-3}$ | 3.00 x | $7.77 \cdot 10^{-3}$ | $2.86 \cdot 10^{-3}$ | 2.72 x | General |
| conv4.1 | $8.58 \cdot 10^{-3}$ | $1.75 \cdot 10^{-3}$ | 4.91 x | $7.77 \cdot 10^{-3}$ | $1.75 \cdot 10^{-3}$ | 4.45 x | General |
| conv5.1 | $1.67 \cdot 10^{-2}$ | $2.91 \cdot 10^{-3}$ | 5.74 x | $1.51 \cdot 10^{-2}$ | $2.91 \cdot 10^{-3}$ | 5.19 x | General |
| conv6.1 | $5.13 \cdot 10^{-3}$ | $2.24 \cdot 10^{-3}$ | 2.29 x | $5.08 \cdot 10^{-3}$ | $2.24 \cdot 10^{-3}$ | 2.27 x | General |
| conv7.0 | $2.58 \cdot 10^{-3}$ | $8.26 \cdot 10^{-4}$ | 3.12 x | $2.51 \cdot 10^{-3}$ | $8.27 \cdot 10^{-4}$ | 3.03 x | General |
| conv8.1 | $8.20 \cdot 10^{-4}$ | $2.96 \cdot 10^{-4}$ | 2.77 x | $3.42 \cdot 10^{-4}$ | $2.97 \cdot 10^{-4}$ | 1.15 x | Dense |
| conv9.1 | $7.52 \cdot 10^{-4}$ | $2.35 \cdot 10^{-4}$ | 3.19 x | $3.01 \cdot 10^{-4}$ | $2.35 \cdot 10^{-4}$ | 1.28 x | Dense |

(d) Alexnet, input shape (32, 3, 256, 256)

| Name | TN [s] | PT [s] | Factor | TN + opt [s] | PT [s] | Factor | Type |
|-------------|----------------------|----------------------|--------|----------------------|----------------------|--------|---------|
| features.0 | $1.83 \cdot 10^{-2}$ | $2.45 \cdot 10^{-3}$ | 7.47 x | $1.79 \cdot 10^{-2}$ | $2.44 \cdot 10^{-3}$ | 7.35 x | General |
| features.3 | $7.43 \cdot 10^{-3}$ | $2.67 \cdot 10^{-3}$ | 2.79 x | $7.27 \cdot 10^{-3}$ | $2.85 \cdot 10^{-3}$ | 2.55 x | General |
| features.6 | $4.68 \cdot 10^{-3}$ | $1.04 \cdot 10^{-3}$ | 4.52 x | $3.22 \cdot 10^{-3}$ | $1.02 \cdot 10^{-3}$ | 3.14 x | General |
| features.8 | $6.15 \cdot 10^{-3}$ | $1.86 \cdot 10^{-3}$ | 3.31 x | $6.16 \cdot 10^{-3}$ | $1.84 \cdot 10^{-3}$ | 3.34 x | General |
| features.10 | $4.41 \cdot 10^{-3}$ | $1.31 \cdot 10^{-3}$ | 3.36 x | $4.38 \cdot 10^{-3}$ | $1.31 \cdot 10^{-3}$ | 3.35 x | General |

(e) ResNet18, input shape (32, 3, 256, 256)

| Name | TN [s] | PT [s] | Factor | TN + opt [s] | PT [s] | Factor | Type |
|-----------------------|----------------------|----------------------|--------|----------------------|----------------------|--------|---------|
| conv1 | $1.44 \cdot 10^{-2}$ | $4.07 \cdot 10^{-3}$ | 3.53 x | $1.44 \cdot 10^{-2}$ | $4.08 \cdot 10^{-3}$ | 3.53 x | General |
| layer1.0.conv1 | $1.05 \cdot 10^{-2}$ | $1.78 \cdot 10^{-3}$ | 5.91 x | $1.05 \cdot 10^{-2}$ | $1.79 \cdot 10^{-3}$ | 5.87 x | General |
| layer2.0.conv1 | $6.44 \cdot 10^{-3}$ | $1.89 \cdot 10^{-3}$ | 3.41 x | $6.46 \cdot 10^{-3}$ | $1.89 \cdot 10^{-3}$ | 3.42 x | General |
| layer2.0.conv2 | $6.88 \cdot 10^{-3}$ | $1.51 \cdot 10^{-3}$ | 4.54 x | $6.91 \cdot 10^{-3}$ | $1.52 \cdot 10^{-3}$ | 4.54 x | General |
| layer2.0.downsample.0 | $1.60 \cdot 10^{-3}$ | $3.79 \cdot 10^{-4}$ | 4.23 x | $5.19 \cdot 10^{-4}$ | $3.80 \cdot 10^{-4}$ | 1.37 x | Down |
| layer3.0.conv1 | $3.82 \cdot 10^{-3}$ | $2.00 \cdot 10^{-3}$ | 1.91 x | $3.56 \cdot 10^{-3}$ | $2.01 \cdot 10^{-3}$ | 1.77 x | General |
| layer3.0.conv2 | $5.02 \cdot 10^{-3}$ | $1.30 \cdot 10^{-3}$ | 3.85 x | $5.05 \cdot 10^{-3}$ | $1.31 \cdot 10^{-3}$ | 3.87 x | General |
| layer3.0.downsample.0 | $1.10 \cdot 10^{-3}$ | $3.78 \cdot 10^{-4}$ | 2.91 x | $5.61 \cdot 10^{-4}$ | $3.79 \cdot 10^{-4}$ | 1.48 x | Down |
| layer4.0.conv1 | $2.87 \cdot 10^{-3}$ | $2.36 \cdot 10^{-3}$ | 1.21 x | $2.86 \cdot 10^{-3}$ | $2.36 \cdot 10^{-3}$ | 1.21 x | General |
| layer4.0.conv2 | $4.47 \cdot 10^{-3}$ | $1.40 \cdot 10^{-3}$ | 3.18 x | $4.51 \cdot 10^{-3}$ | $1.40 \cdot 10^{-3}$ | 3.21 x | General |
| layer4.0.downsample.0 | $9.90 \cdot 10^{-4}$ | $3.81 \cdot 10^{-4}$ | 2.60 x | $5.16 \cdot 10^{-4}$ | $3.83 \cdot 10^{-4}$ | 1.35 x | Down |

(f) ResNext101, input shape (32, 3, 256, 256)

| Name | TN [s] | PT [s] | Factor | TN + opt [s] | PT [s] | Factor | Type |
|-----------------------|----------------------|----------------------|--------|----------------------|----------------------|---------------|---------|
| conv1 | $1.45 \cdot 10^{-2}$ | $4.07 \cdot 10^{-3}$ | 3.57 x | $1.44 \cdot 10^{-2}$ | $4.07 \cdot 10^{-3}$ | 3.54 x | General |
| layer1.0.conv1 | $4.31 \cdot 10^{-3}$ | $1.22 \cdot 10^{-3}$ | 3.54 x | $2.26 \cdot 10^{-3}$ | $1.22 \cdot 10^{-3}$ | 1.85 x | Dense |
| layer1.0.conv2 | $3.03 \cdot 10^{-2}$ | $9.86 \cdot 10^{-3}$ | 3.07 x | $3.03 \cdot 10^{-2}$ | $9.86 \cdot 10^{-3}$ | 3.08 x | General |
| layer1.0.conv3 | $1.51 \cdot 10^{-2}$ | $6.54 \cdot 10^{-3}$ | 2.31 x | $7.49 \cdot 10^{-3}$ | $6.54 \cdot 10^{-3}$ | 1.15 x | Dense |
| layer2.0.conv1 | $2.08 \cdot 10^{-2}$ | $1.29 \cdot 10^{-2}$ | 1.61 x | $1.36 \cdot 10^{-2}$ | $1.29 \cdot 10^{-2}$ | 1.05 x | Dense |
| layer2.0.conv2 | $3.33 \cdot 10^{-2}$ | $4.93 \cdot 10^{-3}$ | 6.75 x | $3.33 \cdot 10^{-2}$ | $4.93 \cdot 10^{-3}$ | 6.75 x | General |
| layer2.0.conv3 | $1.05 \cdot 10^{-2}$ | $6.24 \cdot 10^{-3}$ | 1.69 x | $6.84 \cdot 10^{-3}$ | $6.24 \cdot 10^{-3}$ | 1.10 x | Dense |
| layer2.0.downsample.0 | $7.65 \cdot 10^{-3}$ | $3.30 \cdot 10^{-3}$ | 2.31 x | $3.71 \cdot 10^{-3}$ | $3.31 \cdot 10^{-3}$ | 1.12 x | Down |
| layer2.1.conv2 | $1.50 \cdot 10^{-2}$ | $4.59 \cdot 10^{-3}$ | 3.27 x | $1.50 \cdot 10^{-2}$ | $4.59 \cdot 10^{-3}$ | 3.27 x | General |
| layer3.0.conv1 | $1.67 \cdot 10^{-2}$ | $1.23 \cdot 10^{-2}$ | 1.35 x | $1.28 \cdot 10^{-2}$ | $1.23 \cdot 10^{-2}$ | 1.04 x | Dense |
| layer3.0.conv2 | $1.76 \cdot 10^{-2}$ | $2.65 \cdot 10^{-3}$ | 6.65 x | $1.76 \cdot 10^{-2}$ | $2.66 \cdot 10^{-3}$ | 6.65 x | General |
| layer3.0.conv3 | $8.27 \cdot 10^{-3}$ | $6.14 \cdot 10^{-3}$ | 1.35 x | $6.44 \cdot 10^{-3}$ | $6.14 \cdot 10^{-3}$ | 1.05 x | Dense |
| layer3.0.downsample.0 | $5.58 \cdot 10^{-3}$ | $3.20 \cdot 10^{-3}$ | 1.74 x | $3.42 \cdot 10^{-3}$ | $3.20 \cdot 10^{-3}$ | 1.07 x | Down |
| layer3.1.conv2 | $7.64 \cdot 10^{-3}$ | $2.49 \cdot 10^{-3}$ | 3.07 x | $7.64 \cdot 10^{-3}$ | $2.48 \cdot 10^{-3}$ | 3.07 x | General |
| layer4.0.conv1 | $1.43 \cdot 10^{-2}$ | $1.22 \cdot 10^{-2}$ | 1.18 x | $1.24 \cdot 10^{-2}$ | $1.22 \cdot 10^{-2}$ | 1.02 x | Dense |
| layer4.0.conv2 | $8.07 \cdot 10^{-3}$ | $2.02 \cdot 10^{-3}$ | 3.99 x | $8.08 \cdot 10^{-3}$ | $2.02 \cdot 10^{-3}$ | 4.00 x | General |
| layer4.0.conv3 | $7.85 \cdot 10^{-3}$ | $6.28 \cdot 10^{-3}$ | 1.25 x | $6.33 \cdot 10^{-3}$ | $6.28 \cdot 10^{-3}$ | 1.01 x | Dense |
| layer4.0.downsample.0 | $4.73 \cdot 10^{-3}$ | $3.44 \cdot 10^{-3}$ | 1.37 x | $3.34 \cdot 10^{-3}$ | $3.44 \cdot 10^{-3}$ | 0.97 x | Down |
| layer4.1.conv2 | $4.76 \cdot 10^{-3}$ | $1.36 \cdot 10^{-3}$ | 3.51 x | $4.77 \cdot 10^{-3}$ | $1.35 \cdot 10^{-3}$ | 3.52 x | General |

(g) InceptionV3, input shape (32, 3, 299, 299)

| Name | TN [s] | PT [s] | Factor | TN + opt [s] | PT [s] | Factor | Type |
|------------------------------|----------------------|----------------------|---------------|----------------------|----------------------|---------------|-----------|
| Conv2d_1a_3x3.conv | $1.02 \cdot 10^{-2}$ | $9.85 \cdot 10^{-4}$ | 10.35 x | $1.01 \cdot 10^{-2}$ | $9.79 \cdot 10^{-4}$ | 10.30 x | General |
| Conv2d_2a_3x3.conv | $3.23 \cdot 10^{-2}$ | $5.14 \cdot 10^{-3}$ | 6.30 x | $3.19 \cdot 10^{-2}$ | $5.16 \cdot 10^{-3}$ | 6.18 x | General |
| Conv2d_2b_3x3.conv | $4.83 \cdot 10^{-2}$ | $8.14 \cdot 10^{-3}$ | 5.93 x | $4.78 \cdot 10^{-2}$ | $8.14 \cdot 10^{-3}$ | 5.87 x | General |
| Conv2d_3b_1x1.conv | $4.96 \cdot 10^{-3}$ | $1.17 \cdot 10^{-3}$ | 4.24 x | $1.72 \cdot 10^{-3}$ | $1.17 \cdot 10^{-3}$ | 1.48 x | Dense |
| Conv2d_4a_3x3.conv | $3.69 \cdot 10^{-2}$ | $7.64 \cdot 10^{-3}$ | 4.83 x | $3.65 \cdot 10^{-2}$ | $7.64 \cdot 10^{-3}$ | 4.77 x | General |
| Mixed_5b.branch1x1.conv | $1.85 \cdot 10^{-3}$ | $5.04 \cdot 10^{-4}$ | 3.68 x | $8.17 \cdot 10^{-4}$ | $5.03 \cdot 10^{-4}$ | 1.62 x | Dense |
| Mixed_5b.branch5x5.1.conv | $1.64 \cdot 10^{-3}$ | $4.97 \cdot 10^{-4}$ | 3.30 x | $8.11 \cdot 10^{-4}$ | $4.99 \cdot 10^{-4}$ | 1.63 x | Dense |
| Mixed_5b.branch5x5.2.conv | $5.01 \cdot 10^{-3}$ | $1.23 \cdot 10^{-3}$ | 4.07 x | $4.83 \cdot 10^{-3}$ | $1.23 \cdot 10^{-3}$ | 3.94 x | General |
| Mixed_5b.branch3x3dbl.2.conv | $4.40 \cdot 10^{-3}$ | $1.31 \cdot 10^{-3}$ | 3.38 x | $4.31 \cdot 10^{-3}$ | $1.31 \cdot 10^{-3}$ | 3.30 x | General |
| Mixed_5b.branch3x3dbl.3.conv | $5.82 \cdot 10^{-3}$ | $1.66 \cdot 10^{-3}$ | 3.50 x | $5.66 \cdot 10^{-3}$ | $1.66 \cdot 10^{-3}$ | 3.40 x | General |
| Mixed_5b.branch.pool.conv | $1.33 \cdot 10^{-3}$ | $3.26 \cdot 10^{-4}$ | 4.09 x | $7.04 \cdot 10^{-4}$ | $3.27 \cdot 10^{-4}$ | 2.15 x | Dense |
| Mixed_5c.branch1x1.conv | $2.08 \cdot 10^{-3}$ | $6.41 \cdot 10^{-4}$ | 3.24 x | $1.03 \cdot 10^{-3}$ | $6.40 \cdot 10^{-4}$ | 1.61 x | Dense |
| Mixed_5c.branch5x5.1.conv | $1.87 \cdot 10^{-3}$ | $6.29 \cdot 10^{-4}$ | 2.97 x | $1.03 \cdot 10^{-3}$ | $6.30 \cdot 10^{-4}$ | 1.63 x | Dense |
| Mixed_5d.branch1x1.conv | $2.18 \cdot 10^{-3}$ | $6.99 \cdot 10^{-4}$ | 3.12 x | $1.13 \cdot 10^{-3}$ | $6.98 \cdot 10^{-4}$ | 1.62 x | Dense |
| Mixed_5d.branch5x5.1.conv | $1.96 \cdot 10^{-3}$ | $6.91 \cdot 10^{-4}$ | 2.84 x | $1.13 \cdot 10^{-3}$ | $6.88 \cdot 10^{-4}$ | 1.64 x | Dense |
| Mixed_6a.branch3x3.conv | $1.15 \cdot 10^{-2}$ | $7.12 \cdot 10^{-3}$ | 1.61 x | $1.07 \cdot 10^{-2}$ | $7.13 \cdot 10^{-3}$ | 1.51 x | General |
| Mixed_6a.branch3x3dbl.3.conv | $2.61 \cdot 10^{-3}$ | $8.99 \cdot 10^{-4}$ | 2.90 x | $2.36 \cdot 10^{-3}$ | $9.00 \cdot 10^{-4}$ | 2.62 x | General |
| Mixed_6b.branch1x1.conv | $2.16 \cdot 10^{-3}$ | $1.22 \cdot 10^{-3}$ | 1.77 x | $1.41 \cdot 10^{-3}$ | $1.22 \cdot 10^{-3}$ | 1.15 x | Dense |
| Mixed_6b.branch7x7.1.conv | $1.67 \cdot 10^{-3}$ | $8.15 \cdot 10^{-4}$ | 2.05 x | $1.10 \cdot 10^{-3}$ | $8.16 \cdot 10^{-4}$ | 1.35 x | Dense |
| Mixed_6b.branch7x7.2.conv | $2.14 \cdot 10^{-3}$ | $8.04 \cdot 10^{-4}$ | 2.66 x | $1.76 \cdot 10^{-3}$ | $8.05 \cdot 10^{-4}$ | 2.19 x | Dense mix |
| Mixed_6b.branch7x7.3.conv | $2.59 \cdot 10^{-3}$ | $1.06 \cdot 10^{-3}$ | 2.45 x | $2.27 \cdot 10^{-3}$ | $1.06 \cdot 10^{-3}$ | 2.15 x | Dense mix |
| Mixed_6b.branch7x7dbl.2.conv | $2.17 \cdot 10^{-3}$ | $7.88 \cdot 10^{-4}$ | 2.76 x | $1.78 \cdot 10^{-3}$ | $7.88 \cdot 10^{-4}$ | 2.26 x | Dense mix |
| Mixed_6b.branch7x7dbl.5.conv | $2.63 \cdot 10^{-3}$ | $1.07 \cdot 10^{-3}$ | 2.46 x | $2.25 \cdot 10^{-3}$ | $1.07 \cdot 10^{-3}$ | 2.11 x | Dense mix |
| Mixed_6c.branch7x7.1.conv | $2.05 \cdot 10^{-3}$ | $1.16 \cdot 10^{-3}$ | 1.77 x | $1.41 \cdot 10^{-3}$ | $1.16 \cdot 10^{-3}$ | 1.21 x | Dense |
| Mixed_6c.branch7x7.2.conv | $3.19 \cdot 10^{-3}$ | $1.12 \cdot 10^{-3}$ | 2.84 x | $2.72 \cdot 10^{-3}$ | $1.12 \cdot 10^{-3}$ | 2.42 x | Dense mix |
| Mixed_6c.branch7x7.3.conv | $3.12 \cdot 10^{-3}$ | $1.25 \cdot 10^{-3}$ | 2.50 x | $2.76 \cdot 10^{-3}$ | $1.25 \cdot 10^{-3}$ | 2.21 x | Dense mix |
| Mixed_6c.branch7x7dbl.2.conv | $3.25 \cdot 10^{-3}$ | $1.10 \cdot 10^{-3}$ | 2.96 x | $2.75 \cdot 10^{-3}$ | $1.10 \cdot 10^{-3}$ | 2.51 x | Dense mix |
| Mixed_6c.branch7x7dbl.5.conv | $3.19 \cdot 10^{-3}$ | $1.28 \cdot 10^{-3}$ | 2.49 x | $2.73 \cdot 10^{-3}$ | $1.29 \cdot 10^{-3}$ | 2.12 x | Dense mix |
| Mixed_6e.branch7x7.2.conv | $3.78 \cdot 10^{-3}$ | $1.48 \cdot 10^{-3}$ | 2.54 x | $3.21 \cdot 10^{-3}$ | $1.48 \cdot 10^{-3}$ | 2.16 x | Dense mix |
| Mixed_6e.branch7x7.3.conv | $3.87 \cdot 10^{-3}$ | $1.45 \cdot 10^{-3}$ | 2.66 x | $3.26 \cdot 10^{-3}$ | $1.46 \cdot 10^{-3}$ | 2.24 x | Dense mix |
| AuxLogits.conv0.conv | $6.40 \cdot 10^{-4}$ | $2.38 \cdot 10^{-4}$ | 2.69 x | $3.20 \cdot 10^{-4}$ | $2.39 \cdot 10^{-4}$ | 1.34 x | Dense |
| AuxLogits.conv1.conv | $8.06 \cdot 10^{-4}$ | $1.53 \cdot 10^{-3}$ | 0.53 x | $6.98 \cdot 10^{-4}$ | $1.52 \cdot 10^{-3}$ | 0.46 x | General |
| Mixed_7a.branch3x3.2.conv | $1.08 \cdot 10^{-3}$ | $4.37 \cdot 10^{-4}$ | 2.48 x | $1.09 \cdot 10^{-3}$ | $5.01 \cdot 10^{-4}$ | 2.18 x | General |
| Mixed_7a.branch7x7x3.4.conv | $1.54 \cdot 10^{-3}$ | $8.89 \cdot 10^{-4}$ | 1.73 x | $1.52 \cdot 10^{-3}$ | $8.88 \cdot 10^{-4}$ | 1.71 x | General |
| Mixed_7b.branch1x1.conv | $1.29 \cdot 10^{-3}$ | $7.43 \cdot 10^{-4}$ | 1.73 x | $8.76 \cdot 10^{-4}$ | $7.43 \cdot 10^{-4}$ | 1.18 x | Dense |
| Mixed_7b.branch3x3.1.conv | $1.47 \cdot 10^{-3}$ | $1.03 \cdot 10^{-3}$ | 1.42 x | $1.02 \cdot 10^{-3}$ | $1.03 \cdot 10^{-3}$ | 0.99 x | Dense |
| Mixed_7b.branch3x3.2a.conv | $1.49 \cdot 10^{-3}$ | $9.36 \cdot 10^{-4}$ | 1.59 x | $1.26 \cdot 10^{-3}$ | $9.38 \cdot 10^{-4}$ | 1.34 x | Dense mix |
| Mixed_7b.branch3x3.2b.conv | $1.46 \cdot 10^{-3}$ | $9.37 \cdot 10^{-4}$ | 1.56 x | $1.28 \cdot 10^{-3}$ | $9.37 \cdot 10^{-4}$ | 1.37 x | Dense mix |
| Mixed_7b.branch3x3dbl.1.conv | $1.67 \cdot 10^{-3}$ | $1.04 \cdot 10^{-3}$ | 1.61 x | $1.17 \cdot 10^{-3}$ | $1.04 \cdot 10^{-3}$ | 1.13 x | Dense |
| Mixed_7b.branch3x3dbl.2.conv | $3.18 \cdot 10^{-3}$ | $9.82 \cdot 10^{-4}$ | 3.23 x | $3.21 \cdot 10^{-3}$ | $9.83 \cdot 10^{-4}$ | 3.26 x | General |
| Mixed_7b.branch.pool.conv | $9.54 \cdot 10^{-4}$ | $6.76 \cdot 10^{-4}$ | 1.41 x | $6.30 \cdot 10^{-4}$ | $6.75 \cdot 10^{-4}$ | 0.93 x | Dense |
| Mixed_7c.branch1x1.conv | $1.68 \cdot 10^{-3}$ | $1.08 \cdot 10^{-3}$ | 1.56 x | $1.27 \cdot 10^{-3}$ | $1.08 \cdot 10^{-3}$ | 1.18 x | Dense |
| Mixed_7c.branch3x3.1.conv | $1.98 \cdot 10^{-3}$ | $1.60 \cdot 10^{-3}$ | 1.23 x | $1.51 \cdot 10^{-3}$ | $1.60 \cdot 10^{-3}$ | 0.94 x | Dense |
| Mixed_7c.branch3x3dbl.1.conv | $2.25 \cdot 10^{-3}$ | $1.56 \cdot 10^{-3}$ | 1.44 x | $1.73 \cdot 10^{-3}$ | $1.56 \cdot 10^{-3}$ | 1.11 x | Dense |
| Mixed_7c.branch.pool.conv | $1.25 \cdot 10^{-3}$ | $1.04 \cdot 10^{-3}$ | 1.20 x | $9.35 \cdot 10^{-4}$ | $1.04 \cdot 10^{-3}$ | 0.90 x | Dense |

(h) MobileNetV2, input shape (32, 3, 256, 256)

| Name | TN [s] | PT [s] | Factor | TN + opt [s] | PT [s] | Factor | Type |
|----------------------|----------------------|----------------------|---------|----------------------|----------------------|---------------|---------|
| features.0.0 | $6.91 \cdot 10^{-3}$ | $7.23 \cdot 10^{-4}$ | 9.55 x | $6.92 \cdot 10^{-3}$ | $7.24 \cdot 10^{-4}$ | 9.56 x | General |
| features.1.conv.0.0 | $2.28 \cdot 10^{-2}$ | $2.05 \cdot 10^{-3}$ | 11.11 x | $2.28 \cdot 10^{-2}$ | $2.06 \cdot 10^{-3}$ | 11.09 x | General |
| features.1.conv.1 | $5.64 \cdot 10^{-3}$ | $7.61 \cdot 10^{-4}$ | 7.42 x | $1.56 \cdot 10^{-3}$ | $7.57 \cdot 10^{-4}$ | 2.06 x | Dense |
| features.2.conv.0.0 | $4.27 \cdot 10^{-3}$ | $1.74 \cdot 10^{-3}$ | 2.45 x | $2.02 \cdot 10^{-3}$ | $1.74 \cdot 10^{-3}$ | 1.16 x | Dense |
| features.2.conv.1.0 | $3.31 \cdot 10^{-2}$ | $1.69 \cdot 10^{-3}$ | 19.55 x | $3.31 \cdot 10^{-2}$ | $1.69 \cdot 10^{-3}$ | 19.56 x | General |
| features.2.conv.2 | $2.53 \cdot 10^{-3}$ | $4.93 \cdot 10^{-4}$ | 5.13 x | $1.08 \cdot 10^{-3}$ | $4.99 \cdot 10^{-4}$ | 2.16 x | Dense |
| features.3.conv.0.0 | $1.78 \cdot 10^{-3}$ | $7.88 \cdot 10^{-4}$ | 2.26 x | $9.63 \cdot 10^{-4}$ | $7.88 \cdot 10^{-4}$ | 1.22 x | Dense |
| features.3.conv.1.0 | $2.09 \cdot 10^{-2}$ | $2.30 \cdot 10^{-3}$ | 9.07 x | $2.09 \cdot 10^{-2}$ | $2.30 \cdot 10^{-3}$ | 9.06 x | General |
| features.3.conv.2 | $2.93 \cdot 10^{-3}$ | $6.33 \cdot 10^{-4}$ | 4.63 x | $1.47 \cdot 10^{-3}$ | $6.34 \cdot 10^{-4}$ | 2.33 x | Dense |
| features.4.conv.1.0 | $1.04 \cdot 10^{-2}$ | $6.62 \cdot 10^{-4}$ | 15.76 x | $1.04 \cdot 10^{-2}$ | $6.63 \cdot 10^{-4}$ | 15.72 x | General |
| features.4.conv.2 | $1.10 \cdot 10^{-3}$ | $2.61 \cdot 10^{-4}$ | 4.23 x | $5.03 \cdot 10^{-4}$ | $2.61 \cdot 10^{-4}$ | 1.92 x | Dense |
| features.5.conv.0.0 | $9.24 \cdot 10^{-4}$ | $3.32 \cdot 10^{-4}$ | 2.78 x | $5.07 \cdot 10^{-4}$ | $3.33 \cdot 10^{-4}$ | 1.52 x | Dense |
| features.5.conv.1.0 | $5.44 \cdot 10^{-3}$ | $7.87 \cdot 10^{-4}$ | 6.91 x | $5.42 \cdot 10^{-3}$ | $7.88 \cdot 10^{-4}$ | 6.88 x | General |
| features.5.conv.2 | $1.22 \cdot 10^{-3}$ | $3.11 \cdot 10^{-4}$ | 3.93 x | $6.16 \cdot 10^{-4}$ | $3.11 \cdot 10^{-4}$ | 1.98 x | Dense |
| features.7.conv.1.0 | $2.38 \cdot 10^{-3}$ | $2.49 \cdot 10^{-4}$ | 9.58 x | $2.37 \cdot 10^{-3}$ | $2.51 \cdot 10^{-4}$ | 9.44 x | General |
| features.7.conv.2 | $7.49 \cdot 10^{-4}$ | $2.09 \cdot 10^{-4}$ | 3.58 x | $3.20 \cdot 10^{-4}$ | $2.10 \cdot 10^{-4}$ | 1.53 x | Dense |
| features.8.conv.0.0 | $8.05 \cdot 10^{-4}$ | $2.91 \cdot 10^{-4}$ | 2.77 x | $4.42 \cdot 10^{-4}$ | $2.92 \cdot 10^{-4}$ | 1.51 x | Dense |
| features.8.conv.1.0 | $2.29 \cdot 10^{-3}$ | $4.14 \cdot 10^{-4}$ | 5.53 x | $2.27 \cdot 10^{-3}$ | $4.15 \cdot 10^{-4}$ | 5.48 x | General |
| features.8.conv.2 | $7.98 \cdot 10^{-4}$ | $3.07 \cdot 10^{-4}$ | 2.60 x | $4.63 \cdot 10^{-4}$ | $3.06 \cdot 10^{-4}$ | 1.51 x | Dense |
| features.11.conv.2 | $9.88 \cdot 10^{-4}$ | $4.08 \cdot 10^{-4}$ | 2.42 x | $5.67 \cdot 10^{-4}$ | $4.07 \cdot 10^{-4}$ | 1.39 x | Dense |
| features.12.conv.0.0 | $1.06 \cdot 10^{-3}$ | $4.92 \cdot 10^{-4}$ | 2.16 x | $5.64 \cdot 10^{-4}$ | $4.92 \cdot 10^{-4}$ | 1.14 x | Dense |
| features.12.conv.1.0 | $4.18 \cdot 10^{-3}$ | $6.04 \cdot 10^{-4}$ | 6.91 x | $4.16 \cdot 10^{-3}$ | $6.05 \cdot 10^{-4}$ | 6.87 x | General |
| features.12.conv.2 | $1.16 \cdot 10^{-3}$ | $5.53 \cdot 10^{-4}$ | 2.10 x | $7.40 \cdot 10^{-4}$ | $5.55 \cdot 10^{-4}$ | 1.33 x | Dense |
| features.14.conv.1.0 | $1.73 \cdot 10^{-3}$ | $2.29 \cdot 10^{-4}$ | 7.57 x | $1.72 \cdot 10^{-3}$ | $2.28 \cdot 10^{-4}$ | 7.53 x | General |
| features.14.conv.2 | $6.95 \cdot 10^{-4}$ | $3.90 \cdot 10^{-4}$ | 1.78 x | $4.10 \cdot 10^{-4}$ | $3.90 \cdot 10^{-4}$ | 1.05 x | Dense |
| features.15.conv.0.0 | $9.24 \cdot 10^{-4}$ | $3.53 \cdot 10^{-4}$ | 2.62 x | $4.36 \cdot 10^{-4}$ | $3.53 \cdot 10^{-4}$ | 1.23 x | Dense |
| features.15.conv.1.0 | $1.49 \cdot 10^{-3}$ | $2.72 \cdot 10^{-4}$ | 5.46 x | $1.47 \cdot 10^{-3}$ | $2.73 \cdot 10^{-4}$ | 5.39 x | General |
| features.15.conv.2 | $8.32 \cdot 10^{-4}$ | $5.80 \cdot 10^{-4}$ | 1.43 x | $5.44 \cdot 10^{-4}$ | $5.80 \cdot 10^{-4}$ | 0.94 x | Dense |
| features.17.conv.2 | $1.12 \cdot 10^{-3}$ | $9.74 \cdot 10^{-4}$ | 1.15 x | $7.14 \cdot 10^{-4}$ | $9.75 \cdot 10^{-4}$ | 0.73 x | Dense |
| features.18.0 | $1.25 \cdot 10^{-3}$ | $7.31 \cdot 10^{-4}$ | 1.71 x | $8.01 \cdot 10^{-4}$ | $7.31 \cdot 10^{-4}$ | 1.10 x | Dense |

E.3 INPUT VJP

We compare TN and TN+opt with a PyTorch implementation of the input VJP via `torch.autograd.grad`. Figure E17 visualizes the performance ratios for different convolution categories. Table E5 contains the detailed run times and performance factors.

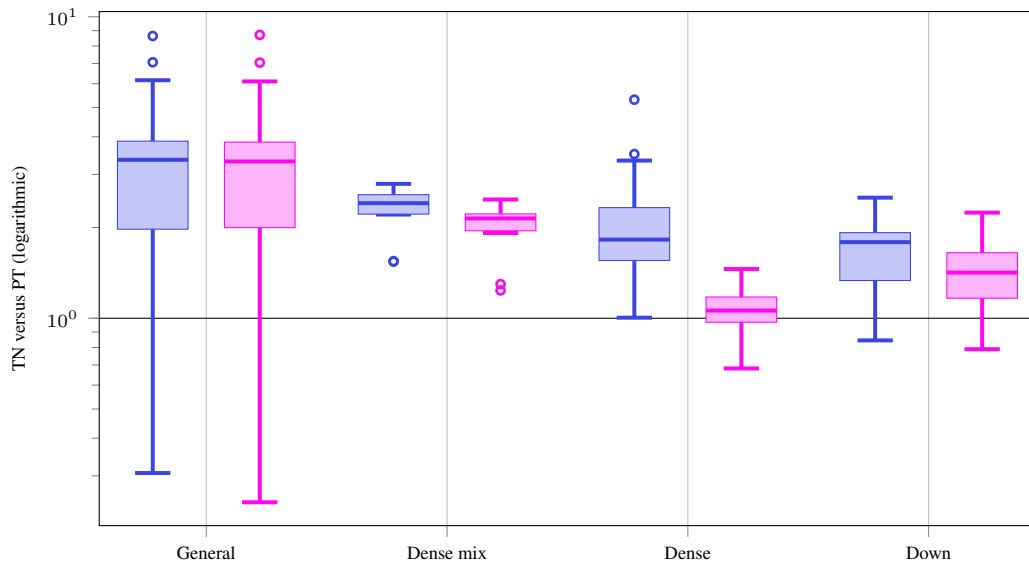


Figure E17: Input VJP performance ratios of TN versus PT and TN+opt versus PT for different convolution types on GPU.

Table E5: Input VJP performance comparison on GPU.

(a) 3c3d, CIFAR-10, input shape (128, 3, 32, 32)

| Name | TN [s] | PT [s] | Factor | TN + opt [s] | PT [s] | Factor | Type |
|---------|----------------------|----------------------|--------|----------------------|----------------------|--------|---------|
| conv1.0 | $2.24 \cdot 10^{-3}$ | $1.39 \cdot 10^{-3}$ | 1.61 x | $2.19 \cdot 10^{-3}$ | $1.34 \cdot 10^{-3}$ | 1.63 x | General |
| conv2.0 | $2.61 \cdot 10^{-3}$ | $8.29 \cdot 10^{-4}$ | 3.15 x | $2.55 \cdot 10^{-3}$ | $7.86 \cdot 10^{-4}$ | 3.25 x | General |
| conv3.1 | $1.46 \cdot 10^{-3}$ | $5.04 \cdot 10^{-4}$ | 2.90 x | $1.42 \cdot 10^{-3}$ | $4.69 \cdot 10^{-4}$ | 3.02 x | General |

(b) F-MNIST 2c2d, input shape (128, 1, 28, 28)

| Name | TN [s] | PT [s] | Factor | TN + opt [s] | PT [s] | Factor | Type |
|---------|----------------------|----------------------|--------|----------------------|----------------------|--------|---------|
| conv1.1 | $9.47 \cdot 10^{-4}$ | $4.36 \cdot 10^{-4}$ | 2.17 x | $8.86 \cdot 10^{-4}$ | $4.40 \cdot 10^{-4}$ | 2.02 x | General |
| conv2.1 | $3.67 \cdot 10^{-3}$ | $9.83 \cdot 10^{-4}$ | 3.74 x | $3.62 \cdot 10^{-3}$ | $9.83 \cdot 10^{-4}$ | 3.69 x | General |

(c) CIFAR-100 All-CNN-C, input shape (128, 3, 32, 32)

| Name | TN [s] | PT [s] | Factor | TN + opt [s] | PT [s] | Factor | Type |
|---------|----------------------|----------------------|--------|----------------------|----------------------|--------|---------|
| conv1.1 | $1.91 \cdot 10^{-3}$ | $9.84 \cdot 10^{-4}$ | 1.94 x | $1.87 \cdot 10^{-3}$ | $9.37 \cdot 10^{-4}$ | 2.00 x | General |
| conv2.1 | $2.00 \cdot 10^{-2}$ | $5.95 \cdot 10^{-3}$ | 3.35 x | $2.00 \cdot 10^{-2}$ | $5.92 \cdot 10^{-3}$ | 3.37 x | General |
| conv3.1 | $7.82 \cdot 10^{-3}$ | $5.05 \cdot 10^{-3}$ | 1.55 x | $7.77 \cdot 10^{-3}$ | $5.01 \cdot 10^{-3}$ | 1.55 x | General |
| conv4.1 | $8.23 \cdot 10^{-3}$ | $3.11 \cdot 10^{-3}$ | 2.65 x | $8.17 \cdot 10^{-3}$ | $3.10 \cdot 10^{-3}$ | 2.63 x | General |
| conv5.1 | $1.56 \cdot 10^{-2}$ | $4.36 \cdot 10^{-3}$ | 3.57 x | $1.55 \cdot 10^{-2}$ | $4.36 \cdot 10^{-3}$ | 3.56 x | General |
| conv6.1 | $4.58 \cdot 10^{-3}$ | $3.96 \cdot 10^{-3}$ | 1.16 x | $4.53 \cdot 10^{-3}$ | $3.96 \cdot 10^{-3}$ | 1.14 x | General |
| conv7.0 | $2.86 \cdot 10^{-3}$ | $8.32 \cdot 10^{-4}$ | 3.44 x | $2.81 \cdot 10^{-3}$ | $8.68 \cdot 10^{-4}$ | 3.24 x | General |
| conv8.1 | $8.31 \cdot 10^{-4}$ | $2.91 \cdot 10^{-4}$ | 2.85 x | $3.47 \cdot 10^{-4}$ | $3.32 \cdot 10^{-4}$ | 1.04 x | Dense |
| conv9.1 | $7.76 \cdot 10^{-4}$ | $2.21 \cdot 10^{-4}$ | 3.51 x | $2.90 \cdot 10^{-4}$ | $2.61 \cdot 10^{-4}$ | 1.11 x | Dense |

(d) Alexnet, input shape (32, 3, 256, 256)

| Name | TN [s] | PT [s] | Factor | TN + opt [s] | PT [s] | Factor | Type |
|-------------|----------------------|----------------------|--------|----------------------|----------------------|--------|---------|
| features.0 | $1.92 \cdot 10^{-2}$ | $5.48 \cdot 10^{-3}$ | 3.50 x | $1.92 \cdot 10^{-2}$ | $5.54 \cdot 10^{-3}$ | 3.46 x | General |
| features.3 | $1.15 \cdot 10^{-2}$ | $4.16 \cdot 10^{-3}$ | 2.77 x | $1.15 \cdot 10^{-2}$ | $4.20 \cdot 10^{-3}$ | 2.75 x | General |
| features.6 | $5.36 \cdot 10^{-3}$ | $1.49 \cdot 10^{-3}$ | 3.60 x | $5.36 \cdot 10^{-3}$ | $1.49 \cdot 10^{-3}$ | 3.60 x | General |
| features.8 | $6.26 \cdot 10^{-3}$ | $1.86 \cdot 10^{-3}$ | 3.36 x | $6.25 \cdot 10^{-3}$ | $1.86 \cdot 10^{-3}$ | 3.37 x | General |
| features.10 | $4.41 \cdot 10^{-3}$ | $1.32 \cdot 10^{-3}$ | 3.35 x | $4.40 \cdot 10^{-3}$ | $1.35 \cdot 10^{-3}$ | 3.26 x | General |

(e) ResNet18, input shape (32, 3, 256, 256)

| Name | TN [s] | PT [s] | Factor | TN + opt [s] | PT [s] | Factor | Type |
|-----------------------|----------------------|----------------------|---------------|----------------------|----------------------|---------------|---------|
| conv1 | $3.38 \cdot 10^{-2}$ | $8.56 \cdot 10^{-3}$ | 3.96 x | $3.38 \cdot 10^{-2}$ | $8.49 \cdot 10^{-3}$ | 3.98 x | General |
| layer1.0.conv1 | $1.06 \cdot 10^{-2}$ | $2.17 \cdot 10^{-3}$ | 4.87 x | $1.05 \cdot 10^{-2}$ | $2.11 \cdot 10^{-3}$ | 4.99 x | General |
| layer2.0.conv1 | $7.03 \cdot 10^{-3}$ | $3.72 \cdot 10^{-3}$ | 1.89 x | $6.95 \cdot 10^{-3}$ | $3.66 \cdot 10^{-3}$ | 1.90 x | General |
| layer2.0.conv2 | $6.91 \cdot 10^{-3}$ | $1.55 \cdot 10^{-3}$ | 4.47 x | $6.90 \cdot 10^{-3}$ | $1.51 \cdot 10^{-3}$ | 4.56 x | General |
| layer2.0.downsample.0 | $2.02 \cdot 10^{-3}$ | $8.02 \cdot 10^{-4}$ | 2.51 x | $1.71 \cdot 10^{-3}$ | $7.64 \cdot 10^{-4}$ | 2.24 x | Down |
| layer3.0.conv1 | $3.94 \cdot 10^{-3}$ | $3.05 \cdot 10^{-3}$ | 1.29 x | $3.88 \cdot 10^{-3}$ | $3.01 \cdot 10^{-3}$ | 1.29 x | General |
| layer3.0.conv2 | $5.07 \cdot 10^{-3}$ | $1.31 \cdot 10^{-3}$ | 3.87 x | $5.07 \cdot 10^{-3}$ | $1.36 \cdot 10^{-3}$ | 3.74 x | General |
| layer3.0.downsample.0 | $1.15 \cdot 10^{-3}$ | $5.96 \cdot 10^{-4}$ | 1.94 x | $9.54 \cdot 10^{-4}$ | $6.40 \cdot 10^{-4}$ | 1.49 x | Down |
| layer4.0.conv1 | $2.89 \cdot 10^{-3}$ | $3.08 \cdot 10^{-3}$ | 0.94 x | $2.84 \cdot 10^{-3}$ | $3.12 \cdot 10^{-3}$ | 0.91 x | General |
| layer4.0.conv2 | $4.50 \cdot 10^{-3}$ | $1.40 \cdot 10^{-3}$ | 3.21 x | $4.49 \cdot 10^{-3}$ | $1.44 \cdot 10^{-3}$ | 3.12 x | General |
| layer4.0.downsample.0 | $9.35 \cdot 10^{-4}$ | $5.51 \cdot 10^{-4}$ | 1.70 x | $7.93 \cdot 10^{-4}$ | $5.90 \cdot 10^{-4}$ | 1.34 x | Down |

(f) ResNext101, input shape (32, 3, 256, 256)

| Name | TN [s] | PT [s] | Factor | TN + opt [s] | PT [s] | Factor | Type |
|-----------------------|----------------------|----------------------|---------------|----------------------|----------------------|---------------|---------|
| conv1 | $3.38 \cdot 10^{-2}$ | $8.52 \cdot 10^{-3}$ | 3.97 x | $3.38 \cdot 10^{-2}$ | $8.48 \cdot 10^{-3}$ | 3.98 x | General |
| layer1.0.conv1 | $6.18 \cdot 10^{-3}$ | $1.96 \cdot 10^{-3}$ | 3.15 x | $2.86 \cdot 10^{-3}$ | $1.96 \cdot 10^{-3}$ | 1.46 x | Dense |
| layer1.0.conv2 | $3.04 \cdot 10^{-2}$ | $1.17 \cdot 10^{-2}$ | 2.60 x | $3.05 \cdot 10^{-2}$ | $1.17 \cdot 10^{-2}$ | 2.61 x | General |
| layer1.0.conv3 | $1.46 \cdot 10^{-2}$ | $6.57 \cdot 10^{-3}$ | 2.22 x | $7.39 \cdot 10^{-3}$ | $6.58 \cdot 10^{-3}$ | 1.12 x | Dense |
| layer2.0.conv1 | $2.40 \cdot 10^{-2}$ | $1.14 \cdot 10^{-2}$ | 2.10 x | $1.44 \cdot 10^{-2}$ | $1.17 \cdot 10^{-2}$ | 1.23 x | Dense |
| layer2.0.conv2 | $2.75 \cdot 10^{-2}$ | $1.96 \cdot 10^{-2}$ | 1.40 x | $2.75 \cdot 10^{-2}$ | $1.95 \cdot 10^{-2}$ | 1.41 x | General |
| layer2.0.conv3 | $1.04 \cdot 10^{-2}$ | $6.43 \cdot 10^{-3}$ | 1.61 x | $6.74 \cdot 10^{-3}$ | $6.43 \cdot 10^{-3}$ | 1.05 x | Dense |
| layer2.0.downsample.0 | $8.99 \cdot 10^{-3}$ | $4.78 \cdot 10^{-3}$ | 1.88 x | $8.06 \cdot 10^{-3}$ | $4.74 \cdot 10^{-3}$ | 1.70 x | Down |
| layer2.1.conv2 | $1.51 \cdot 10^{-2}$ | $4.46 \cdot 10^{-3}$ | 3.38 x | $1.51 \cdot 10^{-2}$ | $4.45 \cdot 10^{-3}$ | 3.39 x | General |
| layer3.0.conv1 | $1.94 \cdot 10^{-2}$ | $1.25 \cdot 10^{-2}$ | 1.55 x | $1.32 \cdot 10^{-2}$ | $1.25 \cdot 10^{-2}$ | 1.06 x | Dense |
| layer3.0.conv2 | $1.76 \cdot 10^{-2}$ | $8.33 \cdot 10^{-3}$ | 2.11 x | $1.76 \cdot 10^{-2}$ | $8.34 \cdot 10^{-3}$ | 2.11 x | General |
| layer3.0.conv3 | $8.21 \cdot 10^{-3}$ | $6.32 \cdot 10^{-3}$ | 1.30 x | $6.39 \cdot 10^{-3}$ | $6.32 \cdot 10^{-3}$ | 1.01 x | Dense |
| layer3.0.downsample.0 | $5.51 \cdot 10^{-3}$ | $4.54 \cdot 10^{-3}$ | 1.21 x | $5.00 \cdot 10^{-3}$ | $4.52 \cdot 10^{-3}$ | 1.11 x | Down |
| layer3.1.conv2 | $7.60 \cdot 10^{-3}$ | $1.97 \cdot 10^{-3}$ | 3.85 x | $7.60 \cdot 10^{-3}$ | $1.98 \cdot 10^{-3}$ | 3.84 x | General |
| layer4.0.conv1 | $1.51 \cdot 10^{-2}$ | $1.24 \cdot 10^{-2}$ | 1.22 x | $1.26 \cdot 10^{-2}$ | $1.24 \cdot 10^{-2}$ | 1.02 x | Dense |
| layer4.0.conv2 | $8.24 \cdot 10^{-3}$ | $5.43 \cdot 10^{-3}$ | 1.52 x | $8.24 \cdot 10^{-3}$ | $5.44 \cdot 10^{-3}$ | 1.51 x | General |
| layer4.0.conv3 | $7.65 \cdot 10^{-3}$ | $6.72 \cdot 10^{-3}$ | 1.14 x | $6.25 \cdot 10^{-3}$ | $6.73 \cdot 10^{-3}$ | 0.93 x | Dense |
| layer4.0.downsample.0 | $4.61 \cdot 10^{-3}$ | $5.45 \cdot 10^{-3}$ | 0.84 x | $4.31 \cdot 10^{-3}$ | $5.45 \cdot 10^{-3}$ | 0.79 x | Down |
| layer4.1.conv2 | $4.79 \cdot 10^{-3}$ | $1.34 \cdot 10^{-3}$ | 3.57 x | $4.79 \cdot 10^{-3}$ | $1.39 \cdot 10^{-3}$ | 3.44 x | General |

(g) InceptionV3, input shape (32, 3, 299, 299)

| Name | TN [s] | PT [s] | Factor | TN + opt [s] | PT [s] | Factor | Type |
|------------------------------|----------------------|----------------------|---------------|----------------------|----------------------|---------------|-----------|
| Conv2d_1a_3x3.conv | $1.27 \cdot 10^{-2}$ | $3.19 \cdot 10^{-3}$ | 3.97 x | $1.26 \cdot 10^{-2}$ | $3.21 \cdot 10^{-3}$ | 3.92 x | General |
| Conv2d_2a_3x3.conv | $3.16 \cdot 10^{-2}$ | $5.13 \cdot 10^{-3}$ | 6.16 x | $3.16 \cdot 10^{-2}$ | $5.17 \cdot 10^{-3}$ | 6.10 x | General |
| Conv2d_2b_3x3.conv | $4.32 \cdot 10^{-2}$ | $8.11 \cdot 10^{-3}$ | 5.33 x | $4.24 \cdot 10^{-2}$ | $8.17 \cdot 10^{-3}$ | 5.19 x | General |
| Conv2d_3b_1x1.conv | $5.76 \cdot 10^{-3}$ | $1.09 \cdot 10^{-3}$ | 5.31 x | $1.37 \cdot 10^{-3}$ | $1.09 \cdot 10^{-3}$ | 1.25 x | Dense |
| Conv2d_4a_3x3.conv | $3.71 \cdot 10^{-2}$ | $1.12 \cdot 10^{-2}$ | 3.30 x | $3.71 \cdot 10^{-2}$ | $1.12 \cdot 10^{-2}$ | 3.30 x | General |
| Mixed_5b.branch1x1.conv | $1.37 \cdot 10^{-3}$ | $6.89 \cdot 10^{-4}$ | 1.99 x | $6.67 \cdot 10^{-4}$ | $6.88 \cdot 10^{-4}$ | 0.97 x | Dense |
| Mixed_5b.branch5x5.1.conv | $1.13 \cdot 10^{-3}$ | $5.87 \cdot 10^{-4}$ | 1.92 x | $5.70 \cdot 10^{-4}$ | $5.88 \cdot 10^{-4}$ | 0.97 x | Dense |
| Mixed_5b.branch5x5.2.conv | $4.97 \cdot 10^{-3}$ | $1.39 \cdot 10^{-3}$ | 3.58 x | $4.97 \cdot 10^{-3}$ | $1.39 \cdot 10^{-3}$ | 3.57 x | General |
| Mixed_5b.branch3x3dbl.2.conv | $4.23 \cdot 10^{-3}$ | $1.07 \cdot 10^{-3}$ | 3.98 x | $4.23 \cdot 10^{-3}$ | $1.06 \cdot 10^{-3}$ | 3.98 x | General |
| Mixed_5b.branch3x3dbl.3.conv | $5.68 \cdot 10^{-3}$ | $1.66 \cdot 10^{-3}$ | 3.41 x | $5.68 \cdot 10^{-3}$ | $1.66 \cdot 10^{-3}$ | 3.41 x | General |
| Mixed_5b.branch.pool.conv | $9.70 \cdot 10^{-4}$ | $5.10 \cdot 10^{-4}$ | 1.90 x | $4.77 \cdot 10^{-4}$ | $5.13 \cdot 10^{-4}$ | 0.93 x | Dense |
| Mixed_5c.branch1x1.conv | $1.48 \cdot 10^{-3}$ | $8.10 \cdot 10^{-4}$ | 1.82 x | $8.07 \cdot 10^{-4}$ | $8.10 \cdot 10^{-4}$ | 1.00 x | Dense |
| Mixed_5c.branch5x5.1.conv | $1.23 \cdot 10^{-3}$ | $6.85 \cdot 10^{-4}$ | 1.79 x | $6.81 \cdot 10^{-4}$ | $6.87 \cdot 10^{-4}$ | 0.99 x | Dense |
| Mixed_5d.branch1x1.conv | $1.68 \cdot 10^{-3}$ | $1.04 \cdot 10^{-3}$ | 1.61 x | $9.40 \cdot 10^{-4}$ | $1.05 \cdot 10^{-3}$ | 0.90 x | Dense |
| Mixed_5d.branch5x5.1.conv | $1.38 \cdot 10^{-3}$ | $8.69 \cdot 10^{-4}$ | 1.59 x | $7.84 \cdot 10^{-4}$ | $8.12 \cdot 10^{-4}$ | 0.96 x | Dense |
| Mixed_6a.branch3x3.conv | $1.14 \cdot 10^{-2}$ | $1.32 \cdot 10^{-2}$ | 0.86 x | $1.14 \cdot 10^{-2}$ | $1.32 \cdot 10^{-2}$ | 0.86 x | General |
| Mixed_6a.branch3x3dbl.3.conv | $2.52 \cdot 10^{-3}$ | $1.70 \cdot 10^{-3}$ | 1.48 x | $2.46 \cdot 10^{-3}$ | $1.70 \cdot 10^{-3}$ | 1.45 x | General |
| Mixed_6b.branch1x1.conv | $1.78 \cdot 10^{-3}$ | $1.18 \cdot 10^{-3}$ | 1.50 x | $1.24 \cdot 10^{-3}$ | $1.19 \cdot 10^{-3}$ | 1.05 x | Dense |
| Mixed_6b.branch7x7.1.conv | $1.37 \cdot 10^{-3}$ | $8.69 \cdot 10^{-4}$ | 1.58 x | $9.27 \cdot 10^{-4}$ | $8.70 \cdot 10^{-4}$ | 1.07 x | Dense |
| Mixed_6b.branch7x7.2.conv | $2.13 \cdot 10^{-3}$ | $8.27 \cdot 10^{-4}$ | 2.58 x | $1.79 \cdot 10^{-3}$ | $8.27 \cdot 10^{-4}$ | 2.16 x | Dense mix |
| Mixed_6b.branch7x7.3.conv | $2.54 \cdot 10^{-3}$ | $1.08 \cdot 10^{-3}$ | 2.36 x | $2.22 \cdot 10^{-3}$ | $1.08 \cdot 10^{-3}$ | 2.05 x | Dense mix |
| Mixed_6b.branch7x7dbl.2.conv | $2.08 \cdot 10^{-3}$ | $8.10 \cdot 10^{-4}$ | 2.57 x | $1.80 \cdot 10^{-3}$ | $8.09 \cdot 10^{-4}$ | 2.22 x | Dense mix |
| Mixed_6b.branch7x7dbl.5.conv | $2.45 \cdot 10^{-3}$ | $1.11 \cdot 10^{-3}$ | 2.21 x | $2.14 \cdot 10^{-3}$ | $1.11 \cdot 10^{-3}$ | 1.92 x | Dense mix |
| Mixed_6c.branch7x7.1.conv | $1.56 \cdot 10^{-3}$ | $1.03 \cdot 10^{-3}$ | 1.52 x | $1.09 \cdot 10^{-3}$ | $1.03 \cdot 10^{-3}$ | 1.06 x | Dense |
| Mixed_6c.branch7x7.2.conv | $3.19 \cdot 10^{-3}$ | $1.14 \cdot 10^{-3}$ | 2.79 x | $2.76 \cdot 10^{-3}$ | $1.13 \cdot 10^{-3}$ | 2.43 x | Dense mix |
| Mixed_6c.branch7x7.3.conv | $3.06 \cdot 10^{-3}$ | $1.28 \cdot 10^{-3}$ | 2.40 x | $2.72 \cdot 10^{-3}$ | $1.28 \cdot 10^{-3}$ | 2.12 x | Dense mix |
| Mixed_6c.branch7x7dbl.2.conv | $3.10 \cdot 10^{-3}$ | $1.12 \cdot 10^{-3}$ | 2.78 x | $2.77 \cdot 10^{-3}$ | $1.12 \cdot 10^{-3}$ | 2.48 x | Dense mix |
| Mixed_6c.branch7x7dbl.5.conv | $2.96 \cdot 10^{-3}$ | $1.33 \cdot 10^{-3}$ | 2.22 x | $2.61 \cdot 10^{-3}$ | $1.33 \cdot 10^{-3}$ | 1.96 x | Dense mix |
| Mixed_6c.branch7x7.2.conv | $3.77 \cdot 10^{-3}$ | $1.54 \cdot 10^{-3}$ | 2.45 x | $3.26 \cdot 10^{-3}$ | $1.50 \cdot 10^{-3}$ | 2.17 x | Dense mix |
| Mixed_6c.branch7x7.3.conv | $3.65 \cdot 10^{-3}$ | $1.51 \cdot 10^{-3}$ | 2.42 x | $3.27 \cdot 10^{-3}$ | $1.47 \cdot 10^{-3}$ | 2.22 x | Dense mix |
| AuxLogits.conv0.conv | $5.53 \cdot 10^{-4}$ | $2.74 \cdot 10^{-4}$ | 2.02 x | $3.03 \cdot 10^{-4}$ | $2.34 \cdot 10^{-4}$ | 1.30 x | Dense |
| AuxLogits.conv1.conv | $6.27 \cdot 10^{-4}$ | $2.04 \cdot 10^{-3}$ | 0.31 x | $4.94 \cdot 10^{-4}$ | $2.02 \cdot 10^{-3}$ | 0.25 x | General |
| Mixed_7a.branch3x3.2.conv | $1.56 \cdot 10^{-3}$ | $7.08 \cdot 10^{-4}$ | 2.21 x | $1.47 \cdot 10^{-3}$ | $6.64 \cdot 10^{-4}$ | 2.22 x | General |
| Mixed_7a.branch7x7x3.4.conv | $1.46 \cdot 10^{-3}$ | $1.10 \cdot 10^{-3}$ | 1.33 x | $1.42 \cdot 10^{-3}$ | $1.14 \cdot 10^{-3}$ | 1.25 x | General |
| Mixed_7b.branch1x1.conv | $1.31 \cdot 10^{-3}$ | $7.40 \cdot 10^{-4}$ | 1.77 x | $8.47 \cdot 10^{-4}$ | $7.89 \cdot 10^{-4}$ | 1.07 x | Dense |
| Mixed_7b.branch3x3.1.conv | $1.44 \cdot 10^{-3}$ | $8.55 \cdot 10^{-4}$ | 1.69 x | $9.54 \cdot 10^{-4}$ | $9.00 \cdot 10^{-4}$ | 1.06 x | Dense |
| Mixed_7b.branch3x3.2a.conv | $1.51 \cdot 10^{-3}$ | $9.77 \cdot 10^{-4}$ | 1.55 x | $1.26 \cdot 10^{-3}$ | $1.02 \cdot 10^{-3}$ | 1.24 x | Dense mix |
| Mixed_7b.branch3x3.2b.conv | $1.50 \cdot 10^{-3}$ | $9.77 \cdot 10^{-4}$ | 1.54 x | $1.27 \cdot 10^{-3}$ | $9.78 \cdot 10^{-4}$ | 1.30 x | Dense mix |
| Mixed_7b.branch3x3dbl.1.conv | $1.56 \cdot 10^{-3}$ | $1.02 \cdot 10^{-3}$ | 1.54 x | $1.07 \cdot 10^{-3}$ | $9.72 \cdot 10^{-4}$ | 1.10 x | Dense |
| Mixed_7b.branch3x3dbl.2.conv | $3.32 \cdot 10^{-3}$ | $1.02 \cdot 10^{-3}$ | 3.24 x | $3.28 \cdot 10^{-3}$ | $9.91 \cdot 10^{-4}$ | 3.31 x | General |
| Mixed_7b.branch.pool.conv | $1.01 \cdot 10^{-3}$ | $5.57 \cdot 10^{-4}$ | 1.81 x | $6.18 \cdot 10^{-4}$ | $5.10 \cdot 10^{-4}$ | 1.21 x | Dense |
| Mixed_7c.branch1x1.conv | $1.69 \cdot 10^{-3}$ | $1.25 \cdot 10^{-3}$ | 1.35 x | $1.21 \cdot 10^{-3}$ | $1.22 \cdot 10^{-3}$ | 0.99 x | Dense |
| Mixed_7c.branch3x3.1.conv | $1.86 \cdot 10^{-3}$ | $1.45 \cdot 10^{-3}$ | 1.28 x | $1.39 \cdot 10^{-3}$ | $1.45 \cdot 10^{-3}$ | 0.95 x | Dense |
| Mixed_7c.branch3x3dbl.1.conv | $2.05 \cdot 10^{-3}$ | $1.66 \cdot 10^{-3}$ | 1.23 x | $1.57 \cdot 10^{-3}$ | $1.66 \cdot 10^{-3}$ | 0.95 x | Dense |
| Mixed_7c.branch.pool.conv | $1.27 \cdot 10^{-3}$ | $8.35 \cdot 10^{-4}$ | 1.53 x | $8.32 \cdot 10^{-4}$ | $8.35 \cdot 10^{-4}$ | 1.00 x | Dense |

(h) MobileNetV2, input shape (32, 3, 256, 256)

| Name | TN [s] | PT [s] | Factor | TN + opt [s] | PT [s] | Factor | Type |
|----------------------|----------------------|----------------------|--------|----------------------|----------------------|---------------|---------|
| features.0.0 | $8.32 \cdot 10^{-3}$ | $2.08 \cdot 10^{-3}$ | 4.01 x | $8.26 \cdot 10^{-3}$ | $2.02 \cdot 10^{-3}$ | 4.09 x | General |
| features.1.conv.0.0 | $2.27 \cdot 10^{-2}$ | $2.63 \cdot 10^{-3}$ | 8.64 x | $2.27 \cdot 10^{-2}$ | $2.60 \cdot 10^{-3}$ | 8.71 x | General |
| features.1.conv.1 | $3.22 \cdot 10^{-3}$ | $1.17 \cdot 10^{-3}$ | 2.75 x | $1.02 \cdot 10^{-3}$ | $1.16 \cdot 10^{-3}$ | 0.87 x | Dense |
| features.2.conv.0.0 | $7.67 \cdot 10^{-3}$ | $2.61 \cdot 10^{-3}$ | 2.94 x | $3.66 \cdot 10^{-3}$ | $2.61 \cdot 10^{-3}$ | 1.40 x | Dense |
| features.2.conv.1.0 | $2.79 \cdot 10^{-2}$ | $8.11 \cdot 10^{-3}$ | 3.44 x | $2.79 \cdot 10^{-2}$ | $8.11 \cdot 10^{-3}$ | 3.43 x | General |
| features.2.conv.2 | $1.48 \cdot 10^{-3}$ | $6.38 \cdot 10^{-4}$ | 2.33 x | $7.53 \cdot 10^{-4}$ | $6.40 \cdot 10^{-4}$ | 1.18 x | Dense |
| features.3.conv.0.0 | $2.86 \cdot 10^{-3}$ | $1.05 \cdot 10^{-3}$ | 2.73 x | $1.45 \cdot 10^{-3}$ | $1.05 \cdot 10^{-3}$ | 1.38 x | Dense |
| features.3.conv.1.0 | $2.08 \cdot 10^{-2}$ | $2.95 \cdot 10^{-3}$ | 7.07 x | $2.08 \cdot 10^{-2}$ | $2.95 \cdot 10^{-3}$ | 7.05 x | General |
| features.3.conv.2 | $1.77 \cdot 10^{-3}$ | $1.04 \cdot 10^{-3}$ | 1.70 x | $9.75 \cdot 10^{-4}$ | $1.04 \cdot 10^{-3}$ | 0.94 x | Dense |
| features.4.conv.1.0 | $7.63 \cdot 10^{-3}$ | $3.15 \cdot 10^{-3}$ | 2.42 x | $7.62 \cdot 10^{-3}$ | $3.15 \cdot 10^{-3}$ | 2.42 x | General |
| features.4.conv.2 | $9.49 \cdot 10^{-4}$ | $4.32 \cdot 10^{-4}$ | 2.20 x | $4.38 \cdot 10^{-4}$ | $3.88 \cdot 10^{-4}$ | 1.13 x | Dense |
| features.5.conv.0.0 | $1.20 \cdot 10^{-3}$ | $5.26 \cdot 10^{-4}$ | 2.29 x | $6.09 \cdot 10^{-4}$ | $4.83 \cdot 10^{-4}$ | 1.26 x | Dense |
| features.5.conv.1.0 | $5.41 \cdot 10^{-3}$ | $1.02 \cdot 10^{-3}$ | 5.29 x | $5.39 \cdot 10^{-3}$ | $1.02 \cdot 10^{-3}$ | 5.27 x | General |
| features.5.conv.2 | $9.53 \cdot 10^{-4}$ | $4.00 \cdot 10^{-4}$ | 2.38 x | $4.35 \cdot 10^{-4}$ | $3.98 \cdot 10^{-4}$ | 1.09 x | Dense |
| features.7.conv.1.0 | $2.11 \cdot 10^{-3}$ | $1.07 \cdot 10^{-3}$ | 1.97 x | $2.10 \cdot 10^{-3}$ | $1.07 \cdot 10^{-3}$ | 1.97 x | General |
| features.7.conv.2 | $7.77 \cdot 10^{-4}$ | $2.33 \cdot 10^{-4}$ | 3.34 x | $3.04 \cdot 10^{-4}$ | $2.33 \cdot 10^{-4}$ | 1.30 x | Dense |
| features.8.conv.0.0 | $8.13 \cdot 10^{-4}$ | $3.41 \cdot 10^{-4}$ | 2.38 x | $4.63 \cdot 10^{-4}$ | $3.40 \cdot 10^{-4}$ | 1.36 x | Dense |
| features.8.conv.1.0 | $2.09 \cdot 10^{-3}$ | $5.48 \cdot 10^{-4}$ | 3.81 x | $2.07 \cdot 10^{-3}$ | $5.47 \cdot 10^{-4}$ | 3.79 x | General |
| features.8.conv.2 | $8.65 \cdot 10^{-4}$ | $3.16 \cdot 10^{-4}$ | 2.74 x | $4.04 \cdot 10^{-4}$ | $3.16 \cdot 10^{-4}$ | 1.28 x | Dense |
| features.11.conv.2 | $9.34 \cdot 10^{-4}$ | $4.22 \cdot 10^{-4}$ | 2.21 x | $4.74 \cdot 10^{-4}$ | $4.24 \cdot 10^{-4}$ | 1.12 x | Dense |
| features.12.conv.0.0 | $1.16 \cdot 10^{-3}$ | $7.11 \cdot 10^{-4}$ | 1.64 x | $7.37 \cdot 10^{-4}$ | $7.10 \cdot 10^{-4}$ | 1.04 x | Dense |
| features.12.conv.1.0 | $3.84 \cdot 10^{-3}$ | $7.91 \cdot 10^{-4}$ | 4.85 x | $3.82 \cdot 10^{-3}$ | $7.91 \cdot 10^{-4}$ | 4.83 x | General |
| features.12.conv.2 | $1.08 \cdot 10^{-3}$ | $5.71 \cdot 10^{-4}$ | 1.90 x | $6.13 \cdot 10^{-4}$ | $5.73 \cdot 10^{-4}$ | 1.07 x | Dense |
| features.14.conv.1.0 | $1.61 \cdot 10^{-3}$ | $8.26 \cdot 10^{-4}$ | 1.95 x | $1.60 \cdot 10^{-3}$ | $8.26 \cdot 10^{-4}$ | 1.93 x | General |
| features.14.conv.2 | $8.14 \cdot 10^{-4}$ | $2.87 \cdot 10^{-4}$ | 2.83 x | $3.84 \cdot 10^{-4}$ | $2.87 \cdot 10^{-4}$ | 1.34 x | Dense |
| features.15.conv.0.0 | $8.46 \cdot 10^{-4}$ | $6.29 \cdot 10^{-4}$ | 1.34 x | $5.55 \cdot 10^{-4}$ | $6.08 \cdot 10^{-4}$ | 0.91 x | Dense |
| features.15.conv.1.0 | $1.52 \cdot 10^{-3}$ | $3.62 \cdot 10^{-4}$ | 4.21 x | $1.50 \cdot 10^{-3}$ | $3.61 \cdot 10^{-4}$ | 4.17 x | General |
| features.15.conv.2 | $9.64 \cdot 10^{-4}$ | $4.43 \cdot 10^{-4}$ | 2.18 x | $4.82 \cdot 10^{-4}$ | $4.44 \cdot 10^{-4}$ | 1.09 x | Dense |
| features.17.conv.2 | $1.23 \cdot 10^{-3}$ | $7.30 \cdot 10^{-4}$ | 1.69 x | $6.98 \cdot 10^{-4}$ | $7.32 \cdot 10^{-4}$ | 0.95 x | Dense |
| features.18.0 | $1.29 \cdot 10^{-3}$ | $1.28 \cdot 10^{-3}$ | 1.00 x | $8.76 \cdot 10^{-4}$ | $1.28 \cdot 10^{-3}$ | 0.68 x | Dense |

E.4 WEIGHT VJP

We compare TN and TN+opt with a PyTorch implementation of the weight VJP via `torch.autograd.grad`. Figure E18 visualizes the performance ratios for different convolution categories. Table E6 contains the detailed run times and performance factors.

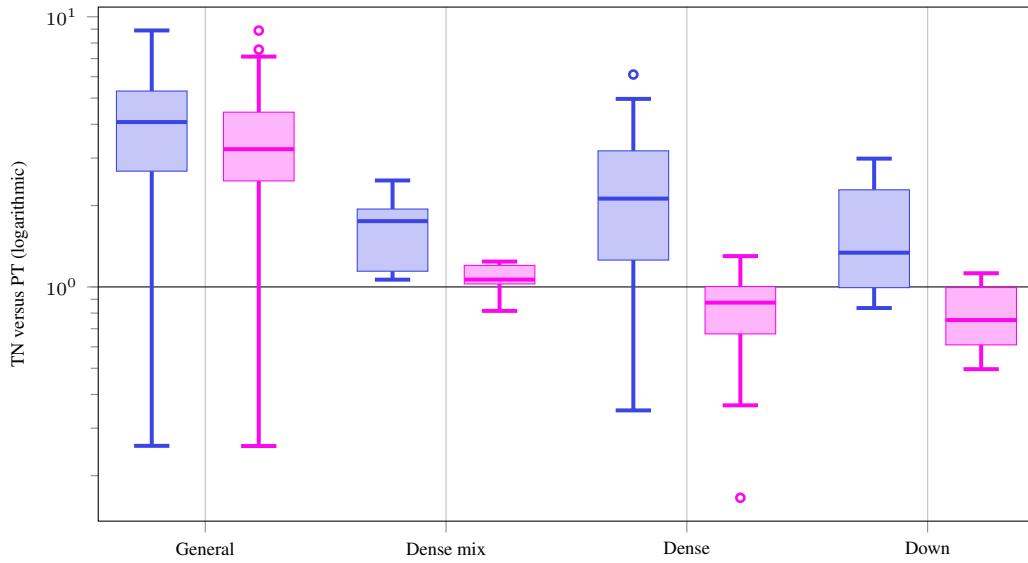


Figure E18: Weight VJP performance ratios of TN versus PT and TN+opt versus PT for different convolution types on GPU.

Table E6: Weight VJP performance comparison on GPU.

(a) 3c3d, CIFAR-10, input shape (128, 3, 32, 32)

| Name | TN [s] | PT [s] | Factor | TN + opt [s] | PT [s] | Factor | Type |
|---------|----------------------|----------------------|--------|----------------------|----------------------|--------|---------|
| conv1.0 | $2.27 \cdot 10^{-3}$ | $1.50 \cdot 10^{-3}$ | 1.52 x | $2.27 \cdot 10^{-3}$ | $1.50 \cdot 10^{-3}$ | 1.51 x | General |
| conv2.0 | $3.00 \cdot 10^{-3}$ | $1.12 \cdot 10^{-3}$ | 2.68 x | $2.99 \cdot 10^{-3}$ | $1.07 \cdot 10^{-3}$ | 2.78 x | General |
| conv3.1 | $1.29 \cdot 10^{-3}$ | $5.46 \cdot 10^{-4}$ | 2.37 x | $1.25 \cdot 10^{-3}$ | $5.08 \cdot 10^{-4}$ | 2.47 x | General |

(b) F-MNIST 2c2d, input shape (128, 1, 28, 28)

| Name | TN [s] | PT [s] | Factor | TN + opt [s] | PT [s] | Factor | Type |
|---------|----------------------|----------------------|--------|----------------------|----------------------|--------|---------|
| conv1.1 | $1.08 \cdot 10^{-3}$ | $3.81 \cdot 10^{-4}$ | 2.83 x | $1.03 \cdot 10^{-3}$ | $4.05 \cdot 10^{-4}$ | 2.54 x | General |
| conv2.1 | $4.12 \cdot 10^{-3}$ | $1.02 \cdot 10^{-3}$ | 4.02 x | $4.09 \cdot 10^{-3}$ | $1.03 \cdot 10^{-3}$ | 3.98 x | General |

(c) CIFAR-100 All-CNN-C, input shape (128, 3, 32, 32)

| Name | TN [s] | PT [s] | Factor | TN + opt [s] | PT [s] | Factor | Type |
|---------|----------------------|----------------------|---------------|----------------------|----------------------|---------------|---------|
| conv1.1 | $2.43 \cdot 10^{-3}$ | $1.02 \cdot 10^{-3}$ | 2.39 x | $2.42 \cdot 10^{-3}$ | $1.02 \cdot 10^{-3}$ | 2.37 x | General |
| conv2.1 | $3.83 \cdot 10^{-2}$ | $5.62 \cdot 10^{-3}$ | 6.81 x | $1.97 \cdot 10^{-2}$ | $5.62 \cdot 10^{-3}$ | 3.51 x | General |
| conv3.1 | $8.30 \cdot 10^{-3}$ | $4.14 \cdot 10^{-3}$ | 2.00 x | $8.33 \cdot 10^{-3}$ | $4.21 \cdot 10^{-3}$ | 1.98 x | General |
| conv4.1 | $8.66 \cdot 10^{-3}$ | $2.64 \cdot 10^{-3}$ | 3.28 x | $8.68 \cdot 10^{-3}$ | $2.68 \cdot 10^{-3}$ | 3.24 x | General |
| conv5.1 | $1.60 \cdot 10^{-2}$ | $3.38 \cdot 10^{-3}$ | 4.75 x | $1.61 \cdot 10^{-2}$ | $3.42 \cdot 10^{-3}$ | 4.70 x | General |
| conv6.1 | $5.23 \cdot 10^{-3}$ | $2.80 \cdot 10^{-3}$ | 1.87 x | $5.17 \cdot 10^{-3}$ | $2.81 \cdot 10^{-3}$ | 1.84 x | General |
| conv7.0 | $2.68 \cdot 10^{-3}$ | $9.97 \cdot 10^{-4}$ | 2.68 x | $2.59 \cdot 10^{-3}$ | $1.04 \cdot 10^{-3}$ | 2.49 x | General |
| conv8.1 | $9.13 \cdot 10^{-4}$ | $2.62 \cdot 10^{-3}$ | 0.35 x | $4.33 \cdot 10^{-4}$ | $2.62 \cdot 10^{-3}$ | 0.17 x | Dense |
| conv9.1 | $8.78 \cdot 10^{-4}$ | $3.54 \cdot 10^{-4}$ | 2.48 x | $3.93 \cdot 10^{-4}$ | $3.50 \cdot 10^{-4}$ | 1.12 x | Dense |

(d) Alexnet, input shape (32, 3, 256, 256)

| Name | TN [s] | PT [s] | Factor | TN + opt [s] | PT [s] | Factor | Type |
|-------------|----------------------|----------------------|--------|----------------------|----------------------|--------|---------|
| features.0 | $1.82 \cdot 10^{-2}$ | $3.31 \cdot 10^{-3}$ | 5.50 x | $1.82 \cdot 10^{-2}$ | $3.33 \cdot 10^{-3}$ | 5.46 x | General |
| features.3 | $2.02 \cdot 10^{-2}$ | $2.57 \cdot 10^{-3}$ | 7.85 x | $1.14 \cdot 10^{-2}$ | $2.58 \cdot 10^{-3}$ | 4.44 x | General |
| features.6 | $6.98 \cdot 10^{-3}$ | $1.67 \cdot 10^{-3}$ | 4.19 x | $5.17 \cdot 10^{-3}$ | $1.67 \cdot 10^{-3}$ | 3.10 x | General |
| features.8 | $8.16 \cdot 10^{-3}$ | $1.97 \cdot 10^{-3}$ | 4.15 x | $6.13 \cdot 10^{-3}$ | $1.97 \cdot 10^{-3}$ | 3.11 x | General |
| features.10 | $5.80 \cdot 10^{-3}$ | $1.47 \cdot 10^{-3}$ | 3.94 x | $4.34 \cdot 10^{-3}$ | $1.47 \cdot 10^{-3}$ | 2.95 x | General |

(e) ResNet18, input shape (32, 3, 256, 256)

| Name | TN [s] | PT [s] | Factor | TN + opt [s] | PT [s] | Factor | Type |
|-----------------------|----------------------|----------------------|---------------|----------------------|----------------------|---------------|---------|
| conv1 | $3.00 \cdot 10^{-2}$ | $8.23 \cdot 10^{-3}$ | 3.65 x | $2.99 \cdot 10^{-2}$ | $7.83 \cdot 10^{-3}$ | 3.82 x | General |
| layer1.0.conv1 | $2.34 \cdot 10^{-2}$ | $3.18 \cdot 10^{-3}$ | 7.37 x | $1.10 \cdot 10^{-2}$ | $3.22 \cdot 10^{-3}$ | 3.43 x | General |
| layer2.0.conv1 | $5.88 \cdot 10^{-3}$ | $2.97 \cdot 10^{-3}$ | 1.98 x | $5.87 \cdot 10^{-3}$ | $2.96 \cdot 10^{-3}$ | 1.98 x | General |
| layer2.0.conv2 | $1.17 \cdot 10^{-2}$ | $1.66 \cdot 10^{-3}$ | 7.03 x | $6.98 \cdot 10^{-3}$ | $1.66 \cdot 10^{-3}$ | 4.20 x | General |
| layer2.0.downsample.0 | $1.85 \cdot 10^{-3}$ | $7.39 \cdot 10^{-4}$ | 2.51 x | $7.60 \cdot 10^{-4}$ | $7.33 \cdot 10^{-4}$ | 1.04 x | Down |
| layer3.0.conv1 | $3.79 \cdot 10^{-3}$ | $2.71 \cdot 10^{-3}$ | 1.40 x | $3.76 \cdot 10^{-3}$ | $2.71 \cdot 10^{-3}$ | 1.39 x | General |
| layer3.0.conv2 | $6.62 \cdot 10^{-3}$ | $1.48 \cdot 10^{-3}$ | 4.46 x | $4.87 \cdot 10^{-3}$ | $1.48 \cdot 10^{-3}$ | 3.28 x | General |
| layer3.0.downsample.0 | $1.61 \cdot 10^{-3}$ | $5.39 \cdot 10^{-4}$ | 2.99 x | $6.12 \cdot 10^{-4}$ | $5.45 \cdot 10^{-4}$ | 1.12 x | Down |
| layer4.0.conv1 | $2.85 \cdot 10^{-3}$ | $2.46 \cdot 10^{-3}$ | 1.16 x | $2.82 \cdot 10^{-3}$ | $2.46 \cdot 10^{-3}$ | 1.15 x | General |
| layer4.0.conv2 | $4.83 \cdot 10^{-3}$ | $1.72 \cdot 10^{-3}$ | 2.80 x | $4.31 \cdot 10^{-3}$ | $1.72 \cdot 10^{-3}$ | 2.50 x | General |
| layer4.0.downsample.0 | $1.00 \cdot 10^{-3}$ | $1.02 \cdot 10^{-3}$ | 0.98 x | $5.07 \cdot 10^{-4}$ | $1.02 \cdot 10^{-3}$ | 0.50 x | Down |

(f) ResNext101, input shape (32, 3, 256, 256)

| Name | TN [s] | PT [s] | Factor | TN + opt [s] | PT [s] | Factor | Type |
|-----------------------|----------------------|----------------------|---------------|----------------------|----------------------|---------------|---------|
| conv1 | $3.00 \cdot 10^{-2}$ | $8.22 \cdot 10^{-3}$ | 3.65 x | $2.99 \cdot 10^{-2}$ | $7.83 \cdot 10^{-3}$ | 3.82 x | General |
| layer1.0.conv1 | $7.08 \cdot 10^{-3}$ | $2.92 \cdot 10^{-3}$ | 2.42 x | $3.75 \cdot 10^{-3}$ | $2.89 \cdot 10^{-3}$ | 1.30 x | Dense |
| layer1.0.conv2 | $6.70 \cdot 10^{-2}$ | $2.53 \cdot 10^{-2}$ | 2.65 x | $6.72 \cdot 10^{-2}$ | $1.91 \cdot 10^{-2}$ | 3.51 x | General |
| layer1.0.conv3 | $3.12 \cdot 10^{-2}$ | $8.78 \cdot 10^{-3}$ | 3.55 x | $1.04 \cdot 10^{-2}$ | $1.02 \cdot 10^{-2}$ | 1.02 x | Dense |
| layer2.0.conv1 | $2.29 \cdot 10^{-2}$ | $1.80 \cdot 10^{-2}$ | 1.28 x | $1.77 \cdot 10^{-2}$ | $1.76 \cdot 10^{-2}$ | 1.01 x | Dense |
| layer2.0.conv2 | $6.64 \cdot 10^{-2}$ | $1.23 \cdot 10^{-2}$ | 5.40 x | $6.63 \cdot 10^{-2}$ | $1.23 \cdot 10^{-2}$ | 5.39 x | General |
| layer2.0.conv3 | $1.82 \cdot 10^{-2}$ | $5.90 \cdot 10^{-3}$ | 3.08 x | $8.44 \cdot 10^{-3}$ | $6.50 \cdot 10^{-3}$ | 1.30 x | Dense |
| layer2.0.downsample.0 | $8.57 \cdot 10^{-3}$ | $5.24 \cdot 10^{-3}$ | 1.64 x | $4.55 \cdot 10^{-3}$ | $5.24 \cdot 10^{-3}$ | 0.87 x | Down |
| layer2.1.conv2 | $4.04 \cdot 10^{-2}$ | $1.21 \cdot 10^{-2}$ | 3.33 x | $4.04 \cdot 10^{-2}$ | $1.22 \cdot 10^{-2}$ | 3.32 x | General |
| layer3.0.conv1 | $1.84 \cdot 10^{-2}$ | $2.03 \cdot 10^{-2}$ | 0.91 x | $1.48 \cdot 10^{-2}$ | $2.03 \cdot 10^{-2}$ | 0.73 x | Dense |
| layer3.0.conv2 | $1.63 \cdot 10^{-2}$ | $5.77 \cdot 10^{-3}$ | 2.83 x | $1.63 \cdot 10^{-2}$ | $5.82 \cdot 10^{-3}$ | 2.81 x | General |
| layer3.0.conv3 | $1.17 \cdot 10^{-2}$ | $1.07 \cdot 10^{-2}$ | 1.10 x | $7.19 \cdot 10^{-3}$ | $1.07 \cdot 10^{-2}$ | 0.67 x | Dense |
| layer3.0.downsample.0 | $6.19 \cdot 10^{-3}$ | $5.95 \cdot 10^{-3}$ | 1.04 x | $3.85 \cdot 10^{-3}$ | $6.01 \cdot 10^{-3}$ | 0.64 x | Down |
| layer3.1.conv2 | $1.47 \cdot 10^{-2}$ | $3.17 \cdot 10^{-3}$ | 4.65 x | $1.47 \cdot 10^{-2}$ | $3.14 \cdot 10^{-3}$ | 4.67 x | General |
| layer4.0.conv1 | $1.55 \cdot 10^{-2}$ | $2.10 \cdot 10^{-2}$ | 0.74 x | $1.33 \cdot 10^{-2}$ | $2.11 \cdot 10^{-2}$ | 0.63 x | Dense |
| layer4.0.conv2 | $8.07 \cdot 10^{-3}$ | $3.13 \cdot 10^{-2}$ | 0.26 x | $8.06 \cdot 10^{-3}$ | $3.13 \cdot 10^{-2}$ | 0.26 x | General |
| layer4.0.conv3 | $8.23 \cdot 10^{-3}$ | $1.06 \cdot 10^{-2}$ | 0.78 x | $6.75 \cdot 10^{-3}$ | $1.06 \cdot 10^{-2}$ | 0.63 x | Dense |
| layer4.0.downsample.0 | $4.96 \cdot 10^{-3}$ | $5.94 \cdot 10^{-3}$ | 0.84 x | $3.59 \cdot 10^{-3}$ | $5.99 \cdot 10^{-3}$ | 0.60 x | Down |
| layer4.1.conv2 | $6.63 \cdot 10^{-3}$ | $1.40 \cdot 10^{-3}$ | 4.72 x | $6.62 \cdot 10^{-3}$ | $1.45 \cdot 10^{-3}$ | 4.55 x | General |

(g) InceptionV3, input shape (32, 3, 299, 299)

| Name | TN [s] | PT [s] | Factor | TN + opt [s] | PT [s] | Factor | Type |
|------------------------------|----------------------|----------------------|---------------|----------------------|----------------------|---------------|-----------|
| Conv2d_1a_3x3.conv | $1.07 \cdot 10^{-2}$ | $1.70 \cdot 10^{-3}$ | 6.31 x | $1.07 \cdot 10^{-2}$ | $1.70 \cdot 10^{-3}$ | 6.29 x | General |
| Conv2d_2a_3x3.conv | $6.00 \cdot 10^{-2}$ | $1.16 \cdot 10^{-2}$ | 5.18 x | $3.11 \cdot 10^{-2}$ | $1.16 \cdot 10^{-2}$ | 2.68 x | General |
| Conv2d_2b_3x3.conv | $6.10 \cdot 10^{-2}$ | $1.34 \cdot 10^{-2}$ | 4.55 x | $4.27 \cdot 10^{-2}$ | $1.53 \cdot 10^{-2}$ | 2.78 x | General |
| Conv2d_3b_1x1.conv | $5.48 \cdot 10^{-3}$ | $1.82 \cdot 10^{-3}$ | 3.01 x | $2.26 \cdot 10^{-3}$ | $2.12 \cdot 10^{-3}$ | 1.07 x | Dense |
| Conv2d_4a_3x3.conv | $5.28 \cdot 10^{-2}$ | $1.29 \cdot 10^{-2}$ | 4.08 x | $3.39 \cdot 10^{-2}$ | $1.29 \cdot 10^{-2}$ | 2.62 x | General |
| Mixed_5b.branch1x1.conv | $5.14 \cdot 10^{-3}$ | $1.16 \cdot 10^{-3}$ | 4.43 x | $1.41 \cdot 10^{-3}$ | $1.48 \cdot 10^{-3}$ | 0.95 x | Dense |
| Mixed_5b.branch5x5_1.conv | $4.92 \cdot 10^{-3}$ | $1.46 \cdot 10^{-3}$ | 3.37 x | $1.39 \cdot 10^{-3}$ | $1.47 \cdot 10^{-3}$ | 0.95 x | Dense |
| Mixed_5b.branch3x3dbl_1.conv | $9.28 \cdot 10^{-3}$ | $1.28 \cdot 10^{-3}$ | 7.23 x | $4.83 \cdot 10^{-3}$ | $1.28 \cdot 10^{-3}$ | 3.77 x | General |
| Mixed_5b.branch3x3dbl_2.conv | $7.78 \cdot 10^{-3}$ | $1.75 \cdot 10^{-3}$ | 4.45 x | $4.22 \cdot 10^{-3}$ | $1.75 \cdot 10^{-3}$ | 2.41 x | General |
| Mixed_5b.branch3x3dbl_3.conv | $1.05 \cdot 10^{-2}$ | $1.86 \cdot 10^{-3}$ | 5.63 x | $6.00 \cdot 10^{-3}$ | $1.87 \cdot 10^{-3}$ | 3.21 x | General |
| Mixed_5b.branch.pool.conv | $4.52 \cdot 10^{-3}$ | $9.10 \cdot 10^{-4}$ | 4.97 x | $1.16 \cdot 10^{-3}$ | $8.96 \cdot 10^{-4}$ | 1.30 x | Dense |
| Mixed_5c.branch1x1.conv | $6.55 \cdot 10^{-3}$ | $2.00 \cdot 10^{-3}$ | 3.27 x | $1.67 \cdot 10^{-3}$ | $1.93 \cdot 10^{-3}$ | 0.86 x | Dense |
| Mixed_5c.branch5x5_1.conv | $6.33 \cdot 10^{-3}$ | $1.93 \cdot 10^{-3}$ | 3.28 x | $1.64 \cdot 10^{-3}$ | $1.86 \cdot 10^{-3}$ | 0.88 x | Dense |
| Mixed_5d.branch1x1.conv | $7.46 \cdot 10^{-3}$ | $2.34 \cdot 10^{-3}$ | 3.19 x | $2.03 \cdot 10^{-3}$ | $2.31 \cdot 10^{-3}$ | 0.88 x | Dense |
| Mixed_5d.branch5x5_1.conv | $7.24 \cdot 10^{-3}$ | $2.16 \cdot 10^{-3}$ | 3.36 x | $2.00 \cdot 10^{-3}$ | $2.15 \cdot 10^{-3}$ | 0.93 x | Dense |
| Mixed_6a.branch3x3.conv | $1.10 \cdot 10^{-2}$ | $8.34 \cdot 10^{-3}$ | 1.32 x | $1.09 \cdot 10^{-2}$ | $8.34 \cdot 10^{-3}$ | 1.31 x | General |
| Mixed_6a.branch3x3dbl_3.conv | $2.46 \cdot 10^{-3}$ | $1.12 \cdot 10^{-3}$ | 2.20 x | $2.42 \cdot 10^{-3}$ | $1.12 \cdot 10^{-3}$ | 2.17 x | General |
| Mixed_6b.branch1x1.conv | $5.17 \cdot 10^{-3}$ | $2.05 \cdot 10^{-3}$ | 2.52 x | $1.86 \cdot 10^{-3}$ | $2.07 \cdot 10^{-3}$ | 0.90 x | Dense |
| Mixed_6b.branch7x7_1.conv | $4.63 \cdot 10^{-3}$ | $1.56 \cdot 10^{-3}$ | 2.96 x | $1.46 \cdot 10^{-3}$ | $1.61 \cdot 10^{-3}$ | 0.91 x | Dense |
| Mixed_6b.branch7x7_2.conv | $3.09 \cdot 10^{-3}$ | $1.59 \cdot 10^{-3}$ | 1.94 x | $2.01 \cdot 10^{-3}$ | $1.64 \cdot 10^{-3}$ | 1.22 x | Dense mix |
| Mixed_6b.branch7x7_3.conv | $3.44 \cdot 10^{-3}$ | $2.29 \cdot 10^{-3}$ | 1.50 x | $2.37 \cdot 10^{-3}$ | $2.33 \cdot 10^{-3}$ | 1.01 x | Dense mix |
| Mixed_6b.branch7x7dbl_2.conv | $4.06 \cdot 10^{-3}$ | $1.64 \cdot 10^{-3}$ | 2.48 x | $1.81 \cdot 10^{-3}$ | $1.68 \cdot 10^{-3}$ | 1.08 x | Dense mix |
| Mixed_6b.branch7x7dbl_5.conv | $2.51 \cdot 10^{-3}$ | $2.24 \cdot 10^{-3}$ | 1.12 x | $2.85 \cdot 10^{-3}$ | $2.29 \cdot 10^{-3}$ | 1.24 x | Dense mix |
| Mixed_6c.branch7x7_1.conv | $4.99 \cdot 10^{-3}$ | $1.98 \cdot 10^{-3}$ | 2.53 x | $1.77 \cdot 10^{-3}$ | $2.03 \cdot 10^{-3}$ | 0.87 x | Dense |
| Mixed_6c.branch7x7_2.conv | $4.87 \cdot 10^{-3}$ | $2.71 \cdot 10^{-3}$ | 1.80 x | $3.30 \cdot 10^{-3}$ | $2.75 \cdot 10^{-3}$ | 1.20 x | Dense mix |
| Mixed_6c.branch7x7_3.conv | $4.85 \cdot 10^{-3}$ | $2.84 \cdot 10^{-3}$ | 1.71 x | $2.99 \cdot 10^{-3}$ | $2.87 \cdot 10^{-3}$ | 1.04 x | Dense mix |
| Mixed_6c.branch7x7dbl_2.conv | $5.43 \cdot 10^{-3}$ | $2.80 \cdot 10^{-3}$ | 1.94 x | $2.95 \cdot 10^{-3}$ | $2.80 \cdot 10^{-3}$ | 1.05 x | Dense mix |
| Mixed_6c.branch7x7dbl_5.conv | $3.20 \cdot 10^{-3}$ | $2.78 \cdot 10^{-3}$ | 1.15 x | $3.41 \cdot 10^{-3}$ | $2.82 \cdot 10^{-3}$ | 1.21 x | Dense mix |
| Mixed_6e.branch7x7_2.conv | $5.96 \cdot 10^{-3}$ | $3.19 \cdot 10^{-3}$ | 1.87 x | $3.83 \cdot 10^{-3}$ | $3.24 \cdot 10^{-3}$ | 1.18 x | Dense mix |
| Mixed_6e.branch7x7_3.conv | $6.50 \cdot 10^{-3}$ | $3.26 \cdot 10^{-3}$ | 1.99 x | $3.40 \cdot 10^{-3}$ | $3.30 \cdot 10^{-3}$ | 1.03 x | Dense mix |
| AuxLogits.conv0.conv | $6.48 \cdot 10^{-4}$ | $3.45 \cdot 10^{-4}$ | 1.87 x | $3.45 \cdot 10^{-4}$ | $3.88 \cdot 10^{-4}$ | 0.89 x | Dense |
| AuxLogits.conv1.conv | $5.34 \cdot 10^{-4}$ | $2.09 \cdot 10^{-4}$ | 2.56 x | $4.59 \cdot 10^{-4}$ | $2.76 \cdot 10^{-4}$ | 1.66 x | General |
| Mixed_7a.branch3x3_2.conv | $1.80 \cdot 10^{-3}$ | $5.61 \cdot 10^{-4}$ | 3.22 x | $1.78 \cdot 10^{-3}$ | $6.16 \cdot 10^{-4}$ | 2.90 x | General |
| Mixed_7a.branch7x7x3_4.conv | $1.55 \cdot 10^{-3}$ | $8.46 \cdot 10^{-4}$ | 1.83 x | $1.52 \cdot 10^{-3}$ | $8.50 \cdot 10^{-4}$ | 1.79 x | General |
| Mixed_7b.branch1x1.conv | $2.08 \cdot 10^{-3}$ | $1.62 \cdot 10^{-3}$ | 1.28 x | $1.07 \cdot 10^{-3}$ | $1.63 \cdot 10^{-3}$ | 0.66 x | Dense |
| Mixed_7b.branch3x3_1.conv | $2.19 \cdot 10^{-3}$ | $1.65 \cdot 10^{-3}$ | 1.33 x | $1.17 \cdot 10^{-3}$ | $1.65 \cdot 10^{-3}$ | 0.71 x | Dense |
| Mixed_7b.branch3x3_2a.conv | $1.56 \cdot 10^{-3}$ | $1.47 \cdot 10^{-3}$ | 1.06 x | $1.20 \cdot 10^{-3}$ | $1.47 \cdot 10^{-3}$ | 0.82 x | Dense mix |
| Mixed_7b.branch3x3_2b.conv | $1.66 \cdot 10^{-3}$ | $1.50 \cdot 10^{-3}$ | 1.11 x | $1.22 \cdot 10^{-3}$ | $1.50 \cdot 10^{-3}$ | 0.82 x | Dense mix |
| Mixed_7b.branch3x3dbl_1.conv | $2.34 \cdot 10^{-3}$ | $1.65 \cdot 10^{-3}$ | 1.42 x | $1.33 \cdot 10^{-3}$ | $1.66 \cdot 10^{-3}$ | 0.80 x | Dense |
| Mixed_7b.branch3x3dbl_2.conv | $3.55 \cdot 10^{-3}$ | $1.23 \cdot 10^{-3}$ | 2.90 x | $3.10 \cdot 10^{-3}$ | $1.26 \cdot 10^{-3}$ | 2.45 x | General |
| Mixed_7b.branch.pool.conv | $1.84 \cdot 10^{-3}$ | $1.46 \cdot 10^{-3}$ | 1.26 x | $8.67 \cdot 10^{-4}$ | $1.46 \cdot 10^{-3}$ | 0.59 x | Dense |
| Mixed_7c.branch1x1.conv | $3.07 \cdot 10^{-3}$ | $3.08 \cdot 10^{-3}$ | 1.00 x | $1.55 \cdot 10^{-3}$ | $3.12 \cdot 10^{-3}$ | 0.50 x | Dense |
| Mixed_7c.branch3x3_1.conv | $3.30 \cdot 10^{-3}$ | $3.11 \cdot 10^{-3}$ | 1.06 x | $1.79 \cdot 10^{-3}$ | $3.11 \cdot 10^{-3}$ | 0.58 x | Dense |
| Mixed_7c.branch3x3dbl_1.conv | $3.56 \cdot 10^{-3}$ | $3.11 \cdot 10^{-3}$ | 1.15 x | $2.03 \cdot 10^{-3}$ | $3.10 \cdot 10^{-3}$ | 0.65 x | Dense |
| Mixed_7c.branch.pool.conv | $2.70 \cdot 10^{-3}$ | $1.61 \cdot 10^{-3}$ | 1.68 x | $1.22 \cdot 10^{-3}$ | $1.61 \cdot 10^{-3}$ | 0.76 x | Dense |

(h) MobileNetV2, input shape (32, 3, 256, 256)

| Name | TN [s] | PT [s] | Factor | TN + opt [s] | PT [s] | Factor | Type |
|----------------------|----------------------|----------------------|---------------|----------------------|----------------------|---------------|---------|
| features.0.0 | $7.70 \cdot 10^{-3}$ | $1.45 \cdot 10^{-3}$ | 5.30 x | $7.67 \cdot 10^{-3}$ | $1.46 \cdot 10^{-3}$ | 5.26 x | General |
| features.1.conv.0.0 | $1.59 \cdot 10^{-2}$ | $2.46 \cdot 10^{-3}$ | 6.48 x | $1.59 \cdot 10^{-2}$ | $2.47 \cdot 10^{-3}$ | 6.46 x | General |
| features.1.conv.1 | $1.47 \cdot 10^{-2}$ | $2.40 \cdot 10^{-3}$ | 6.11 x | $2.64 \cdot 10^{-3}$ | $2.39 \cdot 10^{-3}$ | 1.10 x | Dense |
| features.2.conv.0.0 | $8.97 \cdot 10^{-3}$ | $4.95 \cdot 10^{-3}$ | 1.81 x | $4.22 \cdot 10^{-3}$ | $4.95 \cdot 10^{-3}$ | 0.85 x | Dense |
| features.2.conv.1.0 | $2.14 \cdot 10^{-2}$ | $2.40 \cdot 10^{-3}$ | 8.90 x | $2.14 \cdot 10^{-2}$ | $2.41 \cdot 10^{-3}$ | 8.89 x | General |
| features.2.conv.2 | $7.38 \cdot 10^{-3}$ | $1.96 \cdot 10^{-3}$ | 3.76 x | $1.91 \cdot 10^{-3}$ | $1.89 \cdot 10^{-3}$ | 1.01 x | Dense |
| features.3.conv.0.0 | $3.55 \cdot 10^{-3}$ | $2.24 \cdot 10^{-3}$ | 1.58 x | $1.83 \cdot 10^{-3}$ | $2.19 \cdot 10^{-3}$ | 0.84 x | Dense |
| features.3.conv.1.0 | $1.34 \cdot 10^{-2}$ | $2.49 \cdot 10^{-3}$ | 5.38 x | $1.34 \cdot 10^{-2}$ | $2.46 \cdot 10^{-3}$ | 5.43 x | General |
| features.3.conv.2 | $1.04 \cdot 10^{-2}$ | $2.89 \cdot 10^{-3}$ | 3.61 x | $2.89 \cdot 10^{-3}$ | $2.85 \cdot 10^{-3}$ | 1.01 x | Dense |
| features.4.conv.1.0 | $7.46 \cdot 10^{-3}$ | $1.01 \cdot 10^{-3}$ | 7.41 x | $7.44 \cdot 10^{-3}$ | $9.84 \cdot 10^{-4}$ | 7.56 x | General |
| features.4.conv.2 | $3.00 \cdot 10^{-3}$ | $9.40 \cdot 10^{-4}$ | 3.19 x | $9.20 \cdot 10^{-4}$ | $8.94 \cdot 10^{-4}$ | 1.03 x | Dense |
| features.5.conv.0.0 | $1.49 \cdot 10^{-3}$ | $7.46 \cdot 10^{-4}$ | 2.00 x | $7.48 \cdot 10^{-4}$ | $7.46 \cdot 10^{-4}$ | 1.00 x | Dense |
| features.5.conv.1.0 | $4.77 \cdot 10^{-3}$ | $9.10 \cdot 10^{-4}$ | 5.24 x | $4.75 \cdot 10^{-3}$ | $8.88 \cdot 10^{-4}$ | 5.34 x | General |
| features.5.conv.2 | $3.62 \cdot 10^{-3}$ | $1.06 \cdot 10^{-3}$ | 3.41 x | $1.04 \cdot 10^{-3}$ | $1.01 \cdot 10^{-3}$ | 1.03 x | Dense |
| features.7.conv.1.0 | $2.61 \cdot 10^{-3}$ | $3.66 \cdot 10^{-4}$ | 7.13 x | $2.60 \cdot 10^{-3}$ | $3.65 \cdot 10^{-4}$ | 7.13 x | General |
| features.7.conv.2 | $1.43 \cdot 10^{-3}$ | $5.55 \cdot 10^{-4}$ | 2.58 x | $4.64 \cdot 10^{-4}$ | $5.55 \cdot 10^{-4}$ | 0.84 x | Dense |
| features.8.conv.0.0 | $1.14 \cdot 10^{-3}$ | $5.36 \cdot 10^{-4}$ | 2.12 x | $5.22 \cdot 10^{-4}$ | $5.34 \cdot 10^{-4}$ | 0.98 x | Dense |
| features.8.conv.1.0 | $2.44 \cdot 10^{-3}$ | $5.67 \cdot 10^{-4}$ | 4.31 x | $2.43 \cdot 10^{-3}$ | $5.68 \cdot 10^{-4}$ | 4.28 x | General |
| features.8.conv.2 | $2.23 \cdot 10^{-3}$ | $8.32 \cdot 10^{-4}$ | 2.68 x | $6.80 \cdot 10^{-4}$ | $8.82 \cdot 10^{-4}$ | 0.77 x | Dense |
| features.11.conv.2 | $2.36 \cdot 10^{-3}$ | $8.68 \cdot 10^{-4}$ | 2.72 x | $7.89 \cdot 10^{-4}$ | $8.69 \cdot 10^{-4}$ | 0.91 x | Dense |
| features.12.conv.0.0 | $1.55 \cdot 10^{-3}$ | $1.08 \cdot 10^{-3}$ | 1.44 x | $9.00 \cdot 10^{-4}$ | $1.03 \cdot 10^{-3}$ | 0.88 x | Dense |
| features.12.conv.1.0 | $3.52 \cdot 10^{-3}$ | $8.20 \cdot 10^{-4}$ | 4.29 x | $3.50 \cdot 10^{-3}$ | $8.19 \cdot 10^{-4}$ | 4.27 x | General |
| features.12.conv.2 | $3.27 \cdot 10^{-3}$ | $1.26 \cdot 10^{-3}$ | 2.59 x | $1.10 \cdot 10^{-3}$ | $1.26 \cdot 10^{-3}$ | 0.87 x | Dense |
| features.14.conv.1.0 | $2.07 \cdot 10^{-3}$ | $3.90 \cdot 10^{-4}$ | 5.31 x | $2.05 \cdot 10^{-3}$ | $3.90 \cdot 10^{-4}$ | 5.26 x | General |
| features.14.conv.2 | $1.06 \cdot 10^{-3}$ | $1.39 \cdot 10^{-3}$ | 0.76 x | $5.10 \cdot 10^{-4}$ | $1.40 \cdot 10^{-3}$ | 0.36 x | Dense |
| features.15.conv.0.0 | $1.12 \cdot 10^{-3}$ | $7.19 \cdot 10^{-4}$ | 1.56 x | $6.21 \cdot 10^{-4}$ | $7.10 \cdot 10^{-4}$ | 0.87 x | Dense |
| features.15.conv.1.0 | $2.31 \cdot 10^{-3}$ | $5.96 \cdot 10^{-4}$ | 3.87 x | $2.28 \cdot 10^{-3}$ | $5.96 \cdot 10^{-4}$ | 3.83 x | General |
| features.15.conv.2 | $1.34 \cdot 10^{-3}$ | $1.41 \cdot 10^{-3}$ | 0.95 x | $6.53 \cdot 10^{-4}$ | $1.40 \cdot 10^{-3}$ | 0.47 x | Dense |
| features.17.conv.2 | $1.59 \cdot 10^{-3}$ | $1.67 \cdot 10^{-3}$ | 0.95 x | $8.70 \cdot 10^{-4}$ | $1.62 \cdot 10^{-3}$ | 0.54 x | Dense |
| features.18.0 | $1.53 \cdot 10^{-3}$ | $1.68 \cdot 10^{-3}$ | 0.91 x | $1.04 \cdot 10^{-3}$ | $1.63 \cdot 10^{-3}$ | 0.64 x | Dense |

E.5 KFC FACTOR (KFAC-EXPAND)

We compare TN and TN+opt with a PyTorch implementation of the input-based KFC factor based on `torch.nn.functional.unfold`. Figure E19 visualizes the performance ratios for different convolution categories. Table E7 contains the detailed run times and performance factors.

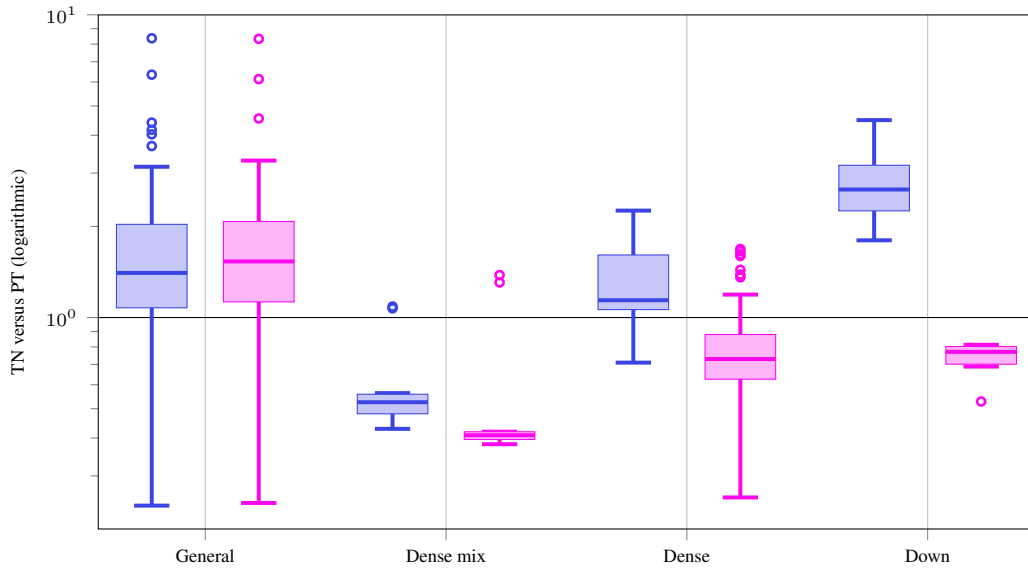


Figure E19: KFC/KFAC-expand factor performance ratios of TN versus PT and TN+opt versus PT for different convolution types on GPU.

Table E7: KFC (KFAC-expand) factor performance comparison on GPU.

(a) 3c3d, CIFAR-10, input shape (128, 3, 32, 32)

| Name | TN [s] | PT [s] | Factor | TN + opt [s] | PT [s] | Factor | Type |
|---------|----------------------|----------------------|---------------|----------------------|----------------------|---------------|---------|
| conv1.0 | $1.03 \cdot 10^{-3}$ | $2.42 \cdot 10^{-3}$ | 0.43 x | $1.03 \cdot 10^{-3}$ | $2.52 \cdot 10^{-3}$ | 0.41 x | General |
| conv2.0 | $6.69 \cdot 10^{-3}$ | $3.83 \cdot 10^{-3}$ | 1.75 x | $6.97 \cdot 10^{-3}$ | $4.52 \cdot 10^{-3}$ | 1.54 x | General |
| conv3.1 | $3.27 \cdot 10^{-3}$ | $2.38 \cdot 10^{-3}$ | 1.37 x | $3.53 \cdot 10^{-3}$ | $2.54 \cdot 10^{-3}$ | 1.39 x | General |

(b) F-MNIST 2c2d, input shape (128, 1, 28, 28)

| Name | TN [s] | PT [s] | Factor | TN + opt [s] | PT [s] | Factor | Type |
|---------|----------------------|----------------------|---------------|----------------------|----------------------|---------------|---------|
| conv1.1 | $1.22 \cdot 10^{-3}$ | $2.01 \cdot 10^{-3}$ | 0.61 x | $9.30 \cdot 10^{-4}$ | $1.72 \cdot 10^{-3}$ | 0.54 x | General |
| conv2.1 | $1.03 \cdot 10^{-2}$ | $9.54 \cdot 10^{-3}$ | 1.08 x | $1.02 \cdot 10^{-2}$ | $9.47 \cdot 10^{-3}$ | 1.08 x | General |

(c) CIFAR-100 All-CNN-C, input shape (128, 3, 32, 32)

| Name | TN [s] | PT [s] | Factor | TN + opt [s] | PT [s] | Factor | Type |
|---------|----------------------|----------------------|---------------|----------------------|----------------------|---------------|---------|
| conv1.1 | $1.37 \cdot 10^{-3}$ | $1.48 \cdot 10^{-3}$ | 0.93 x | $2.72 \cdot 10^{-3}$ | $2.11 \cdot 10^{-3}$ | 1.29 x | General |
| conv2.1 | $1.48 \cdot 10^{-1}$ | $6.95 \cdot 10^{-2}$ | 2.13 x | $1.53 \cdot 10^{-1}$ | $7.14 \cdot 10^{-2}$ | 2.15 x | General |
| conv3.1 | $4.77 \cdot 10^{-2}$ | $1.15 \cdot 10^{-2}$ | 4.17 x | $4.56 \cdot 10^{-2}$ | $1.38 \cdot 10^{-2}$ | 3.30 x | General |
| conv4.1 | $2.32 \cdot 10^{-2}$ | $1.14 \cdot 10^{-2}$ | 2.03 x | $2.25 \cdot 10^{-2}$ | $1.14 \cdot 10^{-2}$ | 1.98 x | General |
| conv5.1 | $7.03 \cdot 10^{-2}$ | $5.82 \cdot 10^{-2}$ | 1.21 x | $1.01 \cdot 10^{-1}$ | $6.19 \cdot 10^{-2}$ | 1.63 x | General |
| conv6.1 | $2.84 \cdot 10^{-2}$ | $1.33 \cdot 10^{-2}$ | 2.14 x | $2.83 \cdot 10^{-2}$ | $9.77 \cdot 10^{-3}$ | 2.90 x | General |
| conv7.0 | $8.68 \cdot 10^{-3}$ | $5.95 \cdot 10^{-3}$ | 1.46 x | $9.30 \cdot 10^{-3}$ | $6.01 \cdot 10^{-3}$ | 1.55 x | General |
| conv8.1 | $1.03 \cdot 10^{-3}$ | $9.97 \cdot 10^{-4}$ | 1.03 x | $3.67 \cdot 10^{-4}$ | $1.44 \cdot 10^{-3}$ | 0.25 x | Dense |
| conv9.1 | $1.06 \cdot 10^{-3}$ | $1.49 \cdot 10^{-3}$ | 0.71 x | $4.61 \cdot 10^{-4}$ | $1.56 \cdot 10^{-3}$ | 0.30 x | Dense |

(d) Alexnet, input shape (32, 3, 256, 256)

| Name | TN [s] | PT [s] | Factor | TN + opt [s] | PT [s] | Factor | Type |
|-------------|----------------------|----------------------|---------------|----------------------|----------------------|--------|---------|
| features.0 | $5.45 \cdot 10^{-2}$ | $1.35 \cdot 10^{-2}$ | 4.03 x | $6.09 \cdot 10^{-2}$ | $1.34 \cdot 10^{-2}$ | 4.55 x | General |
| features.3 | $4.57 \cdot 10^{-2}$ | $4.14 \cdot 10^{-2}$ | 1.10 x | $5.31 \cdot 10^{-2}$ | $3.73 \cdot 10^{-2}$ | 1.42 x | General |
| features.6 | $8.63 \cdot 10^{-3}$ | $7.86 \cdot 10^{-3}$ | 1.10 x | $1.12 \cdot 10^{-2}$ | $8.74 \cdot 10^{-3}$ | 1.28 x | General |
| features.8 | $3.76 \cdot 10^{-2}$ | $4.10 \cdot 10^{-2}$ | 0.92 x | $4.57 \cdot 10^{-2}$ | $4.33 \cdot 10^{-2}$ | 1.06 x | General |
| features.10 | $1.52 \cdot 10^{-2}$ | $1.38 \cdot 10^{-2}$ | 1.10 x | $1.91 \cdot 10^{-2}$ | $1.47 \cdot 10^{-2}$ | 1.30 x | General |

(e) ResNet18, input shape (32, 3, 256, 256)

| Name | TN [s] | PT [s] | Factor | TN + opt [s] | PT [s] | Factor | Type |
|-----------------------|----------------------|----------------------|--------|----------------------|----------------------|---------------|---------|
| conv1 | $5.25 \cdot 10^{-2}$ | $2.07 \cdot 10^{-2}$ | 2.54 x | $5.22 \cdot 10^{-2}$ | $2.06 \cdot 10^{-2}$ | 2.54 x | General |
| layer1.0.conv1 | $4.36 \cdot 10^{-2}$ | $2.98 \cdot 10^{-2}$ | 1.46 x | $5.57 \cdot 10^{-2}$ | $3.02 \cdot 10^{-2}$ | 1.84 x | General |
| layer2.0.conv1 | $2.81 \cdot 10^{-2}$ | $6.38 \cdot 10^{-3}$ | 4.41 x | $2.78 \cdot 10^{-2}$ | $1.23 \cdot 10^{-2}$ | 2.25 x | General |
| layer2.0.conv2 | $2.56 \cdot 10^{-2}$ | $1.90 \cdot 10^{-2}$ | 1.34 x | $3.09 \cdot 10^{-2}$ | $2.01 \cdot 10^{-2}$ | 1.53 x | General |
| layer2.0.downsample.0 | $3.66 \cdot 10^{-3}$ | $8.14 \cdot 10^{-4}$ | 4.49 x | $6.45 \cdot 10^{-4}$ | $7.94 \cdot 10^{-4}$ | 0.81 x | Down |
| layer3.0.conv1 | $1.34 \cdot 10^{-2}$ | $9.19 \cdot 10^{-3}$ | 1.46 x | $1.40 \cdot 10^{-2}$ | $9.17 \cdot 10^{-3}$ | 1.53 x | General |
| layer3.0.conv2 | $1.90 \cdot 10^{-2}$ | $1.84 \cdot 10^{-2}$ | 1.03 x | $2.25 \cdot 10^{-2}$ | $1.95 \cdot 10^{-2}$ | 1.16 x | General |
| layer3.0.downsample.0 | $1.98 \cdot 10^{-3}$ | $7.00 \cdot 10^{-4}$ | 2.83 x | $4.59 \cdot 10^{-4}$ | $5.72 \cdot 10^{-4}$ | 0.80 x | Down |
| layer4.0.conv1 | $8.65 \cdot 10^{-3}$ | $4.79 \cdot 10^{-3}$ | 1.81 x | $9.12 \cdot 10^{-3}$ | $4.60 \cdot 10^{-3}$ | 1.98 x | General |
| layer4.0.conv2 | $2.48 \cdot 10^{-2}$ | $1.63 \cdot 10^{-2}$ | 1.52 x | $2.49 \cdot 10^{-2}$ | $1.88 \cdot 10^{-2}$ | 1.32 x | General |
| layer4.0.downsample.0 | $1.19 \cdot 10^{-3}$ | $5.45 \cdot 10^{-4}$ | 2.18 x | $2.88 \cdot 10^{-4}$ | $5.45 \cdot 10^{-4}$ | 0.53 x | Down |

(f) ResNext101, input shape (32, 3, 256, 256)

| Name | TN [s] | PT [s] | Factor | TN + opt [s] | PT [s] | Factor | Type |
|-----------------------|----------------------|----------------------|--------|----------------------|----------------------|---------------|---------|
| conv1 | $5.13 \cdot 10^{-2}$ | $2.05 \cdot 10^{-2}$ | 2.50 x | $5.06 \cdot 10^{-2}$ | $2.05 \cdot 10^{-2}$ | 2.46 x | General |
| layer1.0.conv1 | $3.33 \cdot 10^{-3}$ | $1.85 \cdot 10^{-3}$ | 1.80 x | $1.70 \cdot 10^{-3}$ | $2.08 \cdot 10^{-3}$ | 0.82 x | Dense |
| layer1.0.conv2 | $1.09 \cdot 10^{-1}$ | $6.60 \cdot 10^{-2}$ | 1.66 x | $1.11 \cdot 10^{-1}$ | $8.12 \cdot 10^{-2}$ | 1.37 x | General |
| layer1.0.conv3 | $1.60 \cdot 10^{-2}$ | $7.49 \cdot 10^{-3}$ | 2.14 x | $1.04 \cdot 10^{-2}$ | $7.52 \cdot 10^{-3}$ | 1.39 x | Dense |
| layer2.0.conv1 | $1.60 \cdot 10^{-2}$ | $1.53 \cdot 10^{-2}$ | 1.05 x | $1.04 \cdot 10^{-2}$ | $1.53 \cdot 10^{-2}$ | 0.68 x | Dense |
| layer2.0.conv2 | $1.40 \cdot 10^{-1}$ | $4.44 \cdot 10^{-2}$ | 3.15 x | $1.44 \cdot 10^{-1}$ | $4.54 \cdot 10^{-2}$ | 3.18 x | General |
| layer2.0.conv3 | $1.14 \cdot 10^{-2}$ | $5.19 \cdot 10^{-3}$ | 2.20 x | $8.41 \cdot 10^{-3}$ | $5.20 \cdot 10^{-3}$ | 1.62 x | Dense |
| layer2.0.downsample.0 | $1.40 \cdot 10^{-2}$ | $4.22 \cdot 10^{-3}$ | 3.30 x | $2.92 \cdot 10^{-3}$ | $4.24 \cdot 10^{-3}$ | 0.69 x | Down |
| layer2.1.conv2 | $5.07 \cdot 10^{-2}$ | $4.23 \cdot 10^{-2}$ | 1.20 x | $5.07 \cdot 10^{-2}$ | $4.24 \cdot 10^{-2}$ | 1.19 x | General |
| layer3.0.conv1 | $1.14 \cdot 10^{-2}$ | $5.21 \cdot 10^{-3}$ | 2.19 x | $8.42 \cdot 10^{-3}$ | $5.27 \cdot 10^{-3}$ | 1.60 x | Dense |
| layer3.0.conv2 | $6.11 \cdot 10^{-2}$ | $3.21 \cdot 10^{-2}$ | 1.90 x | $6.23 \cdot 10^{-2}$ | $2.92 \cdot 10^{-2}$ | 2.14 x | General |
| layer3.0.conv3 | $8.77 \cdot 10^{-3}$ | $4.30 \cdot 10^{-3}$ | 2.04 x | $7.17 \cdot 10^{-3}$ | $4.33 \cdot 10^{-3}$ | 1.66 x | Dense |
| layer3.0.downsample.0 | $7.59 \cdot 10^{-3}$ | $3.08 \cdot 10^{-3}$ | 2.47 x | $2.28 \cdot 10^{-3}$ | $3.08 \cdot 10^{-3}$ | 0.74 x | Down |
| layer3.1.conv2 | $2.12 \cdot 10^{-2}$ | $1.95 \cdot 10^{-2}$ | 1.09 x | $2.05 \cdot 10^{-2}$ | $1.99 \cdot 10^{-2}$ | 1.03 x | General |
| layer4.0.conv1 | $8.75 \cdot 10^{-3}$ | $4.15 \cdot 10^{-3}$ | 2.11 x | $7.18 \cdot 10^{-3}$ | $4.26 \cdot 10^{-3}$ | 1.68 x | Dense |
| layer4.0.conv2 | $4.70 \cdot 10^{-2}$ | $2.47 \cdot 10^{-2}$ | 1.91 x | $4.71 \cdot 10^{-2}$ | $2.47 \cdot 10^{-2}$ | 1.91 x | General |
| layer4.0.conv3 | $7.88 \cdot 10^{-3}$ | $7.66 \cdot 10^{-3}$ | 1.03 x | $6.74 \cdot 10^{-3}$ | $7.67 \cdot 10^{-3}$ | 0.88 x | Dense |
| layer4.0.downsample.0 | $4.54 \cdot 10^{-3}$ | $2.52 \cdot 10^{-3}$ | 1.80 x | $2.03 \cdot 10^{-3}$ | $2.54 \cdot 10^{-3}$ | 0.80 x | Down |
| layer4.1.conv2 | $1.36 \cdot 10^{-2}$ | $1.16 \cdot 10^{-2}$ | 1.16 x | $1.36 \cdot 10^{-2}$ | $1.17 \cdot 10^{-2}$ | 1.16 x | General |

(g) InceptionV3, input shape (32, 3, 299, 299)

| Name | TN [s] | PT [s] | Factor | TN + opt [s] | PT [s] | Factor | Type |
|------------------------------|----------------------|----------------------|---------------|----------------------|----------------------|---------------|-----------|
| Conv2d_1a_3x3.conv | $3.42 \cdot 10^{-2}$ | $4.09 \cdot 10^{-3}$ | 8.36 x | $3.43 \cdot 10^{-2}$ | $4.11 \cdot 10^{-3}$ | 8.33 x | General |
| Conv2d_2a_3x3.conv | $1.58 \cdot 10^{-1}$ | $9.29 \cdot 10^{-2}$ | 1.70 x | $1.91 \cdot 10^{-1}$ | $9.18 \cdot 10^{-2}$ | 2.08 x | General |
| Conv2d_2b_3x3.conv | $1.56 \cdot 10^{-1}$ | $9.66 \cdot 10^{-2}$ | 1.61 x | $1.88 \cdot 10^{-1}$ | $9.44 \cdot 10^{-2}$ | 1.99 x | General |
| Conv2d_3b_1x1.conv | $5.26 \cdot 10^{-3}$ | $2.33 \cdot 10^{-3}$ | 2.26 x | $1.74 \cdot 10^{-3}$ | $2.41 \cdot 10^{-3}$ | 0.72 x | Dense |
| Conv2d_4a_3x3.conv | $1.01 \cdot 10^{-1}$ | $6.34 \cdot 10^{-2}$ | 1.58 x | $1.08 \cdot 10^{-1}$ | $6.16 \cdot 10^{-2}$ | 1.76 x | General |
| Mixed_5b.branch1x1.conv | $4.13 \cdot 10^{-3}$ | $2.02 \cdot 10^{-3}$ | 2.05 x | $2.40 \cdot 10^{-3}$ | $2.13 \cdot 10^{-3}$ | 1.13 x | Dense |
| Mixed_5b.branch5x5.1.conv | $4.12 \cdot 10^{-3}$ | $3.66 \cdot 10^{-3}$ | 1.13 x | $2.41 \cdot 10^{-3}$ | $3.65 \cdot 10^{-3}$ | 0.66 x | Dense |
| Mixed_5b.branch5x5.2.conv | $4.29 \cdot 10^{-2}$ | $3.27 \cdot 10^{-2}$ | 1.31 x | $4.39 \cdot 10^{-2}$ | $3.29 \cdot 10^{-2}$ | 1.33 x | General |
| Mixed_5b.branch3x3dbl.2.conv | $8.57 \cdot 10^{-3}$ | $7.27 \cdot 10^{-3}$ | 1.18 x | $1.38 \cdot 10^{-2}$ | $7.31 \cdot 10^{-3}$ | 1.89 x | General |
| Mixed_5b.branch3x3dbl.3.conv | $1.72 \cdot 10^{-2}$ | $1.42 \cdot 10^{-2}$ | 1.21 x | $2.46 \cdot 10^{-2}$ | $1.42 \cdot 10^{-2}$ | 1.73 x | General |
| Mixed_5b.branch.pool.conv | $4.12 \cdot 10^{-3}$ | $2.05 \cdot 10^{-3}$ | 2.01 x | $2.40 \cdot 10^{-3}$ | $2.02 \cdot 10^{-3}$ | 1.19 x | Dense |
| Mixed_5c.branch1x1.conv | $5.43 \cdot 10^{-3}$ | $4.89 \cdot 10^{-3}$ | 1.11 x | $3.27 \cdot 10^{-3}$ | $4.89 \cdot 10^{-3}$ | 0.67 x | Dense |
| Mixed_5c.branch5x5.1.conv | $5.40 \cdot 10^{-3}$ | $4.87 \cdot 10^{-3}$ | 1.11 x | $3.27 \cdot 10^{-3}$ | $4.88 \cdot 10^{-3}$ | 0.67 x | Dense |
| Mixed_5d.branch1x1.conv | $7.24 \cdot 10^{-3}$ | $6.66 \cdot 10^{-3}$ | 1.09 x | $4.88 \cdot 10^{-3}$ | $6.68 \cdot 10^{-3}$ | 0.73 x | Dense |
| Mixed_5d.branch5x5.1.conv | $7.25 \cdot 10^{-3}$ | $6.67 \cdot 10^{-3}$ | 1.09 x | $4.88 \cdot 10^{-3}$ | $6.69 \cdot 10^{-3}$ | 0.73 x | Dense |
| Mixed_6a.branch3x3.conv | $7.76 \cdot 10^{-2}$ | $3.28 \cdot 10^{-2}$ | 2.37 x | $7.78 \cdot 10^{-2}$ | $3.23 \cdot 10^{-2}$ | 2.41 x | General |
| Mixed_6a.branch3x3dbl.3.conv | $1.29 \cdot 10^{-2}$ | $3.50 \cdot 10^{-3}$ | 3.69 x | $1.41 \cdot 10^{-2}$ | $7.15 \cdot 10^{-3}$ | 1.97 x | General |
| Mixed_6b.branch1x1.conv | $6.56 \cdot 10^{-3}$ | $5.66 \cdot 10^{-3}$ | 1.16 x | $4.80 \cdot 10^{-3}$ | $4.22 \cdot 10^{-3}$ | 1.14 x | Dense |
| Mixed_6b.branch7x7.1.conv | $6.55 \cdot 10^{-3}$ | $6.02 \cdot 10^{-3}$ | 1.09 x | $4.80 \cdot 10^{-3}$ | $6.03 \cdot 10^{-3}$ | 0.80 x | Dense |
| Mixed_6b.branch7x7.2.conv | $2.01 \cdot 10^{-3}$ | $3.60 \cdot 10^{-3}$ | 0.56 x | $1.50 \cdot 10^{-3}$ | $3.58 \cdot 10^{-3}$ | 0.42 x | Dense mix |
| Mixed_6b.branch7x7.3.conv | $1.92 \cdot 10^{-3}$ | $3.50 \cdot 10^{-3}$ | 0.55 x | $1.46 \cdot 10^{-3}$ | $3.58 \cdot 10^{-3}$ | 0.41 x | Dense mix |
| Mixed_6b.branch7x7dbl.2.conv | $1.94 \cdot 10^{-3}$ | $3.54 \cdot 10^{-3}$ | 0.55 x | $1.45 \cdot 10^{-3}$ | $3.56 \cdot 10^{-3}$ | 0.41 x | Dense mix |
| Mixed_6b.branch7x7dbl.5.conv | $1.97 \cdot 10^{-3}$ | $3.49 \cdot 10^{-3}$ | 0.56 x | $1.46 \cdot 10^{-3}$ | $3.49 \cdot 10^{-3}$ | 0.42 x | Dense mix |
| Mixed_6c.branch7x7.1.conv | $6.59 \cdot 10^{-3}$ | $4.60 \cdot 10^{-3}$ | 1.43 x | $4.80 \cdot 10^{-3}$ | $4.90 \cdot 10^{-3}$ | 0.98 x | Dense |
| Mixed_6c.branch7x7.2.conv | $2.59 \cdot 10^{-3}$ | $5.14 \cdot 10^{-3}$ | 0.50 x | $2.08 \cdot 10^{-3}$ | $5.08 \cdot 10^{-3}$ | 0.41 x | Dense mix |
| Mixed_6c.branch7x7.3.conv | $2.58 \cdot 10^{-3}$ | $5.32 \cdot 10^{-3}$ | 0.48 x | $2.04 \cdot 10^{-3}$ | $5.23 \cdot 10^{-3}$ | 0.39 x | Dense mix |
| Mixed_6c.branch7x7dbl.2.conv | $2.51 \cdot 10^{-3}$ | $5.32 \cdot 10^{-3}$ | 0.47 x | $2.05 \cdot 10^{-3}$ | $5.25 \cdot 10^{-3}$ | 0.39 x | Dense mix |
| Mixed_6c.branch7x7dbl.5.conv | $2.53 \cdot 10^{-3}$ | $5.21 \cdot 10^{-3}$ | 0.49 x | $2.04 \cdot 10^{-3}$ | $5.12 \cdot 10^{-3}$ | 0.40 x | Dense mix |
| Mixed_6e.branch7x7.2.conv | $3.35 \cdot 10^{-3}$ | $7.81 \cdot 10^{-3}$ | 0.43 x | $2.90 \cdot 10^{-3}$ | $7.61 \cdot 10^{-3}$ | 0.38 x | Dense mix |
| Mixed_6e.branch7x7.3.conv | $3.35 \cdot 10^{-3}$ | $7.52 \cdot 10^{-3}$ | 0.45 x | $2.91 \cdot 10^{-3}$ | $7.31 \cdot 10^{-3}$ | 0.40 x | Dense mix |
| AuxLogits.conv0.conv | $1.09 \cdot 10^{-3}$ | $6.14 \cdot 10^{-4}$ | 1.77 x | $3.82 \cdot 10^{-4}$ | $6.10 \cdot 10^{-4}$ | 0.63 x | Dense |
| AuxLogits.conv1.conv | $8.95 \cdot 10^{-4}$ | $1.07 \cdot 10^{-3}$ | 0.84 x | $8.52 \cdot 10^{-4}$ | $1.09 \cdot 10^{-3}$ | 0.78 x | General |
| Mixed_7a.branch3x3.2.conv | $6.56 \cdot 10^{-3}$ | $2.67 \cdot 10^{-3}$ | 2.45 x | $6.98 \cdot 10^{-3}$ | $2.68 \cdot 10^{-3}$ | 2.60 x | General |
| Mixed_7a.branch7x7x3.4.conv | $6.93 \cdot 10^{-3}$ | $2.93 \cdot 10^{-3}$ | 2.36 x | $7.04 \cdot 10^{-3}$ | $2.94 \cdot 10^{-3}$ | 2.39 x | General |
| Mixed_7b.branch1x1.conv | $3.27 \cdot 10^{-3}$ | $1.82 \cdot 10^{-3}$ | 1.80 x | $2.39 \cdot 10^{-3}$ | $1.76 \cdot 10^{-3}$ | 1.36 x | Dense |
| Mixed_7b.branch3x3.1.conv | $3.66 \cdot 10^{-3}$ | $3.34 \cdot 10^{-3}$ | 1.10 x | $2.83 \cdot 10^{-3}$ | $3.36 \cdot 10^{-3}$ | 0.84 x | Dense |
| Mixed_7b.branch3x3.2a.conv | $2.51 \cdot 10^{-3}$ | $2.34 \cdot 10^{-3}$ | 1.07 x | $3.03 \cdot 10^{-3}$ | $2.32 \cdot 10^{-3}$ | 1.31 x | Dense mix |
| Mixed_7b.branch3x3.2b.conv | $2.43 \cdot 10^{-3}$ | $2.24 \cdot 10^{-3}$ | 1.09 x | $2.98 \cdot 10^{-3}$ | $2.16 \cdot 10^{-3}$ | 1.38 x | Dense mix |
| Mixed_7b.branch3x3dbl.1.conv | $3.70 \cdot 10^{-3}$ | $2.57 \cdot 10^{-3}$ | 1.44 x | $2.83 \cdot 10^{-3}$ | $2.43 \cdot 10^{-3}$ | 1.17 x | Dense |
| Mixed_7b.branch3x3dbl.2.conv | $2.03 \cdot 10^{-2}$ | $1.45 \cdot 10^{-2}$ | 1.40 x | $1.94 \cdot 10^{-2}$ | $1.40 \cdot 10^{-2}$ | 1.39 x | General |
| Mixed_7b.branch.pool.conv | $2.89 \cdot 10^{-3}$ | $1.57 \cdot 10^{-3}$ | 1.84 x | $2.26 \cdot 10^{-3}$ | $1.57 \cdot 10^{-3}$ | 1.44 x | Dense |
| Mixed_7c.branch1x1.conv | $7.88 \cdot 10^{-3}$ | $7.66 \cdot 10^{-3}$ | 1.03 x | $6.73 \cdot 10^{-3}$ | $7.66 \cdot 10^{-3}$ | 0.88 x | Dense |
| Mixed_7c.branch3x3.1.conv | $7.88 \cdot 10^{-3}$ | $7.66 \cdot 10^{-3}$ | 1.03 x | $6.73 \cdot 10^{-3}$ | $7.66 \cdot 10^{-3}$ | 0.88 x | Dense |
| Mixed_7c.branch3x3dbl.1.conv | $7.92 \cdot 10^{-3}$ | $7.67 \cdot 10^{-3}$ | 1.03 x | $6.74 \cdot 10^{-3}$ | $7.67 \cdot 10^{-3}$ | 0.88 x | Dense |
| Mixed_7c.branch.pool.conv | $7.92 \cdot 10^{-3}$ | $7.67 \cdot 10^{-3}$ | 1.03 x | $6.74 \cdot 10^{-3}$ | $7.67 \cdot 10^{-3}$ | 0.88 x | Dense |

(h) MobileNetV2, input shape (32, 3, 256, 256)

| Name | TN [s] | PT [s] | Factor | TN + opt [s] | PT [s] | Factor | Type |
|----------------------|----------------------|----------------------|---------------|----------------------|----------------------|---------------|---------|
| features.0.0 | $2.30 \cdot 10^{-2}$ | $3.63 \cdot 10^{-3}$ | 6.34 x | $2.24 \cdot 10^{-2}$ | $3.65 \cdot 10^{-3}$ | 6.13 x | General |
| features.1.conv.0.0 | $2.84 \cdot 10^{-2}$ | $3.71 \cdot 10^{-2}$ | 0.76 x | $2.84 \cdot 10^{-2}$ | $3.72 \cdot 10^{-2}$ | 0.76 x | General |
| features.1.conv.1 | $7.35 \cdot 10^{-3}$ | $5.48 \cdot 10^{-3}$ | 1.34 x | $2.95 \cdot 10^{-3}$ | $5.50 \cdot 10^{-3}$ | 0.54 x | Dense |
| features.2.conv.0.0 | $4.28 \cdot 10^{-3}$ | $2.92 \cdot 10^{-3}$ | 1.47 x | $1.50 \cdot 10^{-3}$ | $2.91 \cdot 10^{-3}$ | 0.51 x | Dense |
| features.2.conv.1.0 | $3.98 \cdot 10^{-2}$ | $2.51 \cdot 10^{-2}$ | 1.59 x | $3.98 \cdot 10^{-2}$ | $2.51 \cdot 10^{-2}$ | 1.59 x | General |
| features.2.conv.2 | $5.33 \cdot 10^{-3}$ | $4.67 \cdot 10^{-3}$ | 1.14 x | $3.06 \cdot 10^{-3}$ | $5.04 \cdot 10^{-3}$ | 0.61 x | Dense |
| features.3.conv.0.0 | $1.63 \cdot 10^{-3}$ | $1.37 \cdot 10^{-3}$ | 1.19 x | $7.02 \cdot 10^{-4}$ | $1.39 \cdot 10^{-3}$ | 0.50 x | Dense |
| features.3.conv.1.0 | $2.07 \cdot 10^{-2}$ | $3.67 \cdot 10^{-2}$ | 0.56 x | $2.06 \cdot 10^{-2}$ | $3.68 \cdot 10^{-2}$ | 0.56 x | General |
| features.3.conv.2 | $9.72 \cdot 10^{-3}$ | $9.38 \cdot 10^{-3}$ | 1.04 x | $6.47 \cdot 10^{-3}$ | $9.36 \cdot 10^{-3}$ | 0.69 x | Dense |
| features.4.conv.1.0 | $1.15 \cdot 10^{-2}$ | $1.02 \cdot 10^{-2}$ | 1.13 x | $1.15 \cdot 10^{-2}$ | $1.02 \cdot 10^{-2}$ | 1.13 x | General |
| features.4.conv.2 | $2.82 \cdot 10^{-3}$ | $2.65 \cdot 10^{-3}$ | 1.06 x | $1.77 \cdot 10^{-3}$ | $2.64 \cdot 10^{-3}$ | 0.67 x | Dense |
| features.5.conv.0.0 | $1.05 \cdot 10^{-3}$ | $7.05 \cdot 10^{-4}$ | 1.49 x | $3.84 \cdot 10^{-4}$ | $7.08 \cdot 10^{-4}$ | 0.54 x | Dense |
| features.5.conv.1.0 | $6.38 \cdot 10^{-3}$ | $1.19 \cdot 10^{-2}$ | 0.54 x | $6.36 \cdot 10^{-3}$ | $1.19 \cdot 10^{-2}$ | 0.53 x | General |
| features.5.conv.2 | $3.39 \cdot 10^{-3}$ | $3.16 \cdot 10^{-3}$ | 1.07 x | $2.10 \cdot 10^{-3}$ | $3.18 \cdot 10^{-3}$ | 0.66 x | Dense |
| features.7.conv.1.0 | $3.66 \cdot 10^{-3}$ | $3.66 \cdot 10^{-3}$ | 1.00 x | $3.69 \cdot 10^{-3}$ | $3.67 \cdot 10^{-3}$ | 1.01 x | General |
| features.7.conv.2 | $1.41 \cdot 10^{-3}$ | $1.28 \cdot 10^{-3}$ | 1.10 x | $7.93 \cdot 10^{-4}$ | $1.28 \cdot 10^{-3}$ | 0.62 x | Dense |
| features.8.conv.0.0 | $9.96 \cdot 10^{-4}$ | $6.18 \cdot 10^{-4}$ | 1.61 x | $3.37 \cdot 10^{-4}$ | $6.26 \cdot 10^{-4}$ | 0.54 x | Dense |
| features.8.conv.1.0 | $2.88 \cdot 10^{-3}$ | $6.25 \cdot 10^{-3}$ | 0.46 x | $2.87 \cdot 10^{-3}$ | $6.26 \cdot 10^{-3}$ | 0.46 x | General |
| features.8.conv.2 | $2.36 \cdot 10^{-3}$ | $2.24 \cdot 10^{-3}$ | 1.06 x | $1.55 \cdot 10^{-3}$ | $2.24 \cdot 10^{-3}$ | 0.69 x | Dense |
| features.11.conv.2 | $2.33 \cdot 10^{-3}$ | $2.22 \cdot 10^{-3}$ | 1.05 x | $1.55 \cdot 10^{-3}$ | $2.24 \cdot 10^{-3}$ | 0.69 x | Dense |
| features.12.conv.0.0 | $9.43 \cdot 10^{-4}$ | $7.06 \cdot 10^{-4}$ | 1.34 x | $3.87 \cdot 10^{-4}$ | $7.07 \cdot 10^{-4}$ | 0.55 x | Dense |
| features.12.conv.1.0 | $4.07 \cdot 10^{-3}$ | $8.89 \cdot 10^{-3}$ | 0.46 x | $4.04 \cdot 10^{-3}$ | $8.90 \cdot 10^{-3}$ | 0.45 x | General |
| features.12.conv.2 | $3.97 \cdot 10^{-3}$ | $3.84 \cdot 10^{-3}$ | 1.03 x | $2.97 \cdot 10^{-3}$ | $3.85 \cdot 10^{-3}$ | 0.77 x | Dense |
| features.14.conv.1.0 | $2.41 \cdot 10^{-3}$ | $2.66 \cdot 10^{-3}$ | 0.91 x | $2.39 \cdot 10^{-3}$ | $2.66 \cdot 10^{-3}$ | 0.90 x | General |
| features.14.conv.2 | $1.50 \cdot 10^{-3}$ | $1.23 \cdot 10^{-3}$ | 1.22 x | $9.00 \cdot 10^{-4}$ | $1.23 \cdot 10^{-3}$ | 0.73 x | Dense |
| features.15.conv.0.0 | $9.14 \cdot 10^{-4}$ | $6.34 \cdot 10^{-4}$ | 1.44 x | $3.38 \cdot 10^{-4}$ | $6.23 \cdot 10^{-4}$ | 0.54 x | Dense |
| features.15.conv.1.0 | $9.60 \cdot 10^{-4}$ | $4.01 \cdot 10^{-3}$ | 0.24 x | $9.83 \cdot 10^{-4}$ | $4.03 \cdot 10^{-3}$ | 0.24 x | General |
| features.15.conv.2 | $2.57 \cdot 10^{-3}$ | $2.35 \cdot 10^{-3}$ | 1.10 x | $1.85 \cdot 10^{-3}$ | $2.35 \cdot 10^{-3}$ | 0.79 x | Dense |
| features.17.conv.2 | $2.57 \cdot 10^{-3}$ | $2.35 \cdot 10^{-3}$ | 1.10 x | $1.85 \cdot 10^{-3}$ | $2.35 \cdot 10^{-3}$ | 0.79 x | Dense |
| features.18.0 | $1.15 \cdot 10^{-3}$ | $7.91 \cdot 10^{-4}$ | 1.46 x | $4.79 \cdot 10^{-4}$ | $7.91 \cdot 10^{-4}$ | 0.61 x | Dense |

E.6 KFAC-REDUCE FACTOR

We compare TN and TN+opt with a PyTorch implementation of the input-based KFAC-reduce factor based on `torch.nn.functional.unfold`. Figure E20 visualizes the performance ratios for different convolution categories. Table E8 contains the detailed run times and performance factors.

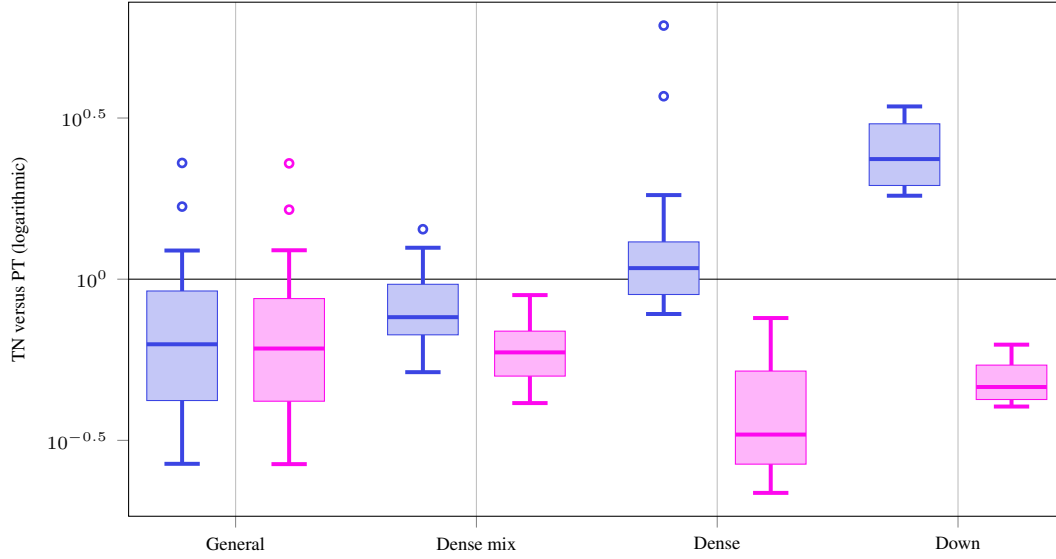


Figure E20: KFAC-reduce factor performance ratios of TN versus PT and TN+opt versus PT for different convolution types on GPU.

Table E8: KFAC-reduce factor performance comparison on GPU.

(a) 3c3d, CIFAR-10, input shape (128, 3, 32, 32)

| Name | TN [s] | PT [s] | Factor | TN + opt [s] | PT [s] | Factor | Type |
|---------|----------------------|----------------------|---------------|----------------------|----------------------|---------------|---------|
| conv1.0 | $8.88 \cdot 10^{-4}$ | $2.26 \cdot 10^{-3}$ | 0.39 x | $8.59 \cdot 10^{-4}$ | $2.41 \cdot 10^{-3}$ | 0.36 x | General |
| conv2.0 | $1.41 \cdot 10^{-3}$ | $1.79 \cdot 10^{-3}$ | 0.79 x | $1.29 \cdot 10^{-3}$ | $1.75 \cdot 10^{-3}$ | 0.74 x | General |
| conv3.1 | $1.33 \cdot 10^{-3}$ | $2.31 \cdot 10^{-3}$ | 0.57 x | $1.46 \cdot 10^{-3}$ | $2.37 \cdot 10^{-3}$ | 0.61 x | General |

(b) F-MNIST 2c2d, input shape (128, 1, 28, 28)

| Name | TN [s] | PT [s] | Factor | TN + opt [s] | PT [s] | Factor | Type |
|---------|----------------------|----------------------|---------------|----------------------|----------------------|---------------|---------|
| conv1.1 | $1.10 \cdot 10^{-3}$ | $1.67 \cdot 10^{-3}$ | 0.66 x | $1.01 \cdot 10^{-3}$ | $1.83 \cdot 10^{-3}$ | 0.55 x | General |
| conv2.1 | $1.58 \cdot 10^{-3}$ | $2.57 \cdot 10^{-3}$ | 0.62 x | $1.54 \cdot 10^{-3}$ | $2.76 \cdot 10^{-3}$ | 0.56 x | General |

(c) CIFAR-100 All-CNN-C, input shape (128, 3, 32, 32)

| Name | TN [s] | PT [s] | Factor | TN + opt [s] | PT [s] | Factor | Type |
|---------|----------------------|----------------------|---------------|----------------------|----------------------|---------------|---------|
| conv1.1 | $1.11 \cdot 10^{-3}$ | $1.84 \cdot 10^{-3}$ | 0.60 x | $1.07 \cdot 10^{-3}$ | $1.89 \cdot 10^{-3}$ | 0.56 x | General |
| conv2.1 | $3.26 \cdot 10^{-3}$ | $8.32 \cdot 10^{-3}$ | 0.39 x | $3.19 \cdot 10^{-3}$ | $8.24 \cdot 10^{-3}$ | 0.39 x | General |
| conv3.1 | $3.09 \cdot 10^{-3}$ | $3.56 \cdot 10^{-3}$ | 0.87 x | $3.08 \cdot 10^{-3}$ | $3.56 \cdot 10^{-3}$ | 0.87 x | General |
| conv4.1 | $1.45 \cdot 10^{-3}$ | $3.09 \cdot 10^{-3}$ | 0.47 x | $1.44 \cdot 10^{-3}$ | $3.09 \cdot 10^{-3}$ | 0.47 x | General |
| conv5.1 | $2.59 \cdot 10^{-3}$ | $5.63 \cdot 10^{-3}$ | 0.46 x | $2.55 \cdot 10^{-3}$ | $5.62 \cdot 10^{-3}$ | 0.45 x | General |
| conv6.1 | $2.46 \cdot 10^{-3}$ | $3.49 \cdot 10^{-3}$ | 0.71 x | $2.43 \cdot 10^{-3}$ | $3.48 \cdot 10^{-3}$ | 0.70 x | General |
| conv7.0 | $1.55 \cdot 10^{-3}$ | $3.03 \cdot 10^{-3}$ | 0.51 x | $1.53 \cdot 10^{-3}$ | $3.02 \cdot 10^{-3}$ | 0.51 x | General |
| conv8.1 | $1.14 \cdot 10^{-3}$ | $1.46 \cdot 10^{-3}$ | 0.78 x | $3.59 \cdot 10^{-4}$ | $1.36 \cdot 10^{-3}$ | 0.26 x | Dense |
| conv9.1 | $1.14 \cdot 10^{-3}$ | $1.46 \cdot 10^{-3}$ | 0.79 x | $3.59 \cdot 10^{-4}$ | $1.36 \cdot 10^{-3}$ | 0.26 x | Dense |

(d) Alexnet, input shape (32, 3, 256, 256)

| Name | TN [s] | PT [s] | Factor | TN + opt [s] | PT [s] | Factor | Type |
|-------------|----------------------|----------------------|---------------|----------------------|----------------------|---------------|---------|
| features.0 | $1.86 \cdot 10^{-3}$ | $4.22 \cdot 10^{-3}$ | 0.44 x | $1.84 \cdot 10^{-3}$ | $4.22 \cdot 10^{-3}$ | 0.44 x | General |
| features.3 | $1.60 \cdot 10^{-3}$ | $3.88 \cdot 10^{-3}$ | 0.41 x | $1.53 \cdot 10^{-3}$ | $3.89 \cdot 10^{-3}$ | 0.39 x | General |
| features.6 | $1.51 \cdot 10^{-3}$ | $1.64 \cdot 10^{-3}$ | 0.92 x | $1.43 \cdot 10^{-3}$ | $1.63 \cdot 10^{-3}$ | 0.88 x | General |
| features.8 | $1.77 \cdot 10^{-3}$ | $3.02 \cdot 10^{-3}$ | 0.59 x | $1.73 \cdot 10^{-3}$ | $3.02 \cdot 10^{-3}$ | 0.57 x | General |
| features.10 | $1.56 \cdot 10^{-3}$ | $1.96 \cdot 10^{-3}$ | 0.79 x | $1.51 \cdot 10^{-3}$ | $1.96 \cdot 10^{-3}$ | 0.77 x | General |

(e) ResNet18, input shape (32, 3, 256, 256)

| Name | TN [s] | PT [s] | Factor | TN + opt [s] | PT [s] | Factor | Type |
|-----------------------|----------------------|----------------------|---------------|----------------------|----------------------|---------------|---------|
| conv1 | $1.79 \cdot 10^{-3}$ | $5.41 \cdot 10^{-3}$ | 0.33 x | $1.78 \cdot 10^{-3}$ | $5.40 \cdot 10^{-3}$ | 0.33 x | General |
| layer1.0.conv1 | $2.24 \cdot 10^{-3}$ | $5.35 \cdot 10^{-3}$ | 0.42 x | $2.20 \cdot 10^{-3}$ | $5.32 \cdot 10^{-3}$ | 0.41 x | General |
| layer2.0.conv1 | $2.23 \cdot 10^{-3}$ | $1.99 \cdot 10^{-3}$ | 1.12 x | $2.16 \cdot 10^{-3}$ | $1.96 \cdot 10^{-3}$ | 1.10 x | General |
| layer2.0.conv2 | $1.47 \cdot 10^{-3}$ | $3.02 \cdot 10^{-3}$ | 0.49 x | $1.47 \cdot 10^{-3}$ | $3.04 \cdot 10^{-3}$ | 0.49 x | General |
| layer3.0.downsample.0 | $1.85 \cdot 10^{-3}$ | $7.70 \cdot 10^{-4}$ | 2.40 x | $3.24 \cdot 10^{-4}$ | $7.49 \cdot 10^{-4}$ | 0.43 x | Down |
| layer3.0.conv1 | $1.46 \cdot 10^{-3}$ | $1.21 \cdot 10^{-3}$ | 1.21 x | $1.45 \cdot 10^{-3}$ | $1.21 \cdot 10^{-3}$ | 1.20 x | General |
| layer3.0.conv2 | $1.49 \cdot 10^{-3}$ | $1.96 \cdot 10^{-3}$ | 0.76 x | $1.36 \cdot 10^{-3}$ | $1.95 \cdot 10^{-3}$ | 0.70 x | General |
| layer3.0.downsample.0 | $1.26 \cdot 10^{-3}$ | $5.44 \cdot 10^{-4}$ | 2.31 x | $2.68 \cdot 10^{-4}$ | $5.44 \cdot 10^{-4}$ | 0.49 x | Down |
| layer4.0.conv1 | $1.49 \cdot 10^{-3}$ | $1.33 \cdot 10^{-3}$ | 1.12 x | $1.44 \cdot 10^{-3}$ | $1.33 \cdot 10^{-3}$ | 1.08 x | General |
| layer4.0.conv2 | $1.60 \cdot 10^{-3}$ | $1.86 \cdot 10^{-3}$ | 0.86 x | $1.62 \cdot 10^{-3}$ | $1.86 \cdot 10^{-3}$ | 0.87 x | General |
| layer4.0.downsample.0 | $9.63 \cdot 10^{-4}$ | $5.25 \cdot 10^{-4}$ | 1.83 x | $2.57 \cdot 10^{-4}$ | $4.11 \cdot 10^{-4}$ | 0.63 x | Down |

(f) ResNext101, input shape (32, 3, 256, 256)

| Name | TN [s] | PT [s] | Factor | TN + opt [s] | PT [s] | Factor | Type |
|-----------------------|----------------------|----------------------|---------------|----------------------|----------------------|---------------|---------|
| conv1 | $1.78 \cdot 10^{-3}$ | $5.38 \cdot 10^{-3}$ | 0.33 x | $1.77 \cdot 10^{-3}$ | $5.39 \cdot 10^{-3}$ | 0.33 x | General |
| layer1.0.conv1 | $1.87 \cdot 10^{-3}$ | $1.73 \cdot 10^{-3}$ | 1.08 x | $4.47 \cdot 10^{-4}$ | $1.73 \cdot 10^{-3}$ | 0.26 x | Dense |
| layer1.0.conv2 | $4.44 \cdot 10^{-2}$ | $1.94 \cdot 10^{-2}$ | 2.29 x | $4.43 \cdot 10^{-2}$ | $1.94 \cdot 10^{-2}$ | 2.29 x | General |
| layer1.0.conv3 | $6.09 \cdot 10^{-3}$ | $5.57 \cdot 10^{-3}$ | 1.09 x | $1.21 \cdot 10^{-3}$ | $5.57 \cdot 10^{-3}$ | 0.22 x | Dense |
| layer2.0.conv1 | $6.09 \cdot 10^{-3}$ | $5.57 \cdot 10^{-3}$ | 1.09 x | $1.21 \cdot 10^{-3}$ | $5.58 \cdot 10^{-3}$ | 0.22 x | Dense |
| layer2.0.conv2 | $1.37 \cdot 10^{-2}$ | $1.18 \cdot 10^{-2}$ | 1.16 x | $1.37 \cdot 10^{-2}$ | $1.18 \cdot 10^{-2}$ | 1.16 x | General |
| layer2.0.conv3 | $3.81 \cdot 10^{-3}$ | $3.02 \cdot 10^{-3}$ | 1.26 x | $7.44 \cdot 10^{-4}$ | $3.02 \cdot 10^{-3}$ | 0.25 x | Dense |
| layer2.0.downsample.0 | $6.08 \cdot 10^{-3}$ | $1.77 \cdot 10^{-3}$ | 3.44 x | $7.12 \cdot 10^{-4}$ | $1.77 \cdot 10^{-3}$ | 0.40 x | Down |
| layer2.1.conv2 | $4.16 \cdot 10^{-3}$ | $9.91 \cdot 10^{-3}$ | 0.42 x | $4.16 \cdot 10^{-3}$ | $9.90 \cdot 10^{-3}$ | 0.42 x | General |
| layer3.0.conv1 | $3.81 \cdot 10^{-3}$ | $3.02 \cdot 10^{-3}$ | 1.26 x | $7.32 \cdot 10^{-4}$ | $3.02 \cdot 10^{-3}$ | 0.24 x | Dense |
| layer3.0.conv2 | $7.88 \cdot 10^{-3}$ | $6.42 \cdot 10^{-3}$ | 1.23 x | $7.90 \cdot 10^{-3}$ | $6.43 \cdot 10^{-3}$ | 1.23 x | General |
| layer3.0.conv3 | $1.61 \cdot 10^{-3}$ | $1.78 \cdot 10^{-3}$ | 0.91 x | $5.42 \cdot 10^{-4}$ | $1.80 \cdot 10^{-3}$ | 0.30 x | Dense |
| layer3.0.downsample.0 | $3.80 \cdot 10^{-3}$ | $1.17 \cdot 10^{-3}$ | 3.24 x | $5.10 \cdot 10^{-4}$ | $1.21 \cdot 10^{-3}$ | 0.42 x | Down |
| layer3.1.conv2 | $2.25 \cdot 10^{-3}$ | $5.41 \cdot 10^{-3}$ | 0.42 x | $2.26 \cdot 10^{-3}$ | $5.41 \cdot 10^{-3}$ | 0.42 x | General |
| layer4.0.conv1 | $1.61 \cdot 10^{-3}$ | $1.77 \cdot 10^{-3}$ | 0.91 x | $5.44 \cdot 10^{-4}$ | $1.80 \cdot 10^{-3}$ | 0.30 x | Dense |
| layer4.0.conv2 | $4.21 \cdot 10^{-3}$ | $5.29 \cdot 10^{-3}$ | 0.80 x | $4.21 \cdot 10^{-3}$ | $5.29 \cdot 10^{-3}$ | 0.80 x | General |
| layer4.0.conv3 | $1.23 \cdot 10^{-3}$ | $1.45 \cdot 10^{-3}$ | 0.85 x | $7.68 \cdot 10^{-4}$ | $1.44 \cdot 10^{-3}$ | 0.53 x | Dense |
| layer4.0.downsample.0 | $1.62 \cdot 10^{-3}$ | $8.91 \cdot 10^{-4}$ | 1.82 x | $4.97 \cdot 10^{-4}$ | $8.93 \cdot 10^{-4}$ | 0.56 x | Down |
| layer4.1.conv2 | $2.18 \cdot 10^{-3}$ | $4.73 \cdot 10^{-3}$ | 0.46 x | $2.16 \cdot 10^{-3}$ | $4.72 \cdot 10^{-3}$ | 0.46 x | General |

(g) InceptionV3, input shape (32, 3, 299, 299)

| Name | TN [s] | PT [s] | Factor | TN + opt [s] | PT [s] | Factor | Type |
|------------------------------|----------------------|----------------------|---------------|----------------------|----------------------|---------------|-----------|
| Conv2d_1a_3x3.conv | $2.39 \cdot 10^{-3}$ | $2.03 \cdot 10^{-3}$ | 1.18 x | $2.36 \cdot 10^{-3}$ | $2.00 \cdot 10^{-3}$ | 1.18 x | General |
| Conv2d_2a_3x3.conv | $4.42 \cdot 10^{-3}$ | $1.30 \cdot 10^{-2}$ | 0.34 x | $4.38 \cdot 10^{-3}$ | $1.30 \cdot 10^{-2}$ | 0.34 x | General |
| Conv2d_2b_3x3.conv | $4.33 \cdot 10^{-3}$ | $1.30 \cdot 10^{-2}$ | 0.33 x | $4.32 \cdot 10^{-3}$ | $1.30 \cdot 10^{-2}$ | 0.33 x | General |
| Conv2d_3b_1x1.conv | $1.32 \cdot 10^{-2}$ | $2.16 \cdot 10^{-3}$ | 6.12 x | $5.53 \cdot 10^{-4}$ | $2.16 \cdot 10^{-3}$ | 0.26 x | Dense |
| Conv2d_4a_3x3.conv | $2.72 \cdot 10^{-3}$ | $8.00 \cdot 10^{-3}$ | 0.34 x | $2.74 \cdot 10^{-3}$ | $8.02 \cdot 10^{-3}$ | 0.34 x | General |
| Mixed_5b.branch1x1.conv | $1.43 \cdot 10^{-3}$ | $1.57 \cdot 10^{-3}$ | 0.91 x | $4.52 \cdot 10^{-4}$ | $1.57 \cdot 10^{-3}$ | 0.29 x | Dense |
| Mixed_5b.branch5x5.1.conv | $1.43 \cdot 10^{-3}$ | $1.57 \cdot 10^{-3}$ | 0.91 x | $4.53 \cdot 10^{-4}$ | $1.57 \cdot 10^{-3}$ | 0.29 x | Dense |
| Mixed_5b.branch3x3dbl.2.conv | $1.56 \cdot 10^{-3}$ | $3.73 \cdot 10^{-3}$ | 0.42 x | $1.35 \cdot 10^{-3}$ | $3.72 \cdot 10^{-3}$ | 0.36 x | General |
| Mixed_5b.branch3x3dbl.1.conv | $1.57 \cdot 10^{-3}$ | $1.91 \cdot 10^{-3}$ | 0.82 x | $1.44 \cdot 10^{-3}$ | $1.91 \cdot 10^{-3}$ | 0.76 x | General |
| Mixed_5b.branch3x3dbl.3.conv | $1.48 \cdot 10^{-3}$ | $2.66 \cdot 10^{-3}$ | 0.56 x | $1.41 \cdot 10^{-3}$ | $2.66 \cdot 10^{-3}$ | 0.53 x | General |
| Mixed_5b.branch.pool.conv | $1.45 \cdot 10^{-3}$ | $1.59 \cdot 10^{-3}$ | 0.91 x | $4.62 \cdot 10^{-4}$ | $1.59 \cdot 10^{-3}$ | 0.29 x | Dense |
| Mixed_5c.branch1x1.conv | $1.79 \cdot 10^{-3}$ | $2.00 \cdot 10^{-3}$ | 0.90 x | $5.48 \cdot 10^{-4}$ | $2.00 \cdot 10^{-3}$ | 0.27 x | Dense |
| Mixed_5c.branch5x5.1.conv | $1.79 \cdot 10^{-3}$ | $2.00 \cdot 10^{-3}$ | 0.90 x | $5.46 \cdot 10^{-4}$ | $2.00 \cdot 10^{-3}$ | 0.27 x | Dense |
| Mixed_5d.branch1x1.conv | $1.99 \cdot 10^{-3}$ | $2.22 \cdot 10^{-3}$ | 0.90 x | $5.90 \cdot 10^{-4}$ | $2.21 \cdot 10^{-3}$ | 0.27 x | Dense |
| Mixed_5d.branch5x5.1.conv | $1.97 \cdot 10^{-3}$ | $2.20 \cdot 10^{-3}$ | 0.89 x | $5.83 \cdot 10^{-4}$ | $2.18 \cdot 10^{-3}$ | 0.27 x | Dense |
| Mixed_6a.branch3x3.conv | $2.81 \cdot 10^{-3}$ | $3.18 \cdot 10^{-3}$ | 0.88 x | $2.76 \cdot 10^{-3}$ | $3.18 \cdot 10^{-3}$ | 0.87 x | General |
| Mixed_6a.branch3x3dbl.3.conv | $1.30 \cdot 10^{-3}$ | $1.22 \cdot 10^{-3}$ | 1.07 x | $1.44 \cdot 10^{-3}$ | $1.29 \cdot 10^{-3}$ | 1.11 x | General |
| Mixed_6b.branch1x1.conv | $1.49 \cdot 10^{-3}$ | $1.64 \cdot 10^{-3}$ | 0.91 x | $5.47 \cdot 10^{-4}$ | $1.62 \cdot 10^{-3}$ | 0.34 x | Dense |
| Mixed_6b.branch7x7.1.conv | $1.46 \cdot 10^{-3}$ | $1.64 \cdot 10^{-3}$ | 0.89 x | $5.60 \cdot 10^{-4}$ | $1.64 \cdot 10^{-3}$ | 0.34 x | Dense |
| Mixed_6b.branch7x7.2.conv | $1.01 \cdot 10^{-3}$ | $1.07 \cdot 10^{-3}$ | 0.94 x | $7.56 \cdot 10^{-4}$ | $1.10 \cdot 10^{-3}$ | 0.69 x | Dense mix |
| Mixed_6b.branch7x7.3.conv | $9.45 \cdot 10^{-4}$ | $1.23 \cdot 10^{-3}$ | 0.77 x | $7.61 \cdot 10^{-4}$ | $1.23 \cdot 10^{-3}$ | 0.62 x | Dense mix |
| Mixed_6b.branch7x7dbl.2.conv | $1.06 \cdot 10^{-3}$ | $1.23 \cdot 10^{-3}$ | 0.86 x | $7.62 \cdot 10^{-4}$ | $1.23 \cdot 10^{-3}$ | 0.62 x | Dense mix |
| Mixed_6b.branch7x7dbl.5.conv | $1.14 \cdot 10^{-3}$ | $1.10 \cdot 10^{-3}$ | 1.04 x | $7.56 \cdot 10^{-4}$ | $1.10 \cdot 10^{-3}$ | 0.69 x | Dense mix |
| Mixed_6c.branch7x7.1.conv | $1.43 \cdot 10^{-3}$ | $1.62 \cdot 10^{-3}$ | 0.88 x | $5.47 \cdot 10^{-4}$ | $1.64 \cdot 10^{-3}$ | 0.33 x | Dense |
| Mixed_6c.branch7x7.2.conv | $1.01 \cdot 10^{-3}$ | $1.34 \cdot 10^{-3}$ | 0.75 x | $7.64 \cdot 10^{-4}$ | $1.35 \cdot 10^{-3}$ | 0.56 x | Dense mix |
| Mixed_6c.branch7x7.3.conv | $1.07 \cdot 10^{-3}$ | $1.69 \cdot 10^{-3}$ | 0.63 x | $7.69 \cdot 10^{-4}$ | $1.68 \cdot 10^{-3}$ | 0.46 x | Dense mix |
| Mixed_6c.branch7x7dbl.2.conv | $8.59 \cdot 10^{-4}$ | $1.67 \cdot 10^{-3}$ | 0.51 x | $7.67 \cdot 10^{-4}$ | $1.69 \cdot 10^{-3}$ | 0.45 x | Dense mix |
| Mixed_6c.branch7x7dbl.5.conv | $1.01 \cdot 10^{-3}$ | $1.33 \cdot 10^{-3}$ | 0.76 x | $7.64 \cdot 10^{-4}$ | $1.35 \cdot 10^{-3}$ | 0.57 x | Dense mix |
| Mixed_6e.branch7x7.2.conv | $1.01 \cdot 10^{-3}$ | $1.48 \cdot 10^{-3}$ | 0.69 x | $7.68 \cdot 10^{-4}$ | $1.49 \cdot 10^{-3}$ | 0.51 x | Dense mix |
| Mixed_6e.branch7x7.3.conv | $9.53 \cdot 10^{-4}$ | $1.77 \cdot 10^{-3}$ | 0.54 x | $7.38 \cdot 10^{-4}$ | $1.79 \cdot 10^{-3}$ | 0.41 x | Dense mix |
| AuxLogits.conv0.conv | $9.97 \cdot 10^{-4}$ | $6.04 \cdot 10^{-4}$ | 1.65 x | $3.66 \cdot 10^{-4}$ | $6.58 \cdot 10^{-4}$ | 0.56 x | Dense |
| AuxLogits.conv1.conv | $1.05 \cdot 10^{-3}$ | $1.09 \cdot 10^{-3}$ | 0.97 x | $9.31 \cdot 10^{-4}$ | $1.09 \cdot 10^{-3}$ | 0.85 x | General |
| Mixed_7a.branch3x3.2.conv | $1.30 \cdot 10^{-3}$ | $7.75 \cdot 10^{-4}$ | 1.68 x | $1.26 \cdot 10^{-3}$ | $7.67 \cdot 10^{-4}$ | 1.64 x | General |
| Mixed_7a.branch7x7x3.4.conv | $1.34 \cdot 10^{-3}$ | $1.14 \cdot 10^{-3}$ | 1.18 x | $1.36 \cdot 10^{-3}$ | $1.14 \cdot 10^{-3}$ | 1.19 x | General |
| Mixed_7b.branch1x1.conv | $1.03 \cdot 10^{-3}$ | $9.07 \cdot 10^{-4}$ | 1.13 x | $5.08 \cdot 10^{-4}$ | $9.07 \cdot 10^{-4}$ | 0.56 x | Dense |
| Mixed_7b.branch3x3.1.conv | $1.16 \cdot 10^{-3}$ | $9.30 \cdot 10^{-4}$ | 1.25 x | $5.20 \cdot 10^{-4}$ | $9.10 \cdot 10^{-4}$ | 0.57 x | Dense |
| Mixed_7b.branch3x3.2a.conv | $1.13 \cdot 10^{-3}$ | $7.94 \cdot 10^{-4}$ | 1.43 x | $6.89 \cdot 10^{-4}$ | $7.93 \cdot 10^{-4}$ | 0.87 x | Dense mix |
| Mixed_7b.branch3x3.2b.conv | $1.07 \cdot 10^{-3}$ | $8.53 \cdot 10^{-4}$ | 1.25 x | $7.60 \cdot 10^{-4}$ | $8.51 \cdot 10^{-4}$ | 0.89 x | Dense mix |
| Mixed_7b.branch3x3dbl.1.conv | $1.16 \cdot 10^{-3}$ | $9.32 \cdot 10^{-4}$ | 1.25 x | $5.38 \cdot 10^{-4}$ | $9.32 \cdot 10^{-4}$ | 0.58 x | Dense |
| Mixed_7b.branch3x3dbl.2.conv | $1.67 \cdot 10^{-3}$ | $1.55 \cdot 10^{-3}$ | 1.08 x | $1.59 \cdot 10^{-3}$ | $1.55 \cdot 10^{-3}$ | 1.02 x | General |
| Mixed_7b.branch.pool.conv | $1.16 \cdot 10^{-3}$ | $6.79 \cdot 10^{-4}$ | 1.71 x | $5.19 \cdot 10^{-4}$ | $6.85 \cdot 10^{-4}$ | 0.76 x | Dense |
| Mixed_7c.branch1x1.conv | $1.23 \cdot 10^{-3}$ | $1.45 \cdot 10^{-3}$ | 0.85 x | $7.69 \cdot 10^{-4}$ | $1.44 \cdot 10^{-3}$ | 0.53 x | Dense |
| Mixed_7c.branch3x3.1.conv | $1.21 \cdot 10^{-3}$ | $1.44 \cdot 10^{-3}$ | 0.84 x | $7.80 \cdot 10^{-4}$ | $1.45 \cdot 10^{-3}$ | 0.54 x | Dense |
| Mixed_7c.branch3x3dbl.1.conv | $1.21 \cdot 10^{-3}$ | $1.43 \cdot 10^{-3}$ | 0.84 x | $7.66 \cdot 10^{-4}$ | $1.44 \cdot 10^{-3}$ | 0.53 x | Dense |
| Mixed_7c.branch.pool.conv | $1.21 \cdot 10^{-3}$ | $1.44 \cdot 10^{-3}$ | 0.84 x | $7.80 \cdot 10^{-4}$ | $1.45 \cdot 10^{-3}$ | 0.54 x | Dense |

(h) MobileNetV2, input shape (32, 3, 256, 256)

| Name | TN [s] | PT [s] | Factor | TN + opt [s] | PT [s] | Factor | Type |
|----------------------|----------------------|----------------------|---------------|----------------------|----------------------|---------------|---------|
| features.0.0 | $1.90 \cdot 10^{-3}$ | $1.66 \cdot 10^{-3}$ | 1.15 x | $1.91 \cdot 10^{-3}$ | $1.68 \cdot 10^{-3}$ | 1.14 x | General |
| features.1.conv.0.0 | $2.69 \cdot 10^{-3}$ | $9.87 \cdot 10^{-3}$ | 0.27 x | $2.70 \cdot 10^{-3}$ | $9.89 \cdot 10^{-3}$ | 0.27 x | General |
| features.1.conv.1 | $1.12 \cdot 10^{-2}$ | $3.03 \cdot 10^{-3}$ | 3.70 x | $7.12 \cdot 10^{-4}$ | $3.00 \cdot 10^{-3}$ | 0.24 x | Dense |
| features.2.conv.0.0 | $1.80 \cdot 10^{-3}$ | $1.77 \cdot 10^{-3}$ | 1.02 x | $4.64 \cdot 10^{-4}$ | $1.76 \cdot 10^{-3}$ | 0.26 x | Dense |
| features.2.conv.1.0 | $7.01 \cdot 10^{-3}$ | $9.06 \cdot 10^{-3}$ | 0.77 x | $6.99 \cdot 10^{-3}$ | $9.06 \cdot 10^{-3}$ | 0.77 x | General |
| features.2.conv.2 | $2.59 \cdot 10^{-3}$ | $2.38 \cdot 10^{-3}$ | 1.09 x | $6.08 \cdot 10^{-4}$ | $2.40 \cdot 10^{-3}$ | 0.25 x | Dense |
| features.3.conv.0.0 | $1.44 \cdot 10^{-3}$ | $9.19 \cdot 10^{-4}$ | 1.57 x | $2.96 \cdot 10^{-4}$ | $9.40 \cdot 10^{-4}$ | 0.31 x | Dense |
| features.3.conv.1.0 | $2.99 \cdot 10^{-3}$ | $1.12 \cdot 10^{-2}$ | 0.27 x | $2.99 \cdot 10^{-3}$ | $1.12 \cdot 10^{-2}$ | 0.27 x | General |
| features.3.conv.2 | $3.65 \cdot 10^{-3}$ | $3.38 \cdot 10^{-3}$ | 1.08 x | $7.92 \cdot 10^{-4}$ | $3.40 \cdot 10^{-3}$ | 0.23 x | Dense |
| features.4.conv.1.0 | $3.01 \cdot 10^{-3}$ | $3.76 \cdot 10^{-3}$ | 0.80 x | $2.99 \cdot 10^{-3}$ | $3.77 \cdot 10^{-3}$ | 0.79 x | General |
| features.4.conv.2 | $1.38 \cdot 10^{-3}$ | $1.16 \cdot 10^{-3}$ | 1.19 x | $3.53 \cdot 10^{-4}$ | $1.16 \cdot 10^{-3}$ | 0.30 x | Dense |
| features.5.conv.0.0 | $8.51 \cdot 10^{-4}$ | $5.17 \cdot 10^{-4}$ | 1.65 x | $2.77 \cdot 10^{-4}$ | $5.34 \cdot 10^{-4}$ | 0.52 x | Dense |
| features.5.conv.1.0 | $1.38 \cdot 10^{-3}$ | $3.99 \cdot 10^{-3}$ | 0.34 x | $1.36 \cdot 10^{-3}$ | $3.99 \cdot 10^{-3}$ | 0.34 x | General |
| features.5.conv.2 | $1.68 \cdot 10^{-3}$ | $1.36 \cdot 10^{-3}$ | 1.24 x | $3.94 \cdot 10^{-4}$ | $1.35 \cdot 10^{-3}$ | 0.29 x | Dense |
| features.7.conv.1.0 | $1.37 \cdot 10^{-3}$ | $1.69 \cdot 10^{-3}$ | 0.81 x | $1.35 \cdot 10^{-3}$ | $1.69 \cdot 10^{-3}$ | 0.80 x | General |
| features.7.conv.2 | $8.59 \cdot 10^{-4}$ | $7.05 \cdot 10^{-4}$ | 1.22 x | $2.52 \cdot 10^{-4}$ | $7.00 \cdot 10^{-4}$ | 0.36 x | Dense |
| features.8.conv.0.0 | $8.45 \cdot 10^{-4}$ | $4.92 \cdot 10^{-4}$ | 1.72 x | $2.49 \cdot 10^{-4}$ | $4.93 \cdot 10^{-4}$ | 0.51 x | Dense |
| features.8.conv.1.0 | $1.16 \cdot 10^{-3}$ | $2.36 \cdot 10^{-3}$ | 0.49 x | $1.12 \cdot 10^{-3}$ | $2.35 \cdot 10^{-3}$ | 0.47 x | General |
| features.8.conv.2 | $8.73 \cdot 10^{-4}$ | $9.30 \cdot 10^{-4}$ | 0.94 x | $3.06 \cdot 10^{-4}$ | $9.29 \cdot 10^{-4}$ | 0.33 x | Dense |
| features.11.conv.2 | $9.89 \cdot 10^{-4}$ | $9.49 \cdot 10^{-4}$ | 1.04 x | $3.06 \cdot 10^{-4}$ | $9.25 \cdot 10^{-4}$ | 0.33 x | Dense |
| features.12.conv.0.0 | $9.55 \cdot 10^{-4}$ | $5.32 \cdot 10^{-4}$ | 1.80 x | $2.50 \cdot 10^{-4}$ | $5.14 \cdot 10^{-4}$ | 0.49 x | Dense |
| features.12.conv.1.0 | $1.51 \cdot 10^{-3}$ | $3.23 \cdot 10^{-3}$ | 0.47 x | $1.27 \cdot 10^{-3}$ | $3.22 \cdot 10^{-3}$ | 0.39 x | General |
| features.12.conv.2 | $1.14 \cdot 10^{-3}$ | $1.24 \cdot 10^{-3}$ | 0.92 x | $3.94 \cdot 10^{-4}$ | $1.17 \cdot 10^{-3}$ | 0.34 x | Dense |
| features.14.conv.1.0 | $1.51 \cdot 10^{-3}$ | $1.61 \cdot 10^{-3}$ | 0.94 x | $1.45 \cdot 10^{-3}$ | $1.61 \cdot 10^{-3}$ | 0.90 x | General |
| features.14.conv.2 | $1.14 \cdot 10^{-3}$ | $6.83 \cdot 10^{-4}$ | 1.67 x | $3.67 \cdot 10^{-4}$ | $6.80 \cdot 10^{-4}$ | 0.54 x | Dense |
| features.15.conv.0.0 | $9.53 \cdot 10^{-4}$ | $5.23 \cdot 10^{-4}$ | 1.82 x | $2.74 \cdot 10^{-4}$ | $5.23 \cdot 10^{-4}$ | 0.52 x | Dense |
| features.15.conv.1.0 | $1.41 \cdot 10^{-3}$ | $2.25 \cdot 10^{-3}$ | 0.63 x | $1.37 \cdot 10^{-3}$ | $2.25 \cdot 10^{-3}$ | 0.61 x | General |
| features.15.conv.2 | $1.15 \cdot 10^{-3}$ | $8.81 \cdot 10^{-4}$ | 1.31 x | $4.46 \cdot 10^{-4}$ | $8.83 \cdot 10^{-4}$ | 0.51 x | Dense |
| features.17.conv.2 | $1.16 \cdot 10^{-3}$ | $8.80 \cdot 10^{-4}$ | 1.31 x | $4.36 \cdot 10^{-4}$ | $8.58 \cdot 10^{-4}$ | 0.51 x | Dense |
| features.18.0 | $9.51 \cdot 10^{-4}$ | $5.40 \cdot 10^{-4}$ | 1.76 x | $2.50 \cdot 10^{-4}$ | $5.22 \cdot 10^{-4}$ | 0.48 x | Dense |

F MISCELLANEOUS

F.1 EXAMPLE: ASSOCIATIVITY OF TENSOR MULTIPLICATION

Here, we demonstrate associativity of tensor multiplication through an example. The technical challenge is that an index can only be summed once there are no remaining tensors sharing it. Therefore, we must carry indices that are summed in later multiplications in the intermediate results, which requires some set arithmetic on the index sets.

Let S_1, S_2, S_3 be index tuples of the input tensors $\mathbf{A}, \mathbf{B}, \mathbf{C}$, and $S_4 \subseteq (S_1 \cup S_2 \cup S_3)$ a valid output index tuple of their tensor multiplication $\mathbf{D} = *_{(S_1, S_2, S_3, S_4)}(\mathbf{A}, \mathbf{B}, \mathbf{C})$. We can either first multiply \mathbf{A} with \mathbf{B} to obtain an intermediate tensor of index structure $S_{1,2}$, or \mathbf{B} with \mathbf{C} to obtain an intermediate tensor of index structure $S_{2,3}$, before carrying out the remaining multiplications. To construct the intermediate index structures, we divide the indices $\tilde{S} = (S_1 \cup S_2 \cup S_3) \setminus S_4$ that are summed over into those only shared between \mathbf{A}, \mathbf{B} given by $\tilde{S}_{1,2} = (S_1 \cup S_2) \setminus (S_4 \cup S_3)$, and those only shared among \mathbf{B}, \mathbf{C} given by $\tilde{S}_{2,3} = (S_2 \cup S_3) \setminus (S_4 \cup S_1)$. This yields the intermediate indices $S_{1,2} = (S_1 \cup S_2) \setminus \tilde{S}_{1,2}$ and $S_{2,3} = (S_2 \cup S_3) \setminus \tilde{S}_{2,3}$, and the parenthesizations

$$\begin{aligned} [\mathbf{D}]_{S_4} &= \left(\sum_{\tilde{S} \setminus \tilde{S}_{1,2}} \left(\sum_{\tilde{S}_{1,2}} [\mathbf{A}]_{S_1} [\mathbf{B}]_{S_2} \right) [\mathbf{C}]_{S_3} \right) = \left(\sum_{\tilde{S} \setminus \tilde{S}_{2,3}} [\mathbf{A}]_{S_1} \left(\sum_{\tilde{S}_{2,3}} [\mathbf{B}]_{S_2} [\mathbf{C}]_{S_3} \right) \right) \quad (\text{F15}) \\ \Leftrightarrow \mathbf{D} &= *_{(S_1, 2, S_3, S_4)} \left(*_{(S_2, S_3, S_{2,3})}(\mathbf{A}, \mathbf{B}), \mathbf{C} \right) = *_{(S_1, S_2, 3, S_4)} \left(\mathbf{A}, *_{(S_1, S_2, S_{1,2})}(\mathbf{B}, \mathbf{C}) \right). \end{aligned}$$

This generalizes to n -ary multiplication, allowing to break it down into smaller multiplications. However, the index notation and set arithmetic from Equation (F15) quickly becomes impractical.